UNIVERSITE DE SHERBROOKE
Faculté de génie
Département de génie chimique et biotechnologique

DÉVELOPPEMENT DE FILMS BARRIÈRES MULTICOUCHES À BASE DE MÉLANGES D'AMIDON THERMOPLASTIQUE ET DE POLYÉTHYLÈNE

DEVELOPMENT OF MULTILAYER BARRIER FILMS BASED ON BLENDS OF THERMOPLASTIC STARCH AND POLYETHYLENE

Thèse de doctorat
Spécialité: génie chimique

Thomas MAZEROLLES

Jury : Pr. Michel Huneault (directeur)
Pr. Marie-Claude Heuzey (co-directrice)
Pr. Nathalie Faucheux
Dr. Hongbo Li
Pr. Frej Mighri

Sherbrooke (Québec), Canada Juillet 2019

À mes parents

RÉSUMÉ

Les emballages jouent un rôle majeur dans la protection des produits. Dans le cas des emballages alimentaires, leur fonction est d'augmenter la durée de conservation des produits et de limiter ainsi les déchets alimentaires. Pour ce faire, ces emballages doivent répondre à des exigences élevées en terme de barrière aux gaz. Les polyoléfines conventionnelles particulièrement hydrophobes comme le polyéthylène ou le polypropylène sont d'excellentes barrières à l'humidité mais de mauvaises barrières face à l'oxygène. Les matériaux présentant de faibles perméabilités à l'oxygène couramment utilisés dans l'industrie sont des polymères polaires comme les polyvinyles alcool ou les polyamides. Typiquement, les films barrières sont des assemblages multicouches de polyoléfines et de matériaux barrières à l'oxygène avec des couches d'adhésif. Ces dernières, souvent des polyoléfines fonctionnalisées, sont utilisées pour éviter la délamination. Cependant, ces matériaux à faible perméabilité à l'oxygène sont pétro-sourcés et relativement chers. De plus, l'utilisation de couches d'adhésif nécessite des équipements de mise en forme plus spécifiques. Grâce à sa faible perméabilité à l'oxygène, l'amidon serait alors une alternative bio-sourcée intéressante pour la production de films barrières. Quand il est correctement déstructuré et plastifié, l'amidon devient thermoplastique (noté TPS) et peut alors être utilisé avec les équipements conventionnels de mise en forme des polymères. Cependant, à cause de son caractère hydrophile, le TPS est très sensible à l'humidité. Le mélange du TPS avec un matériau plus hydrophobe tel le polyéthylène basse densité (LDPE) serait alors un atout en ajoutant une protection au TPS et assurant une bonne barrière à l'humidité au film.

L'objectif de ce projet est le développement de mélanges co-continus de TPS et de LDPE dans le but de produire des films soufflés multicouches présentant une morphologie lamellaire pour des propriétés barrières à l'oxygène améliorées. Une première partie de cette thèse se concentre sur la rhéologie du TPS, en particulier en analysant l'effet de l'eau et du glycérol comme plastifiant. Pour ce faire, les mélanges TPS/LDPE à haut taux de TPS ont été produits par extrusion bi-vis. La transition de morphologie de mélange dispersé à une morphologie co-continue est survenue pour des concentrations en TPS aussi basse que 50% en masse mais cette transition a été déplacée vers des concentrations plus importantes en augmentant le ratio de viscosité TPS/LDPE. La seconde

partie de cette thèse décrit la production de films soufflés 3 couches avec le mélange TPS/LDPE comme couche centrale et des couches externes de LDPE. L'originalité de cette approche se trouve dans la production en continu du film 3 couches sans couche d'adhésif. L'utilisation d'une certaine quantité de compatibilisant dans le mélange est alors nécessaire à sa stabilisation et pour éviter la délamination des couches de film. Un autre point clé de cette étude est l'ajout d'argile naturelle dans le mélange qui améliore significativement la mise en forme du film. De façon globale, la démarche mise en place pour cette thèse a permis la production de films minces et transparents présentant une perméabilité à l'oxygène réduite d'un facteur 20 par rapport au LDPE.

Mots-clés : amidon thermoplastique, multicouche, film soufflé, co-continuité, barrière aux gaz.

ABSTRACT

Packaging plays a crucial role in the protection of goods. In order to increase shelf life and limit product waste, food packaging must comply with very strict standards regarding gas barrier properties. Conventional polyolefins such as polyethylene or polypropylene display very low water permeability due to their hydrophobicity but shows high oxygen permeability. Current industrial solutions to lower oxygen permeability involve the use of highly polar polymers such as polyvinyl alcohol or polyamides. Barrier films are typically a 5-layer assembly with polyolefin outer layers, a central layer comprising the oxygen barrier material and tie layers separating the central and outer layers, improving the interlayer adhesion. The tie layer is commonly a functionalized polyolefin that can react with the barrier material to form covalent bonds. Currently, low oxygen permeability materials are expensive petroleum-based polymers. With its low oxygen permeability, starch could be an interesting bio-based and low-cost alternative material for the preparation of oxygen barrier films. When properly destructurized and plasticized, starch is rendered thermoplastic and can be processed through conventional polymer processing equipment. It is then called thermoplastic starch (TPS). Yet, because of its high hydrophillicity, TPS is very sensitive to moisture. Blending TPS with a more hydrophobic material such as low-density polyethylene (LDPE) would result in the protection of TPS and the addition of a water barrier to the film.

The aim of this project is to develop co-continuous blends of TPS/LDPE in order to produce 3-layer blown films with a center layer comprised of a TPS/LDPE lamellar blend for improved barrier properties. This thesis first focuses on the rheological behavior of TPS and the effect of water and glycerol as plasticizers on TPS viscosity. TPS/LDPE blends with a high TPS fraction were produced in a twin-screw extruder. The transition from dispersed to co-continuous blend morphology appeared at concentration as low as 50 wt% TPS but this transition was pushed to higher concentration when the TPS/LDPE viscosity ratio was increased. The second part of this work describes the successful production of a 3-layer blown film consisting of a TPS/LDPE blend as inner layer and pure LDPE outer layers. The originality of the approach resides in the continuous blown film production of the 3-layer film without the use of a tie layer. The incorporation of a sufficient

amount of compatibilizer in the blend was found to be necessary to its stabilization and to prevent film delamination. Another key point is that the addition of natural clay in the TPS/LDPE blend improves drastically the processing of the multilayer film. Overall, the procedure allows the production of transparent thin films with oxygen barrier properties up to 20 times higher than pure LDPE.

Keywords: thermoplastic starch, multilayer, blown film, co-continuity, gas barrier.

ACKNOWLEDGMENTS

First, I would like to thank my supervisor Pr. Michel Huneault for all his support during my thesis. I learnt a lot from him during these years, both professionally and personally. More than a supervisor, Michel is a friend. I will never forget his warm welcome when I first arrived during the peak of the winter.

I would like to express my sincere gratitude to my co-supervisor Marie-Claude Heuzey for her academic support, suggestions and corrections. It was a pleasure to be part of her research group.

I am very grateful to SABIC for the financial support of this project and especially to Maria Soliman, Hans Martens and Ralf Kleppinger for their suggestions and corrections as well as for giving me this great opportunity.

A particular mention to the research professionals at NRC Boucherville and especially Dr. Hongbo Li for his help with the processing of my product.

I am very grateful to Claire Cerclé and Matthieu Gauthier at Ecole Polytechnique of Montreal for their help in the characterization of my films. A special mention to Richard Silverwood for all the hours spent in Anjou for the production of the films.

I finally wish to thank all the people that have been involved, near of far, in my project at the University of Sherbrooke. I will remember all those late evenings in the laboratory with Valérie Larouche, Isabelle Arsenault, Stéphane Guay and Serge Gagnon. To the research professionals at CCM: Stéphane Gutierrez, Charles Bertrand and Sonia Blais thank you very much for your help with all the characterization of my materials.

Finally, to my colleagues, friends and members of the Team Huneault: Mauricio, Edwin, Christian, Amirjalal, Ariane and Marc-André you will never be forgotten!

TABLE OF CONTENT

TABLE OF FIGURES

TABLE OF TABLES

ABBREVIATIONS

Abbreviation	Definition
EVOH	Ethylene Vinyl Alcohol
LDPE	Low Density Polyethylene
PE	Polyethylene
PP	Polypropylene
MFI	Melt Flow Index
MMT	Montmorillonite
OP	Oxygen Permeability
OTR	Oxygen Transmission Rate
PE-g-MA	Polyethylene grafted maleic anhydride
SEM	Scanning Electron Microscopy
TGA	Thermo Gravimetric Analysis
TPS	Thermoplastic Starch
RH	Humidity Ratio
WVP	Water Vapor Permeability
WVTR	Water Vapor Transmission Rate

CHAPTER 1 INTRODUCTION

1.1 Context of the study

The food packaging industry is driven by socioeconomic needs. The viability of any new packaging depends on its consumer appeal, convenience, safety of use, low-cost, eco-friendliness, recyclability but above all, on its ability to protect its content from the external environment.

One important functional property of food packaging is its ability to reduce the permeation rate of gases from the external environment to the package content. This property is often referred to as the "barrier properties" of the packaging. The aim of gas barrier materials is to reduce the transmission of N_2, O_2, CO_2, CO and/or H_2O depending on the final application. Carbon dioxide barrier is important for gaseous drinks whereas humidity barrier helps preventing dryness and oxygen barrier reduces oxidation thus improving shelf-life. The last two aspects are essential to the conservation of solid food (Lee et al., 2008).

Most of conventional polymers are hydrophobic thus leading to high water barrier whereas the best oxygen barrier material used in packaging is aluminum. 380 million tons of plastic are been produced every year, 45% of which being used for packaging (Geyer et al., 2017). The primary films used in flexible packaging are produced by blown-film or cast film extrusion. The thickness of flexible film packaging is typically between 20 and 250 microns. Moreover, aluminum based packages display the best oxygen barrier performance yet is more expensive and requires lamination facilities.

Polyethylene is the most produced synthetic polymer accounting for approximately 36% of the total plastic market (Geyer et al., 2017). It is due mainly to its low price, excellent chemical resistance and easy processability. Polyethylene is an excellent water barrier but a poor oxygen barrier because of its nonpolar structure. All-polymer packaging with low oxygen permeability are

commercially available. These packaging typically comprise materials like polyamides or Ethylene Vinyl Alcohol copolymers (EVOH). They both display high oxygen barrier performance and easy processing yet they are expensive and highly hydrophilic.

Finding a material combining all desired properties is difficult. One solution is to combine different polymers to take advantage of their specific strengths. In terms of films, it means creating a multilayer structure, each layer having a specific role with regards to properties such as permeability, mechanical performance, optical properties or weldability. Currently, multilayer solution widely used for food packaging applications displays at least five layers: a core layer of Ethylene Vinyl Alcohol (EVOH) as oxygen barrier material, two adhesive layers (known as tie layers) on each side of the core layer to insure interlayer adhesion and two external layers of polyethylene that provides a good water barrier and mechanical strength (Lee et al., 2008).

In the past few years, increasing research activities have been focused on renewable resources aiming to reduce the use of fossil resources. In this perspective, there is a growing interest in food and non-food applications of starch and especially thermoplastic starch (TPS). Starch is rendered thermoplastic by gelatinization, a process in which starch is subjected to shear and heat in presence of a plasticizer. In these conditions, the crystalline structure of starch breaks down and the material becomes fully amorphous opening the way to its processing with conventional polymer processing machinery (Avérous, 2004). TPS exhibits a low oxygen permeability, therefore it could act as an oxygen barrier in a multilayer packaging application.

The pros and cons of Aluminum, EVOH and TPS based packages for food preservation purposes are compared in Table 1.1. Aluminum is the ultimate barrier material but requires specific lamination equipment. Moreover, aluminum-based packages are not see-through and have limited flexibility. EVOH shows a very low oxygen permeability yet it is an expensive petroleum-based material. TPS is cheap, bio-based, it can be processed on conventional polymer processing equipment, it is transparent and shows higher oxygen permeability than EVOH but yet much lower oxygen permeability compared to polyolefins (Jost & Stramm, 2016).

Table 1.1: Comparison between the main oxygen barrier materials used in food packaging and TPS

	Aluminum based packaging	EVOH based packaging	TPS based packaging
Barrier properties	Ultimate gas and moisture barrier for films ≥ 25µm	- Very good oxygen barrier at low Humidity Ratio (RH) - Need another material for water protection - Sensitive to moisture	- Intermediate oxygen barrier material - Very sensitive to moisture - Need another material for water protection
Multilayering	Requires multiple lamination steps i.e. expensive	Co-extrusion easy and cheap	not yet achieved in continuous conditions
Marketing aspects	- Product not visible - Not microwavable	- Easy see-through - Microwavable	- Easy see through - Microwavability not tested

Although TPS seems to be an interesting bio-based alternative as an oxygen barrier material, its continuous processing in films needs to be investigated. It will be important to find a way to protect the TPS from moisture while maximizing the oxygen and water barrier of the film.

1.2 Research objectives

The main objective of this project is to understand the effect of the TPS phase composition and the viscosity ratio on the TPS/LDPE blend morphology for barrier film applications. The first step deals with the study of the TPS/LDPE blend morphology and stability around the phase inversion range. The role of water and glycerol as starch plasticizers and their effect on starch rheology is investigated. The TPS/LDPE blend is then blown as the central layer of a 3-layer blown film along with two continuous LDPE outer layers protecting the TPS from moisture.

Four specific objectives have been identified:

1) Determine the role of TPS/LDPE formulation on the blend morphology developed in the twin-screw compounding process, in particular in the vicinity of the co-continuous morphology concentration range.

2) Monitor the morphology development of TPS/LDPE blends during the multilayer film extrusion step. This includes the role of composition, plasticization (with both water and glycerol) and interface modification on the layer stability and internal blend morphology in the multilayer blown film extrusion.

3) Relate the layer structure and blend morphology within layers with the films barrier and mechanical performance.

4) Determine the potential benefit of platy minerals such as clay for the blown film processing and barrier performance of the multilayer system. This includes natural and organically modified clay and the role of exfoliation during the process.

1.3 Original contribution

First of all, blends of TPS with polyolefins and especially polyethylene have shown interesting properties yet with only limited amount of TPS. The present study investigates blends of both corn and potato-based TPS at high TPS content. In particular, potato starch based TPS blended with polyethylene in the phase inversion range has not yet been explored.

Most blend morphology studies involving TPS focus on blends where the TPS is the dispersed phase. Another original aspect of this thesis is that the effect of blend composition, viscosity ratio (TPS/PE) and compatibilization were investigated in the very high TPS concentration range, in order to identify the concentration range where a co-continuous morphology can be found. Furthermore, the blend morphology was monitored not only after the compounding step but also

after the film blowing enabling us to single out the effect of the film forming process on the blend morphology.

Moreover, multilayer films comprising of a water vapor barrier material and an oxygen barrier material are typically comprised of 5 layers (core functional layers + 2 adhesive layers + 2 polyolefin outer layers). This thesis describes the successful development of an innovative 3-layer blown film composed of a TPS/LDPE blend as an inner layer, protected by pure LDPE outer layers. This strategy allows the continuous production of a film with both oxygen and water barrier properties without the use of adhesive layers (also known as tie-layers).

Another original aspect of this thesis is the use of clay in the TPS phase. Due to its hydrophillicity, natural clay can be easily incorporated in the TPS phase. Mixing clay particles in the first step of the extrusion process is innovative and allows a good exfoliation of the platelets. The subsequent film blowing further improves the positioning of the particles, allowing the production of a clean film.

Finally, although thermoplastic corn starch's production has been widely studied, potato based TPS lacks of investigation due to its high viscosity compared to other starch types. In particular, the effect of plasticizer on potato TPS's viscosity when produced with a twin-screw extruder needs a deeper understanding.

1.4 Structure of the thesis

The thesis has been divided into seven chapters including the introduction. The second chapter gives general information on mathematical and physical aspects of gas permeability through films. Chapter 3 develops the literature review on thermoplastic starch, its blend with polyethylene and the processing of such a blend. Chapter 4 presents the methodology used to conduct the experimental work of this thesis. Chapters 5 and 6 include the two published scientific articles arising from this work. Chapter 5 deals with the development of co-continuous morphology in blends of thermoplastic starch and low-density polyethylene. Chapter 6 focuses

on the development of multilayer barrier film based on thermoplastic starch and polyethylene and the effect of clays in such a system. Finally, chapter 7 aims at drawing conclusions and recommendations from the results of this thesis.

CHAPTER 2 THEORY ON POLYMER FILM PERMEABILITY

2.1 Transfer phenomena through packaging materials

Predicting and controlling product shelf-life and the atmosphere inside the package for the protection and preservation of food product is directly linked to the mass transfer of gas and solute through the packaging. Permeation is the phenomenon by which permeants can penetrate and pass through an entire material in response to a difference in partial pressure or in concentration. Gas and water vapor transmission rates can be measured through films by placing the permeant of interest on one side and measuring the permeant flux in a carrier gas on the other side using a coulometric sensor. The mechanism of measurement is detailed in the Methodology section of this document. To get an intensive property, the transmission rate is multiplied by the film thickness, thus giving the permeability of the membrane. For most polymeric membrane applications, the thickness is small compared to the area through which transfer occurs therefore leading to a single dimension problem.

Figure 2.1 summarizes the mass transfer phenomena happening through a polymer film with C_1 the concentration of permeant of the high concentrated area and C_0 in the low concentrated area. It takes place in three steps. At first, the permeant adsorbs onto the high concentration side of the film. Once the permeant concentration increases at the surface of the membrane, diffusion to the other side of the membrane starts. Diffusion corresponds to the movement of the molecules from the more concentrated areas to the less concentrated areas. Diffusion increases up to a steady-state where the permeation rates on each side of the membrane are equal. Finally, desorption of the permeant on the low concentration side of the film occurs.

Diffusion is described through Fick's law, detailed in Equation (2.1):

$$J_d = -D * \frac{\partial C}{\partial x} \tag{2.1}$$

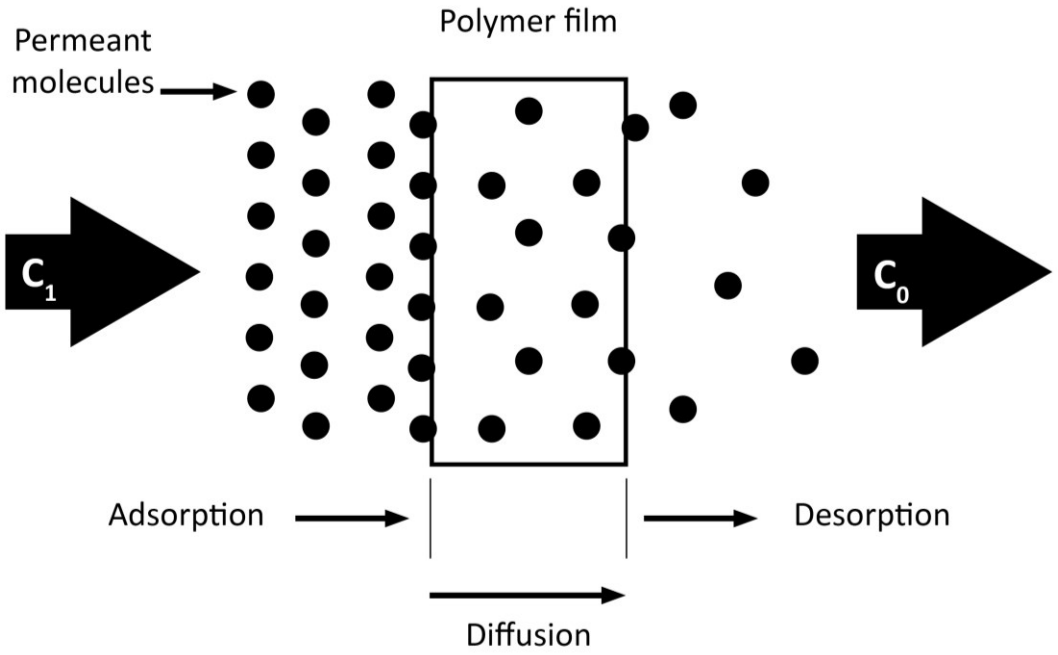

Figure 2.1: Mass transfer phenomena through a polymer film

In Fick's first law, J_d, D, C and x are respectively the flux per unit cross section, the diffusivity coefficient, the concentration of the permeant and the space coordinate in the diffusion direction. If we consider steady-state and that C_{s1} and C_{s0} are the concentrations of permeant at the outer and inner surface of a membrane, Equation (2.2) is obtained by integration of Equation (2.1):

$$J_d = \frac{Q'}{A * t} = D * \frac{(C_{s1} - C_{s0})}{L} \quad i.e. \quad \frac{[Amount_{permeant}]}{[Surface_{membrane}][Time]} = \frac{[kg]}{[m^2][s]} \tag{2.2}$$

Where Q', A and L are the amount of diffused moving substance, the cross sectional diffusing area and the thickness of the membrane, respectively. In order for the gas to diffuse through the membrane, it has to dissolve into the material first and this is usually described with Henry's law, reminded in Equation (2.3):

$$p = k^H * X \tag{2.3}$$

Where p, k^H and X are the partial pressure of permeant, Henry's law constant and the molar fraction of permeant respectively. When dealing with dilute solution such as permeation situations, the approximation $C_s \propto X$, with C_s being the concentration of permeant, can be used. It leads to Equation (2.4), introducing the solubility coefficient S.

$$C_s = S * p \; ; \; [S] = \frac{[mol]}{[m^3][atm]} \tag{2.4}$$

If the solubility coefficient is independent of concentration, this model will be linear otherwise Langmuir type relations may apply. In this thesis, we suppose that Henry's law can be applied. In practice, surface concentration is not always known and it is easier to work with the partial pressures. Hence combining Equations (2.2) and (2.4) and using Q=Q'/t as the steady state permeation rate, it leads to Equation (2.5):

$$Q = D * A * \frac{C_{s1} - C_{s0}}{L} = D * A * \frac{S * (p_1 - p_0)}{L} = P * \frac{A}{L} \Delta p \;\; with \; P = D * S \tag{2.5}$$

This introduces the term permeability P, defined as the product of the diffusion coefficient and the solubility coefficient. The unity of permeability is developed in Equation (2.6).

$$[P] = \frac{Amount_{permeant} * Thickness_{membrane}}{Surface_{membrane} * Time * Pressure_{before\ membrane}} = \frac{kg (or\ m^3) * m}{m^2 * day * atm} \tag{2.6}$$

2.2 Factors influencing permeability

There are different factors influencing polymer permeability, mainly:

1) Size of the permeant

Since the permeability is governed by solubility and diffusivity of the small molecules in the polymer, when increasing the size in a series of chemically similar molecules, higher solubility and lower diffusion coefficients are expected. An increase in size implies an increase in boiling point and therefore a greater solubility coefficient. The decreased diffusion coefficient is due to the

increased activation energy necessary to the diffusion. The competition between these two effects often leads to a decrease in permeability when increasing permeant size since solubility coefficient is expected to increase by a factor 10 when the diffusion coefficient may vary by 10 orders of magnitude in the case of permeant through polymer.

2) Plasticization

Plasticization is used to ease the movement of the polymer chains with regards to each other. Increasing plasticizer's content should then increase permeability.

3) Polymer molecular weight

Increasing the polymer molecular weight decreases the overall number of chain ends thus decreasing the discontinuities in the material. Those discontinuities may form absorption sites for the permeant therefore an increase in polymer molecular weight entails a decrease in permeability.

4) Polymer density

An increase in polymer density often results in a reduction of permeability.

5) Functional groups

Functional groups can show two different types of effects. If the functional groups have a specific interaction with a permeant, it may increase its solubility in the polymer thus leading to a plasticization effect. As explained previously, increasing plasticization would increase permeability. For example, highly polar polymers such as those containing hydroxyl groups are poor water barriers. On the other hand, highly polar polymers are excellent oxygen barrier materials.

6) Fillers

Adding fillers in the polymer may either increase or decrease the permeability. On the first hand, it can create a physical barrier for the permeant to be forced to use longer path thus decreasing permeability. In equation (2.5), the addition of solid fillers increases virtually the film thickness

thus reducing the permeation rate (solubility stays constant since it is a thermodynamic factor). In order to come to such result, the filler particles have to be compatible with the polymer matrix. In case they are not, voids can occur around the particles at the interface thus increasing the permeability.

7) Crystallinity and molecular orientation

In semi-crystalline polymers, crystalline regions and molecular orientation are obstacles to the passage of the penetrating molecules. This forces the penetrant to diffuse along longer path length as in the case of solid fillers (Ketels, 1989).

8) Environmental factors

The two main factors in that category are temperature and relative humidity. The permeability coefficient can be expressed using an Arrhenius-type model, like in Equation (2.7):

$$P = P_0 * exp\left(\frac{-E_a}{RT}\right) \quad (2.7)$$

P_0 being another pre-exponential factor.

As explained earlier, this type of model can be used in the case where the polymer is above the glass transition temperature otherwise the activation energy changes a lot. The permeability would increase with the increase in temperature. In the case of an environment with high humidity, water molecules can be absorbed by the polymer and interact with the polar groups, making the structure swell (plasticization effect). However, it has no effect on non-polar polymers such as polyethylene or polypropylene (PP).

2.3 Gas permeability in polymer blends and multilayer films

In case of a blend of two polymers where one is the dispersed phase and the other one the matrix, the gas permeability P will fall in between lower and upper bonds defined by the series and parallel theoretical models described in Equations (2.8) and (2.9) respectively:

$$P = \alpha_1 P_1 + \alpha_2 P_2 \tag{2.8}$$

$$\frac{1}{P} = \frac{\beta_1}{P_1} + \frac{\beta_2}{P_2} \tag{2.9}$$

P_1 and P_2 are the individual permeability values of the two polymers and α and β are constants. In the case of a blend where the permeability coefficient of the matrix is larger, the series model is preferred. However, when the permeability of the dispersed phase is higher, the parallel model should be preferred.

In a multilayer film, each polymer has its own values of solubility, diffusion and permeability. The global permeability coefficient of the multilayer film may be estimated by using the empirical relationship described in Equation (2.10):

$$flux = \frac{driving\ force}{resistance} \tag{2.10}$$

In the case of permeability, as seen in Equation (2.5), the flux is the one of the permeant, the driving force is the difference in partial pressure and the resistance is the inverse of permeability. In such a model, used for example in Ohm's law, it is known that the total resistance is equal to the sum of individual resistances in series, thus leading in our case to Equation (2.11):

$$\frac{L}{P} = \sum_{i=1}^{n} \frac{L_i}{P_i} \tag{2.11}$$

L and P being respectively the overall thickness and permeability of the multilayer film and L_i and P_i thickness and permeability of the i^{th} layer (n being the total number of layers).

CHAPTER 3 LITERATURE REVIEW

3.1 Current solutions in barrier packaging

Food industry relies on barrier packaging in order to protect their product from external contamination, maintain the humidity level and limit the oxidation thus extending shelf-life.

Reduction in gas permeation rates of packaging can be obtained through several procedures, the most widely found in the industry are metallization, coating, orientation and layering. Metallization uses mostly Aluminum because it becomes totally impermeable to oxygen at thickness greater than 20 µm (Robertson, 2006). Other metals such as copper or silver could be used as well but are more expensive (Cros, 2007). Organic and inorganic coatings can be used as well: silicon or aluminum oxides on polyethylene terephthalate (PET) for example. Since increasing crystallinity increases barrier properties, polymer molecular orientation can also be a way to enhance barrier properties: for example bi-oriented polypropylene and PET are used. Finally, another way is to produce a multilayer film, each layer having a specific role regarding the barrier. Multilayer co-extrusion of polymers is widely used in the industry but cardboard and aluminum can also be combined with polymers in solution such as Tetrapak® packages to protect very sensitive products like milk or fruit juice (Ronzani & Baccaro, 2012). However this last solution is more expensive, requires a very specific equipment allowing multiple lamination steps to produce Aluminum sheets and the package is then non-recyclable and not transparent (Robertson, 2006).

Figure 3.1 shows the permeability to oxygen and water vapor of standard packaging polymers. Polyolefins such as Low Density Polyethylene (LDPE), High Density Polyethylene (HDPE) and PP are very common packaging materials because of their low cost, easy processing and excellent mechanical properties. They boast very low permeability to water vapor but are extremely poor barriers to oxygen. Polyvinylidene chloride (PVDC) has interesting properties being both a good barrier to water vapor and oxygen. It has almost totally disappeared as a packaging material

however because of concerns with its chlorine content, recyclability and cost. The best oxygen barriers are polyvinyl alcohol (PVAL) and copolymers of ethylene and vinyl alcohol (EVOH). The former is a water-soluble polymer that cannot be processed easily using industrial melt-processing techniques. By contrast, EVOH is a widely used oxygen barrier and can be considered as the reference material for this property. A typical barrier multilayer film comprises external layers of polyethylene, an internal layer of EVOH and intermediate layers of polymeric adhesives that insure proper adhesion between the EVOH and PE layers. However, the production of such film requires at least 5-layer film production lines (Robertson, 2013).

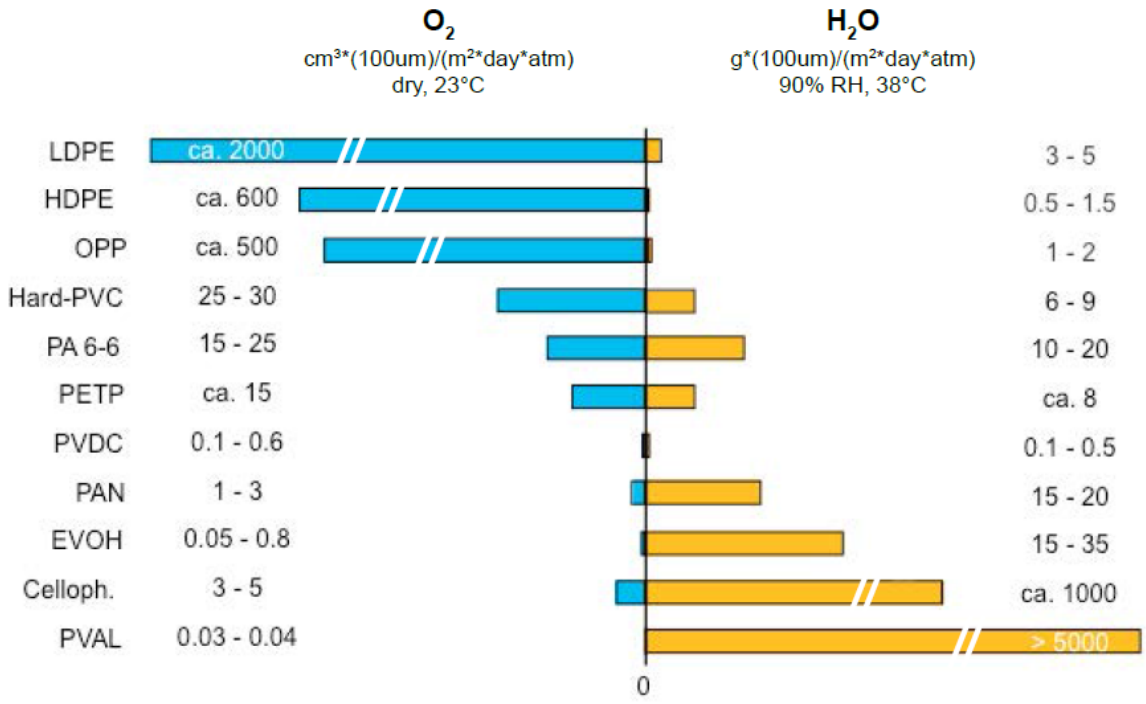

Figure 3.1: Oxygen and water vapor permeability (reproduced with permission from Martens, 2014)

Polyethylene, in all its different forms, is the most used polymer accounting for 36% of the world total polymer production (Geyer et al., 2017). Because of different molecular weights and architecture, it has several sub-categories, such as HDPE (high-density polyethylene, linear structure), LDPE (low-density polyethylene, highly branched), and LLDPE (linear low-density polyethylene) each of which possesses different mechanical properties making it suitable for different applications. For example, due to its regular structure and low branching HDPE has a

high crystallinity (up to 90%), higher density (around 0.96), hardness and tensile strength whereas LDPE is highly branched thus leading to a more amorphous material (about 50% crystallinity) with a density between 0.912-0.935. HDPE will then have applications in more rigid products like bottles, pipes or industrial containers whereas LDPE is widely used in flexible packaging like films, sheets or bags for example. LDPE is opaque because of it being a mixture of amorphous and crystalline regions but since the spherulites are not isolated but homogeneously dispersed in the structure, the refractive index changes thus resulting in a nearly clear film. Moreover, LLDPE is a copolymer of ethylene with around 10% of another olefin such as 1-butene, 1-pentene or 1-octene thus enabling the final product to have properties between those of LDPE and HDPE. Finally LLDPE is tough, transparent and flexible therefore most applications are found to be films for packaging or cables for example (Carraher, 2013).

EVOH has excellent barrier properties compared to common polymers and is a very good odor and aroma barrier as well. In terms of production, ethylene and vinyl acetate are first copolymerized to produce Ethylene Vinyl Acetate (EVA) and then hydrolyzed through a saponification process to produce EVOH. It can then be processed easily with other polymers on common industrial equipment. The molar percentage of ethylene is crucial since it affects most of EVOH properties (Ketels, 1989).

EVOH oxygen permeability depends on the relative humidity: the barrier drops rapidly above 75% humidity ratio. The other important factor is the amount of ethylene: by decreasing the amount of ethylene (typical value of 27 mol% for a low ethylene content) the oxygen barrier increases but so does the water absorption. With a 47 mol% ethylene, EVOH loses an order of magnitude in barrier properties but the water absorption does not affect significantly the permeability up to 85-90% RH. The oxygen permeability depends on the temperature as well. For a film with 0 to 33%RH, oxygen permeability increases by an order of magnitude at 50°C compared to room temperature (Chomon, 2005). Table 3.1 shows a comparison between selected properties for EVOH and LDPE. As discussed previously, due to its low MFI and good mechanical properties in both machine and transverse direction, LDPE is suitable for film applications and so does EVOH.

Moreover, with a water absorption of 0.01%, LDPE stands as a very good humidity barrier but it has an oxygen permeability with five orders of magnitude higher than EVOH.

Table 3.1: Selected properties of LDPE and EVOH

Property	LDPE[1,2]	EVOH[2]
T_g	-125°C	52-65°C (29 mol% ethylene)
Density	0.91-0.95	1.14-1.21[3]
Melt Flow Index	0.15-4.6 g/10min (2.16 kg, 190°C)	1.3 g/10min (32 mol% ethylene) 5.5 g/10min (44 mol% ethylene) (2.16 kg, 210°C)
Water Absorption	0.01% (24h test, ASTM D570)	6.7-8.6% (24h test, 1/8 inch think specimen, ASTM D570)
Water Vapor Permeability	7.9 g.mm/(m^2.day.atm)[4]	25 g.mm/(m^2.day.atm)
Oxygen Permeability	96-236 cm^3.mm/(m^2.day.atm) (20-25°C)	0.006 cm^3.mm/(m^2.day.atm) (27 mol% ethylene, 23°C, dry)[5]
Young's Modulus	190-430 MPa	350 MPa (6.5% moisture content)
Tensile Stress at Break, value and elongation	10-34 MPa (200-600%) MD* 14-21 MPa (480-800%) TD*	43 MPa (4%) film, 44mol% ethylene 66 MPa (5%) film, 32mol% ethylene

[1] (Carraher, 2013)
[2] (ChemNetBase, 2016)
[3] (Chomon, 2005)
[4] (Rindlav-Westling et al., 1998)
[5] (Mokwena & Tang, 2012)
*MD: Machine Direction ; TD: Transverse Direction

Since EVOH is very sensitive to moisture, multilayer structures with another material preventing water from going in the EVOH layer seems to be a solution for a use in food packaging. Blends of EVOH and LDPE have been investigated as well. In order to bridge the gap in interfacial tension between the two polymers, a compatibilizer is used. Polyethylene grafted maleic anhydride (PE-g-MA) has shown to be an efficient compatibilizer without having effect on the inherent

properties of the blend and the oxygen permeability in particular (Huang et al., 2004; Lee & Kim, 1997). LLDPE/EVOH blends were also investigated. The oxygen barrier showed a percolation threshold of around 50% EVOH in the conventional melt blending on pressed sheets, the permeability droped drastically above this value of nearly three orders of magnitude (Su et al., 2015) Uncompatibilized blends of LLDPE/EVOH (50/50 w/w) were also investigated but through multiplication extrusion. This process separates and recombines the polymer flow through multiplication dies in order to create multilayer films with tens of layers. In this case, co-continuous layered morphology displays the best barrier to both oxygen and water vapor compared to dispersed structures (Zhang et al., 2015).

Finally, EVOH is a convenient oxygen barrier material. However it is a petroleum-based material about five to six times more expensive than LDPE. The development of a bio-based alternative to EVOH would be an asset in the packaging industry.

3.2 Starch chemistry and applications

Starch is a carbohydrate composed of two polysaccharides: amylose and amylopectin. It is found in crops such as potatoes, wheat, maize or rice.

Figure 3.2 presents the chain structure of amylose and amylopectin. Largely linear, amylose displays D-glucose units attached through α- (1,4) bonding. Its typical molecular weight is comprised between 10^4 and 10^6 Da. By contrast, amylopectin has a branched structure. The branching takes place via α- (1,6) bonding. Amylopectin exhibits higher molecular weight than amylose, typically in the 10^6 and 10^7 Da range (Carraher, 2013).

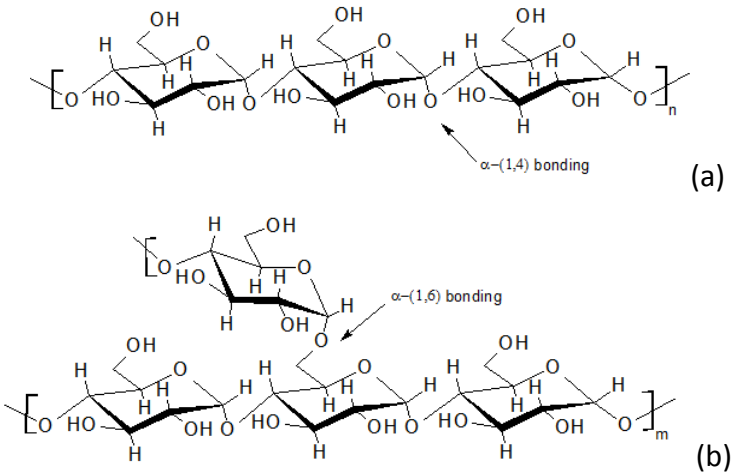

Figure 3.2: Amylose (a) and amylopectin (b) structure

The long chains are able to form helices thus leading to two stable states: single helical structures and double helices, the more hydrophobic side being folded inside the double helices. The regularity of those patterns can be seen via X-ray diffraction (WAXD: Wide Angle X-ray Diffraction) and different types of structures emerge depending on the origin of the starch (Pérez et al., 2009). These structures are useful to analyze the type and evolution of starch (Van Soest et al., 1996b).

The starch crystalline structure can be classified in three classes, A B and C. The A-type is the one found in the starch present in cereals while the B-type originates from tuber crops such as potato and cassava. The C-type, present in legumes, is a mixture of the A and B-types. Figure 3.3 presents a projection of the crystal structure in the A and B-type starches. B-type starch exhibits a hexagonal structure whereas A-type starches are monoclinic (Pérez et al., 2009).

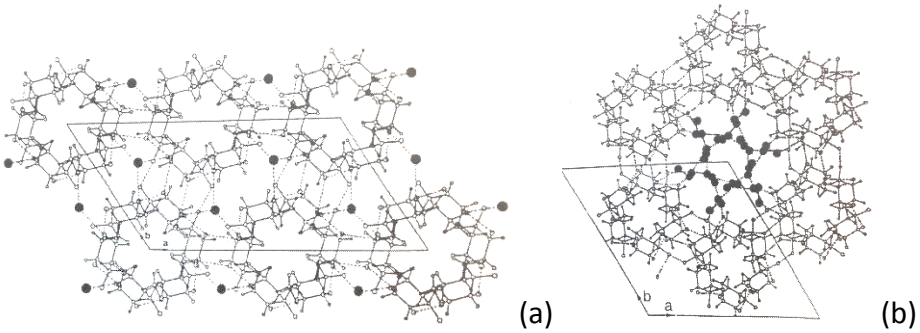

Figure 3.3: Top view of molecular organization of A-type starch (a) and B-type starches (b) (reproduced with permission from Pérez et al., 2009)

When A-type starches have only 4 water molecules that are part of the crystalline unit cell, B-type starches is the most hydrated with 36 water molecules being part of the hexagonal structure. In this case, water molecules are part of the crystalline structure thus meaning they cannot be removed unless by destroying the structure. A-type starches display very compact helices without leaving any space for water molecules in the center whereas B-type starches helices are less compact and their arrangement allows the formation of channels of water molecules inside the hexagonal structure. Half of them are bound to the helix and the other half forms a network through hydrogen bounding. This explains why tubers have higher native moisture content compared to cereals (Pérez et al., 2009).

Figure 3.4 presents the structure of amylopectin at the starch granule level. Amylopectin is responsible for the overall structure of the starch granules. It shows an arborescence with multiple chain length; chains of small branches being organized themselves in double helices thus leading to a crystalline structure.

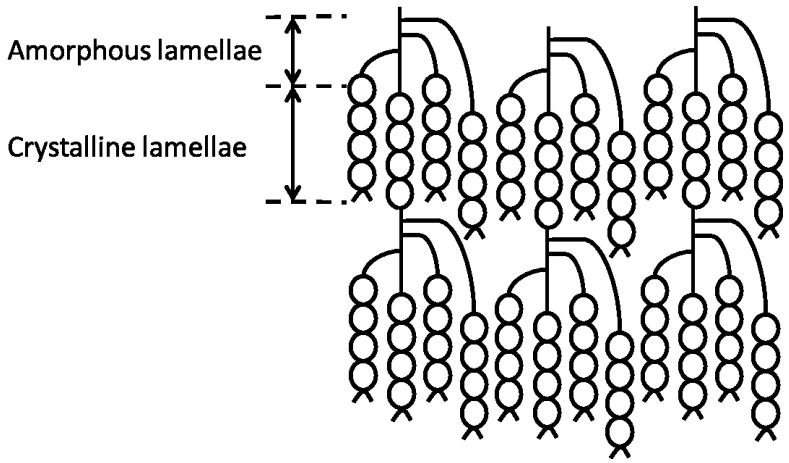

Figure 3.4 : Amylopectin arborescence structure (adapted with permission from Pérez et al., 2009)

The structure of the starch granule has been the subject of numerous studies (Buleon et al., 1998; Tester et al., 2004; Jane, 2009; Pérez et al., 2009). The overall structure is presented in Figure 3.5. The alternating crystalline and amorphous lamellae of amylopectin are arranged into blocklets thus agglomerating into semi crystalline and amorphous shells constituting the whole starch

granule morphology. This organization and the orientation of the crystallites allows observations under polarized light with optical microscopy. Granules show Maltese crosses under those conditions. This positive birefringence generally indicates a radial orientation of the crystallites but in case of starch granules, the pattern remains unchanged on both polar and equatorial sections. This indicates that there are extremely small crystallites with multiple orientations interfering with each other during the observation (Biliaderis, 2009).

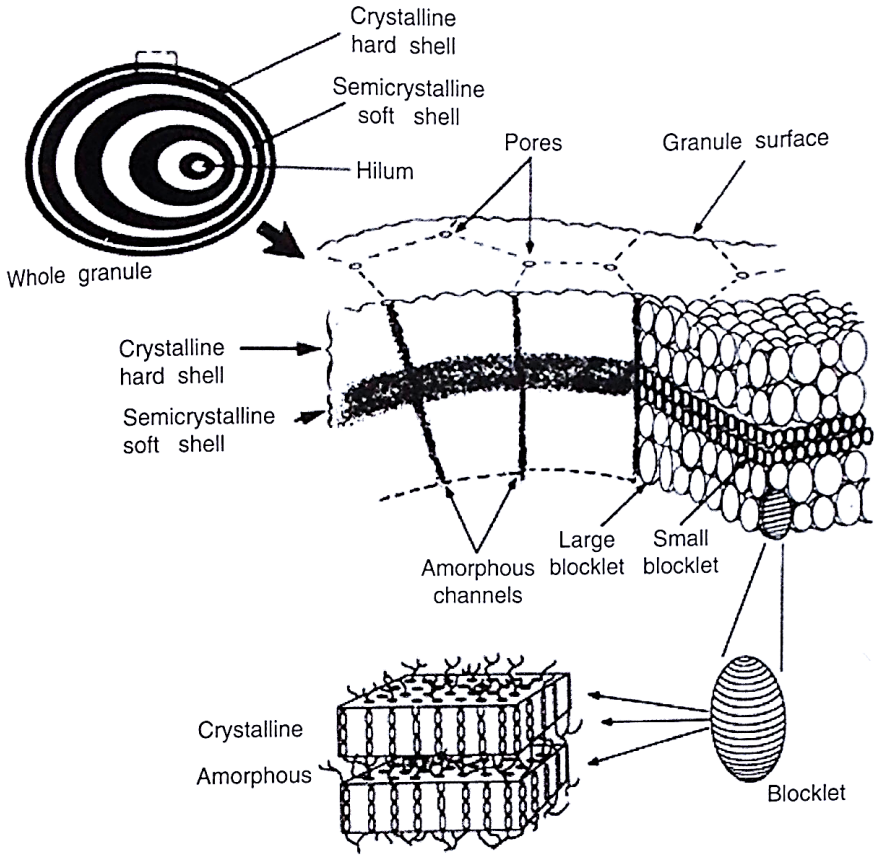

Figure 3.5: Starch granule organization (reproduced with permission from Pérez et al., 2009)

Amylose chains are found between amylopectin groups of helices where they have little opportunity to form double helices but they facilitate the formation of the branches. Since they are not covalently bonded to the amylopectin chains, amylose molecules will leach easily from swollen granules when hydrated at a temperature slightly above the gel temperature (Pérez et

al., 2009). Amylose does usually not contribute to the total crystallinity but partial co-crystallization with amylopectin can occur for example in potato starch (Jane, 2009).

Despite sharing structure and components, starches display some differences thus leading to crucial changes in properties. Table 3.2 shows a comparison with selected properties for four different types of starches. With similar ratios of amylose/amylopectin yet with amylose molecules having different chain length, starches display very different shapes and granule size. This entails great variations at macroscopic scale: for example swelling power, paste clarity or viscosity, which are crucial parameters for film applications, are modified.

Table 3.2: Composition and characteristics of common starches (adapted with permission from Grommers & van der Krogt, 2009)

Characteristics	Potato	Maize (corn)	Wheat	Tapioca
Starch type	B	A	A and B	A
Shape of granules	Oval/ spherical	Round/ polygonal	Round (B type) /lenticular (A type)	Truncated round
Diameter range (µm)	5-100	2-30	0.5-45	4-35
Amylose content (%)	21-25	25-28	30-34 (A type) 25-27 (B type)	17-23
Amylopectin content (%)	75-79	72-75	70-76 (A type) 73-75 (B type)	77-83

It is noteworthy that most natural starches contain around 75% amylopectin but mutants have been developed. Among all mutations (naturally occurring and genetically modified), one of the mostly used contains almost no amylose: it is known as waxy starches. It can be obtained from maize, rice, potato or barley and have applications in food or paper industries (Shannon et al., 2009).

3.3 From starch to Thermoplastic Starch (TPS)

In its raw state, starch is a solid, white and odorless powder. Since starch's crystalline melt temperature is higher than its degradation temperature, dry-starch cannot be melted. It is therefore mostly used as a filler in polymers.

However, when heated in water, native starch granules will lose their semi crystalline structure and go from an ordered to a disordered state. This phenomenon associated with the collapse of molecular order i.e. hydrogen bonds, is called gelatinization. It can be characterized under polarized light through the loss of birefringence. Gelatinization is irreversible and comes with a swelling of the granules and the solubilization of molecules, mainly amylose, thus forming a viscous paste (Avérous, 2004; Biliaderis, 2009).

Gelatinization under quiescent conditions requires excess water in order to be completed: above 63% for waxy maize starch or 65% for wheat starch (Wang et al., 1991). With low moisture content i.e. under 20%, the melting temperature gets close to the degradation temperature (220°C) thus being a problem for any processing. At low water and destructuration, starch can be used only as a filler in opposition with high water and destructuration leading to a gel. Low to medium water content with high destructuring of starch granules leads to plasticized starch, also called thermoplastic starch (Avérous, 2004).

In order to overcome the need for water in semi crystalline destruction and to prevent the dough from being too liquid, another plasticizer can be used to decrease the melt temperature and ease the processing. Generally, a plasticizer is a low molecular weight chemical that is miscible in a polymer and that can reduce its glass transition temperature thus decreasing its melt viscosity in the melt state and its elastic modulus in the glassy state. The effect of a plasticizer on a polymer can be explained through different models. According to the lubricity theory, plasticizers act as internal lubricant and allow polymer chains to slip past one another. Gel model can be applied on amorphous polymers: it assumes that polymers have many intermolecular attractions that are

weakened by the presence of a plasticizer (Carraher, 2013). Table 3.3 displays some properties of common starch gels. It shows that potato starch is the most hydrated with 18% water in comparison to maize and wheat with around 13%. Potato starch is highly viscous compared to other starch types. The higher the amylose content, the lower is the swelling power and the smaller is the gel strength for the same starch concentration. To a certain extent, however, a smaller swelling power due to high amylose content can be counteracted by a larger granule size (Biliaderis, 2009).

Table 3.3: Molecular and physical properties of common starches (adapted with permission from Grommers & van der Krogt, 2009)

Characteristics	Potato	Maize (corn)	Wheat	Tapioca
Amylose content (%)	21-25	25-28	30-34 (A type) 25-27 (B type)	17-23
Moisture content (%)[1]	18-19	12-13	13	n. d.
Pasting temperature (°C)	60-65	75-80	80-85	60-65
Number average DP of amylose	4900	930	1300	2600
Starch paste viscosity	Very high	Medium	Low	High
Paste clarity	Almost clear	Opaque	Cloudy	Quite clear
Paste rate of retrogradation	Medium	High	High	Low

n. d., not determined.
[1] Measured after equilibrium at 65%RH, 20°C (Avérous, 2004)

Plasticization is therefore crucial in forming thermoplastic starch. The most common plasticizer for starch is surely water. However, starch can be plasticized by other molecules especially with higher molecular weight: glycerol, urea or sorbitol for example. For costs and ease of use purposes, glycerol has been widely used in the industry. It improves starch ductility and ability to flow. When blending TPS with LDPE, varying the amount of glycerol will enable the formation of a wide range of morphologies from spherical to co-continuous. In parallel, increasing the amount of plasticizer will increase TPS's ductility (Rodriguez-Gonzalez, Ramsay, & Favis, 2003). Citric acid has also been used as co-plasticizer with glycerol to strengthen the interaction between starch

and plasticizer (Shi et al., 2007). Plasticizers containing amide groups and especially urea have been investigated. The hydrogen bonding ability of urea with starch has shown to be higher than glycerol and retrogradation was limited (Ma & Yu, 2004; Ma et al., 2006; Šoltýs et al., 2019). In blends of TPS with Polylactic Acid, using Sorbitol as a plasticizer for TPS seemed to decrease the interfacial tension in comparison with glycerol thus leading to a finely dispersed morphology (Li & Huneault, 2011).

Gelatinization of starch is different with shear treatment, the last enabling a quicker destructuration of starch granules in excess water and the melting of crystallites with limited water. The advantage of such study is that most polymer are processed using shear treatment. In fact, combining thermal and mechanical treatments can be achieved through regular plastic processing techniques like extrusion. In this case, the loss of crystallinity comes from two mechanisms: water penetration and mechanical disruption of molecular bonds because of the shear within the extruder. The produced thermoplastic starch can then be processed with common thermoplastic processing equipment (Xie et al., 2006).

The processing of starch, however, is much more complex and difficult to control than for most of the conventional polymers. While the processing of most synthetic polymers includes melting, blending/compounding, and shaping, the processing of starch also involves the transformation (granular disruption, crystalline melting, etc.) of starch from a native granular state to a molten state. Therefore, to produce a homogeneous molten state, which is necessary for the processing, a high-energy input is needed. Both granular transformation and macromolecular degradation (especially shear treatment), which are influenced by the processing conditions, can, in turn, impact processibility and product properties (Xie et al., 2012).

The case of potato starch extrusion is even more challenging because of its particularly high viscosity increase during gelatinization. The subsequent processing difficulties are often overcomed by the increase in water content. The high melt viscosity in particular was found to be linked to the high molecular weight of potato starch compared to cereals (Table 3.3). Thermo-

mechanical treatment becomes essential to split the long chains and decrease the molecular weight thus leading to a same melt behavior as cereal starches with similar moisture content. However, achieving this shear treatment requires two to three times higher energy input (Della Valle et al., 1995).

The last phenomenon that has to be taken into account is the retrogradation, or setback, of starch. It is due to the re-association of starch molecules: the chains are going back to the double helices conformation and tends to align in crystallites. This increases the amount of ordered material leading to a decrease in volume and increase in viscosity. Once again, the rate of retrogradation depends on the type of starch (Table 3.3).

The transformation of starch in TPS can be studied easily via WAXD. In order to be sure that the reaction is complete, the destruction of the native crystalline structure, B-type structure in the case of potato starch, can be monitored until a fully amorphous material is obtained. After extrusion, this amorphous materials tends to recrystallize into an unstable structure, V_h or V_a for hydrated or anhydrous starches, which itself tends to come back to the original native structure (Van Soest et al., 1996a; 1996b).

TPS's mechanical properties vary largely upon plasticizer type and amount. Van Soest et al. reported a linear decrease in Young's modulus from 10^3 to 10^1 MPa when increasing the water content from 5 to 20% in water-plasticized potato starch casted films. The tensile stress however decreased exponentially from 30 to around 2 MPa when increasing water content from 5 to 20% (Van Soest et al., 1996). Cyras et al. reported a Young's modulus of around 30 MPa, a tensile stress of 3.3 MPa and an elongation at break of around 63% for pressed films based on potato starch plasticized with water and 30% glycerol (Cyras et al., 2008). Thunwall et al. mentioned a much higher modulus of 500 MPa, a tensile stress of 10 MPa and an elongation at break around 10% for blown films made out of potato starch plasticized with 30 wt% glycerol and 13 wt% water. It is noteworthy that they reported a noticeable difference in values between the flow and perpendicular directions. They attributed this difference to the anisotropy of the film due to the

process and subsequent shrinkage of the film (Thunwall et al., 2008). Dai et al. also reported differences in mechanical properties of films from one botanical source to another. They noticed that potato based films showed the best mechanical properties with the highest tensile strength, Young's modulus and elongation compared to other native starches such as waxy corn, cassava, sweet potato, wheat and corn (Dai et al., 2019). The transparency of starch films varies upon the botanical source. Dai et al. reported potato starch films produced by solution casting to be the most transparent whereas corn starch being the less transparent (Dai et al., 2019).

With regard to oxygen (OP) and water vapor permeability (WVP), thermoplastic starch displays interesting properties. Table 3.4 presents OP and WVP values of different starch types, amylose and amylopectin in comparison with regular LDPE and EVOH. The moisture sensitivity of TPS makes the WVP measurement difficult and very dependent on the testing conditions, the results being globally more than ten times higher for starch compared to LDPE. However, OP is about two orders of magnitude lower for starch compared to LDPE. Consequently, TPS stands as an interesting candidate for barrier material. In comparison with a very high oxygen barrier material such as EVOH, TPS is two orders of magnitude higher in OP.

Table 3.4: Oxygen and water vapor permeability values

Material	Plasticizer type and amount	OP (cm^3.[100]µm.m^{-2}.day^{-1}.atm^{-1})	WVP (g.mm.m^{-2}.day^{-1}.atm^{-1})	References
Pure amylose	Glycerol (40 wt%)	7 (23°C, 50%RH)	10300 (23°C, 50-85%RH)	(Rindlav-Westling et al., 1998)
Pure amylopectin	Glycerol (40 wt%)	14 (23°C, 50%RH)	12400 (23°C, 50-85%RH)	
Rice	Glycerol (30 wt%)	10 ± 1 (23°C, 0%RH)	160 ± 15 (38°C, 90%RH)	(Laohakunjit & Noomhorm, 2004)
Rice	Sorbitol (30 wt%)	16 ± 1 (23°C, 0%RH)	130 ± 30 (38°C, 90%RH)	
Corn	Glycerol (30 wt%)	38.3 ± 2.0 (23°C, 70%RH)	119.0 ± 2.3 (23°C, 85%RH)	(Jost & Stramm, 2016)
Corn	Sorbitol (30 wt%)	1.5 ± 0.4 (23°C, 70%RH)	39 ± 4.0 (23°C, 85%RH)	
LDPE	n.a.	1900	7.9	(Rindlav-Westling et al., 1998; Mokwena & Tang, 2012)
EVOH	n.a.	0.06 (23°C, 0%RH)	25	

It is noteworthy that oxygen permeability of starch depends drastically upon the humidity and therefore stable properties would only be achieved in controlled moisture conditions.

3.4 Blending TPS and LDPE

Blending immiscible polymers can lead to various morphology types such as matrix-dispersed particles, matrix-fiber structures, lamellar structures or co-continuous structures. The latter is a transition state particular to polymers close to phase inversion in which one cannot distinguish the matrix from the dispersed phase. This means that at least two fully continuous structures exist within the same volume (Pötschke & Paul, 2003). The range of composition in which co-continuity happens was found to be depending on numerous parameters such as interfacial tension or the viscosity ratio between the phases (Fortelný, 2005).

Blending TPS and LDPE is challenging due to their immiscibility and high interfacial tension. Different methods for blending TPS and polyethylene have been reported. One of the first process was developed by St-Pierre et al. Starch and plasticizer were mixed together in a mixer until starch granules were completely swollen. This slurry was then added through a single-screw extruder to a main twin-screw extruder where the LDPE was added. TPS and LDPE were then blended together in the second half of the twin-screw extruder. The blend showed matrix-droplets morphology for blends up to 36 wt% wheat-based TPS in LDPE. When increasing the TPS content up to 53 wt%, the blend displayed fiber-like structures due to an increased coalescence (St-Pierre et al., 1997). Another version of the previous process was later proposed by Rodriguez-Gonzalez et al. Alternatively, the starch slurry was here introduced in the primary feed hopper while LDPE was added in molten state at mid-extruder through a side single-screw extruder. In that case, phase inversion was found to occur in the range 45-50 wt% TPS. Elongation at break and maximum tensile strength of the blend were lower than those of pure LDPE. However, they reported a slightly higher Young's modulus for TPS concentration above 40 wt% (Rodriguez-Gonzalez, Ramsay, et al., 2003). Later work by the same research group showed that increasing the plasticizer level in TPS increased the deformability of the TPS phase when subjected to stretching (Rodriguez-Gonzalez, Virgilio et al., 2003). Finally, a very coarse blend morphology was observed with symmetric blends of TPS and LDPE yet with a high level of interconnexion (Li et al., 2011).

The high gap in polarity between LDPE and TPS lead to a very high interfacial tension in the blend of 16.4 $mJ.m^{-2}$ (Schwach & Avérous, 2004). In order to stabilize blend morphology, prevent coalescence and reduce the interfacial tension, a compatibilizer can be used. For LDPE and TPS, they are mostly olefinic compounds with reactive moieties that can react with starch macromolecules to form in situ a polymeric emulsifier. Various compatibilizers for starch/PE have been investigated such as ethylene-co-acrylic acid copolymer (EAA) (Otey et al., 1980; Willett, 1994) or ethylene-vinyl alcohol (EVA) (Bikiaris, Theologidis, & Panayiotou, 1998). Later work suggested a simpler and cheaper way by using polyethylene grafted maleic anhydride (PE-g-MA) either by in situ reactive extrusion (Wang et al., 2005) or adding as a separate component

(Chandra & Rustgi, 1997; Gupta et al., 2008; Huneault & Li, 2012). In this case, the compatibility is enhanced over the esterification reaction between maleic anhydride groups and starch as well as interactions between the long PE chains. Using 10% PE-g-MA was found to be sufficient to assure a good emulsification, a ten times decrease in TPS phase size was observed (Huneault & Li, 2012). With blend composition up to 30 wt% corn-based TPS, the use of PE-g-MA led to a finer and more uniform dispersion of the starch phase (Bikiaris & Panayiotou, 1998; Huneault & Li, 2012). Dispersed TPS drops were also observed in blends of 60 wt% wheat TPS in polyethylene whereas co-continuity was achieved around 75 wt% TPS (Mortazavi et al., 2013, 2014).

It is noteworthy that chemical modification of starch has been investigated in order to increase its compatibility with apolar polymers. For example, stearic acid-grafted starch (ST-SA) have been investigated by Khanoonkon et al. In this study, starch and stearic acid react in DMSO prior to the extrusion with up to 40 wt% plasticized starch in LLDPE. The processability of the blend was slightly enhanced with the ST-SA and interfacial adhesion was improved with only 1% compatibilizer (Khanoonkon et al., 2016b). About barrier properties, adding ST-SA decreased slightly water vapor permeability compared to the uncompatibilized blend but increase significantly oxygen permeability, the blend being more permeable than pure LLDPE (Khanoonkon et al., 2016a).

The first works on blending TPS and LDPE by Rodriguez-Gonzalez et al. Detailed previously were carried out using high water content (up to a 3:2 water:glycerol ratio) to ease the gelatinization in the first part of the extruder. The water was then removed under vacuum before the introduction of LDPE (Rodriguez-Gonzalez, Ramsay, et al., 2003; Rodriguez-Gonzalez, Virgilio, et al., 2003). Later work by Huneault and Li proposed a simpler variation of the previous method where starch was fed in dry form instead of a slurry and where the second polymer was fed in solid form rather than in melt form at mid-extruder. The water content was also drastically reduced. A mix consisting of one part water for nine parts glycerol was found to be efficient enough to plasticize the starch and much less energy consuming. Their process and twin screw configuration are described in Figure 3.6. The starch powder is fed in the first zone of the extruder

before the plasticizer mix is pumped. Starch and plasticizer are then subjected to heat and shear in zones 2 and 3 where the gelatinization of starch happens. The excess water is evacuated in zones 4 and 5 with a vaccum pump or simply by letting the extruder open. A gravimetric feeder introduces the LDPE/compatibilizer pellets in zone 7. The last part of the extruder aims at mixing both polymer and TPS. They reported very similar Young's modulus (around 1 GPa) and tensile strength (around 18 MPa) between pure PE and the blend with 25 wt% TPS. The elongation at break was however drastically reduced from over 800% for PE to 133% for the blend (Huneault & Li, 2012).

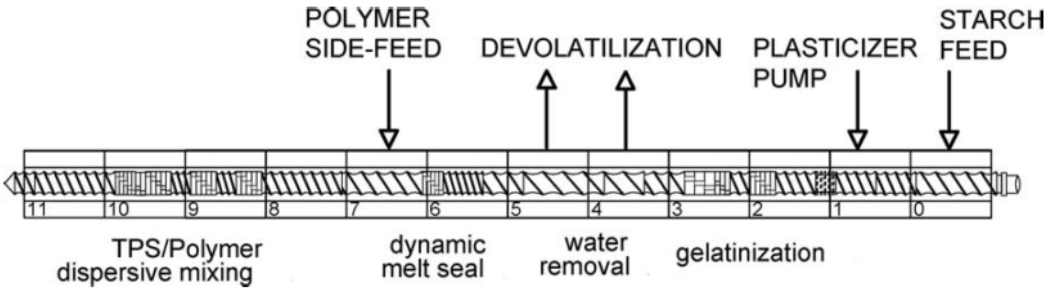

Figure 3.6: Process configuration of the twin screw extruder for LDPE/starch blends (reproduced with permision from Huneault & Li, 2012)

Earlier work have shown the crucial impact of material rheology over morphology development. The viscosity of the material would determine the blend morphology and give indications on the range of composition in which phase inversion can be expected (Avgeropoulos et al., 1976; Paul & Barlow, 1980). Rheology of starch materials, however, is not straightforward. For most TPS, the viscosity shows a power-law behavior without Newtonian plateau. Moreover, empiric models have shown that consistency and power law index depend on many inherent and experimental factors such as botanical source, processing (Singh et al., 2003), testing conditions as well as plasticizer type and content (Liu et al., 2009; Xie et al., 2012). The most common way to study starch rheology is capillary rheometry. This method allows the measurement of viscosity over a wide range of shear rate and limits the evaporation of plasticizer compared to rotational rheometers (Xie et al., 2012). Potato starch in particular was found to have a very high melt viscosity compared to other starch types thus making its process difficult. Equation (3.1) gives the

expression of the power law model with the viscosity η (in Pa.s), the shear rate $\dot{\gamma}$ (in s^{-1}), the consistency K (in $Pa.s^n$) and the power law index n. Della Valle et al. expressed K and n as a function of temperature T, moisture content MC and specific mechanic energy SME. The expression of the consistency is detailed in Equation (3.2) and the one of the power law index in Equation (3.3). The consistency showed an Arrhenius type relation and took into account the activation energy E and R the ideal gas law constant.

$$\eta = K\dot{\gamma}^{n-1} \tag{3.1}$$

$$K = K_0 \exp\left(\frac{E}{RT} - \alpha * MC - \beta * SME\right) \tag{3.2}$$

$$n = n_0 + \alpha_1 T + \alpha_2 MC + \alpha_3 SME + \alpha_{12} T * MC + \alpha_{13} T * SME + \alpha_{23} MC * SME \tag{3.3}$$

The results from Della Valle et al. showed that the consistency of potato starch was more dependent on the moisture content than the SME. Moisture content was also reported to have the biggest effect on the power law index. This aspect highlights the importance of the plasticizer in the variation of TPS's rheology. This model is however limited to water as plasticizer (Della Valle et al., 1995). Similar model have been investigated for different starch types yet with a high variability (Martin et al., 2003; Sandoval & Barreiro, 2007; Tajuddin et al., 2011).

Blend morphology will have a crucial impact over the final product's properties. Previous work by Rodriguez-Gonzalez et al. showed that various morphologies could be achieved with TPS/PE blends: spherical, fibrillar and co-continuous (Rodriguez-Gonzalez, Ramsay, et al., 2003). Huneault and Li reported droplets of TPS in LDPE for compatibilized blends with up to 25 wt% TPS (Huneault & Li, 2012). By contrast, Mortazavi and al. investigated high TPS concentration range and showed that it was possible to achieve co-continuous morphology at 75 wt% TPS. The phase inversion range was found to be slightly above 75 wt% TPS in blends with LDPE compatibilized with 5 wt% PE-g-MA (Mortazavi et al., 2013). Above this limit, TPS becomes the matrix thus resulting in poor mechanical properties and high sensitivity to moisture (Schwach & Avérous, 2004).

3.5 Processing multilayer films

Starch-based and blends with starch have been used to make films through different processing techniques. The most common are compression molding, cast film and blown film.

The easiest procedure to process films out of starch uses a two-step process in which starch and its plasticizer are mixed together until complete swelling of starch granules and then this slurry is being pressed as a thin sheet. Compression molding is a cheap and easy to use procedure but it is not a continuous process and it is mainly limited to laboratory scale experiments. Another procedure uses an extruder where the mixing and heating of starch and its plasticizer happens with other compounds in the case of a blend. The end of the extruder consist of a slit die where the casted film comes out. In this process the film is often wound into rolls and cooled down. The film casting process cannot handle high productivity since it involves long drying time.

Extrusion blown film process is a continuous and widely used technique in the film industry. It consists of an extruder just like cast film where the material is molten and subjected to shear. The die geometry is however different. Blown film process uses an annular die with air coming out of its center in order to blow up the polymer melt into a large bubble of film. At a steady state, this bubble will evolve into a tube that is cooled continually. Finally, it goes through nip rolls where it is flattened to create a flat tube collected by rollers (Lee et al., 2008). Blown film technology allows the production of multilayer structures but it requires a more complex and expensive equipment. Most of the time, an extruder is needed per layer. All the flow is then assembled through different concentric dies into the same bubble.

Some parameters are important to control in order to have the expected film properties and these parameters are to be adapted to each materials (Cantor, 2011). For example: polymer flow rate, gas flow rate, size and shape of the bubble during processing, rolls gap, cooling of the bubble before and after the rolls. Such procedure has to be optimized for a specific material and can be set up knowing some properties of the polymer such as viscosity or melt strength. In order to

characterize properly and control the bubble-forming process, characteristic bubble ratios have been developed, namely the Take-Up Ratio (TUR), the Blow-Up Ratio (BUR) and the Forming ratio (FR). The TUR is defined as the ratio between the film velocity and the melt velocity and gives an indication of the amount of stretching in the Machine Direction (MD). TUR can be expressed as follow in Equation (3.4):

$$TUR = V_{film}/V_{melt} = (\rho A)_{die\ gap}/(\rho A)_{nip\ rollers} \quad (3.4)$$

In this case, the formula takes into account melt and solid densities ρ for the die and rollers respectively. The parameters A and V correspond to the annular area and velocity respectively. The BUR is the ratio between Bubble diameter and die diameter thus giving an indication of the amount of stretching in the Transverse Direction (TD). Lastly, the FR is the ratio between TUR and BUR thus assessing the balance of stretching between machine and transverse direction (Cantor, 2011).

Controlling immiscible polymer blends morphology development is crucial in blown film extrusion. The stretching of the process would deform the dispersed domains depending on material parameters such as initial domain size, viscosity ratio, minor component percentage or interfacial tension but also processing parameters such as the draw ratio of the blown film line.

Although blown film extrusion is a major converting process for manufacturing flexible films and bags from polyethylene, there are few articles in the literature relevant to the blown film extrusion of its blend with thermoplastic starch. Early work on producing films out of TPS/LDPE reported the mixing of water-plasticized starch with LDPE and ethylene co-acrylic acid prior to blown film extrusion (Otey et al., 1980). The process was carried out at laboratory scale equipment for formulations up to 40% starch and lead to poor transparency and mechanical properties at high starch content. Arvanitoyannis et al. have compression-molded LDPE/TPS blends into films. The TPS was plasticized with up to 20 wt% water and was used at concentrations up to 40%. The lack of continuity in the TPS phase at this concentration lead to high oxygen

permeability, higher than that of pure LDPE, as well as an increased water permeability (Arvanitoyannis et al., 1998). As detailed in the previous sections, one way to limit the water sorption and protect the hydrophilic oxygen barrier material is to use multilayer systems. For example, Dole et al. produced 5-layer films by a laboratory-scale combination of solution casting and compression molding. Continuous LDPE outer layers would protect the TPS. They reported the conservation of starch's oxygen barrier performances at high humidity ratio when using a 5-layer film (LDPE/PE-g-MA/TPS/PE-g-MA/LDPE) where PE-g-MA was the tie layer (Dole et al., 2004). These results showed the potential of a multilayer approach for improving oxygen barrier properties and prompted the need for the development of a continuous process for the production of such films.

Sabetzadeh et al. proposed a 3-step process to produce LLDPE/LDPE/TPS films. First they would produce TPS by melt-mixing starch and plasticizer in a internal mixer. The TPS was then blended with a mix of LLDPE/LDPE containing 3wt% PE-g-MA as compatibilizer in a twin-screw extruder. The blend was pelletized and fed to a blow film extrusion line. Sabetzadeh et al. reported the successful production of 45 µm thick films with up to 20 wt% TPS. They also mentionned a decrease of about half the tensile strength and elongation at break at the highest starch loading as well as a decrease in transparency. Finally they mentioned that the requiered mechanical properties for packaging applications can be obtained by using up to 15 wt% TPS (Sabetzadeh et al., 2015).

The production of multilayer films made out of TPS and LDPE showed interesting perspectives in terms of barrier properties yet the processing of such film was reported to be very challenging, especially at high TPS loading(Sabetzadeh et al., 2015). Another solution was needed to further improve barrier properties while keeping most of the mechanical properties in order to fulfil the requirements for packaging film applications (ASTM standard D4635).

3.6 Use of minerals in TPS/LDPE blends

Minerals such as clay or talc have been widely used in polymer science in order to enhance mechanical properties, thermal stability (especially for flame retardant applications) and gas barrier properties. Since minerals are essentially made out of inorganic crystals, they are impermeable to gases thus being an asset in creating barrier materials. The introduction of minerals in a matrix decreases the gas transmission rate by increasing the path length that gas molecules need to follow to go across the film. In this case, the particles create a tortuous path for the gas molecules in the matrix. This effect is however highly dependent on particle parameters such as size and aspect ratio.

For example, talc has been used in polymer blends because of its low cost, availability and its plate form has shown interesting properties with regard to barrier performance. In the example of blends of Polylactic acid (PLA) and Polytrimethylene carbonate, adding 3% talc reduced of around 50% the oxygen permeability of the films (Qin et al., 2014).

Clays are natural inorganic particles. They consist of layered Silicates of Aluminum, Magnesium or Iron. Clay minerals can be seen as a stack of silicon and metal oxides (Silica tetrahedrons SiO_4 and Alumina octahedrons AlO_6). Figure 3.7 illustrates the layered structure of the clay. The arrangement of the atoms creates a layered structure of each type of atom. This pattern is then repeated, creating layers linked to each other by hydrogen bounding. The distance between the sheets varies upon the type of atom or molecule that is in-between. The interlayer spacing can be measured with X-ray diffraction (Giannelis et al., 1999). Native clays have sodium ions in between layers. In the example of Montmorillonite (noted MMT), bonds between the sheets are relatively weak so various cations and water molecules are able to go in between those sheets. This aspect enables various modifications that can be tailored to reach a specific application. For example, Wang et al. reported substituting sodium cations with dioctadecyl dimethyl ammonium in MMT which allowed an increase of 0.5 nm in spacing between the clay platelets (Wang et al., 2018).

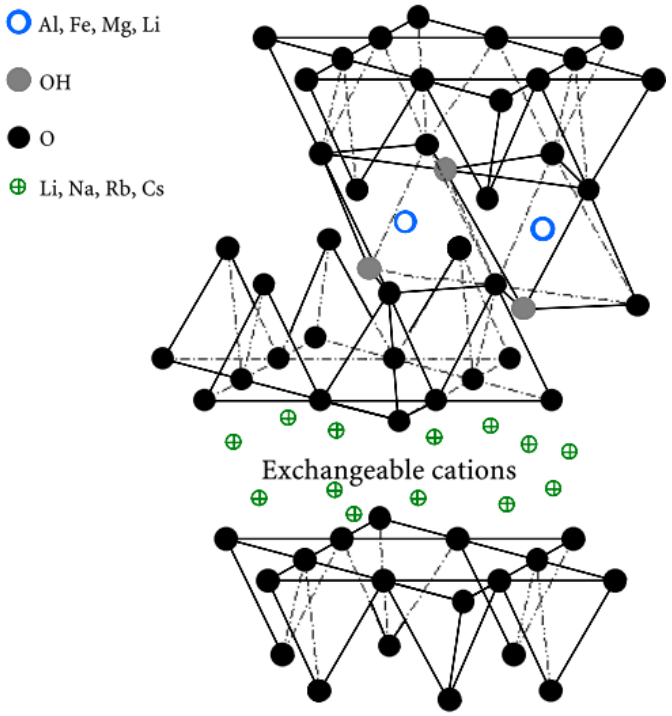

Figure 3.7: Structure of layered silicate such as clay with exchangeable cations in between the layers (reproduced with permision from Giannelis et al., 1999)

Clays are negatively charged and that is the reason why there are many cations between the layers. However, because of the weakness of the bonds and the space between the sheets, the cation exchange capacity is important. Inserting a new cation in the structure allows new properties for the material: for example, bigger cations will increase the size of the agglomerate and decrease the density (swelling) at the macroscopic scale. Moreover, changing cation for a bigger molecule like a quaternary ammonium will increase significantly the spacing. This type of modification is a widely used method to increase the spacing between the clay platelets (Giannelis et al., 1999).

Montmorillonite has a high ability to expand (Wang et al., 2018). The stronger force between the sheets of the kaolinite results in almost no free space between kaolinite sheets. Moreover, clays are highly anisotropic particles. For example, Montmorillonite forms very thin plates whereas Palygorskite shows a needle-like structure. The choice of a specific type of clay will therefore be crucial depending on the final application. In films for example, exfoliated clay platelets with high

surface area and aspect ratio like Montmorillonite can create a tortuous path in the polymer matrix thus reducing the diffusion of gases through the film (Tabatabaei & Ajji, 2011).

Due to their high potential in improving gas barrier properties, this study will focus on Montmorillonite. The clay platelets can be found in various configurations in a polymer matrix depending on their level of exfoliation. Figure 3.8 shows the possible configurations namely agglomerates, intercalated and exfoliated. If the layers are strongly bonded, the platelets stay in agglomerates in the matrix. However, if the intercalation of polymer chains is possible, it becomes possible to increase the spacing between the plates, there is intercalation. If the expansion of the platelets comes to a certain point where there is no more interaction between the platelets then it is complete exfoliation.

The evolution of layer intercalation of silicates can be studied with X-ray diffraction. The spacing between the plates can be found through Bragg's law and a diffraction peak can be noticed. Complete exfoliation would lead to the loss of the peak. In terms of material property, a matrix containing completely exfoliated particles with high aspect ratio and surface area like MMTs would decrease significantly the gas permeability when oriented perpendicularly to the gas flow. For example, Yano et al. reported a decrease of half the permeability of polyimide with the addition of 2 wt% MMT, due to the increase in tortuosity (Yano et al., 1997).

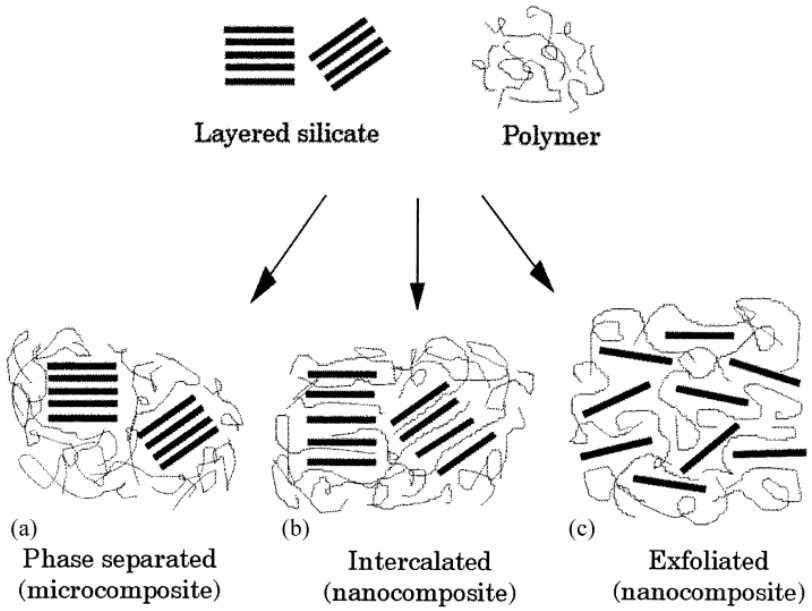

Figure 3.8: Scheme of different types of silicate/polymer composites (reproduced with permision from Alexandre & Dubois, 2000)

Complete exfoliation of clay particles is however not straightforward. In a first step, clay counter ions need to be replaced by organic cations, such as quaternary amines, to form organoclays. The organo-compound is then intercalated between the clay layers. The organoclay needs to be well dispersed and exfoliated during the polymer melt procedure. An important feature here is that the organoclay and polymer should have a good affinity to each other (Xie et al., 2013).

Using highly orienting production technique such as blown film extrusion on a matrix containing exfoliated clay can be an asset in reducing gas permeability. The high stretching that the film undergo during its process should align the clay parallel to the surface of the film.

Using clays in TPS or TPS blends with another polymer has been investigated in the past decades from working on the effect of different types of modified clay (Chiou et al., 2005; Xie et al., 2013) or various plasticizer on the exfoliation (Chivrac et al., 2010). The addition of modifiers to increase the spacing between the platelets being most of the time made out of long apolar chains would increase the interfacial energy with the polar starch molecules. Moreover, plasticizers like urea,

sorbitol or formamide would improve TPS properties yet with no significant improvement on clay exfoliation (Chivrac et al., 2009; Chivrac et al., 2010).

Natural clays being accepted by food compliance regulation, they have been used in films for food packaging application. Complete exfoliation of natural MMT was not achieved with glycerol plasticized starch but intercalated structures were underlined. Concerning the evolution of the blend properties, adding natural MMT was shown to decrease slightly moisture absorption thanks to the tortuous path created by the layered MMT in the TPS matrix (Cyras et al., 2008). An enhancement of about 20% in Young's modulus with 4% clay was reported since the clay can act as reinforcement in the matrix (Avella et al., 2005).

One of the best way to completely exfoliate clay particles is to solubilize them in water. In order to improve clay dispersion in standard polymers, water-assisted melt compounding has been investigated. By injecting clay slurry in the high pressure zone of the extruder and vacuum the steam produced, a higher exfoliation rate was obtained with different polymers. Since starch needs to be plasticized in the process for the gelatinization to happen, the water already present in the blend should help the exfoliation as well (Karger-Kocsis et al., 2014). Usually water is evaporated in the extrusion process except for the plasticizer that remains in the TPS. Mixing pre-plasticized starch with a solution of clays in water prior to melt mixing has yield to a high fraction of exfoliated materials as well (Ayana et al., 2014).

In compatibilized blends of TPS and LDPE, complete exfoliation of the clay particles was reported difficult to achieve. Sabetzadeh et al. reported an increase of about twice the spacing of the clay yet with a small fraction of exfoliated particles. Moreover, they reported a 30% increase in ultimate tensile strength with 5% modified MMT and variations of the film's transparency (Sabetzadeh et al., 2016).

CHAPTER 4 METHODOLOGY

4.1 Material selection

Potato starch from Emsland group (Germany) was selected as the reference starch. As a comparison, a less viscous type of starch was used as well: industrial corn starch supplied by Ingredion (Canada). Native potato and corn starch exhibited initial water content of 16 and 9 wt% respectively. The amount and type of plasticizer are crucial in the production of TPS. For their ability to plasticize starch at a low-cost, water and glycerol have been selected. A 99.5% pure grade glycerol was supplied by Mat Laboratories (Canada).

Four different grades of LDPE were selected, all supplied by SABIC (the Netherlands). Their melt flow index (MFI) varied from about 1 to 8 as described in Table 4.1. LDPEs with a MFI up to 2.5 are suitable for blown film applications. Higher MFIs were used to match TPS's viscosity and investigate the effect of a more liquid LDPE on the blend morphology. Moreover, a random terpolymer of ethylene, acrylic ester and maleic anhydride, namely Lotader 3410 supplied by Arkema (France), was used as compatibilizer for the TPS/LDPE blends.

Table 4.1: MFIs of the selected LDPEs

Sample ID	Supplier reference	MFI (g/10 min measured at 190°C)
PE1	2101TN	0.85
PE2	2102N0W	2.5
PE4	2404TN	4.2
PE8	2008TN	7.5

In the second part of this thesis, the effect of clays on film processing and barrier properties was investigated. Two different types of Montmorillonite clay were used. Natural clay was Cloisite Na whereas organically modified clay was Cloisite 15A, both supplied by Byk (Germany).

4.2 Blend preparation

All blends are prepared by twin-screw extrusion. The LDPE used in the blend was PE1 for all experiments. Two different processes are being used.

The first process used a Leistriz 18 mm co-rotating Twin-Screw Extruder (TSE) with L/D=40 operated at a screw rotation speed of 150 rpm. The screw configuration is presented in Chapter 5 in Figure 5.1. Starch powder and plasticizer were mixed manually for the first step and let to stand for 24 hours enabling complete absorption of the plasticizer in the granular starch. The starch slurry was then introduced in zone 1 of the extruder and starch gelatinization was carried out in barrel section 1-3 by subjecting the mixture to intensive mixing at 130°C using kneading elements. The starch was assumed to be fully gelatinized at the end of barrel section 3. The LDPE and the compatibilizer were dry-blended and then introduced in the extruder in barrel section 4 using a side feeder. The TPS and LDPE were melt blended in the second half of the process mainly using two sets of kneading elements placed in barrel section 5 and 7. Temperature was set to 160°C in section 4-8. It is noteworthy that since section 4 was open to atmospheric pressure, excess water was able to devolatilize through the side-feeder.

For selected experiments, pure TPS was produced through the same process but using lower temperature of 130°C in section 4-6 and around 100°C in section 7-8 to prevent bubble formation at die exit. The first process was used to conduct the experiments detailed in Chapter 5.

For the second process, the TPS/PE blends were prepared in one step on a co-rotating 34 mm Leistritz Twin-Screw Extruder (TSE) with L/D=42 using a screw rotation speed of 160 RPM. Process and detailed screw configuration are presented in Chapter 6 in the Figure 6.1. The main difference with the first process is that in this case the starch was introduced directly as a powder in the extruder in the hopper in zone 0. In specific formulations containing clays, the clay powder was dry-mixed with the starch and introduced in zone 0 as well. The glycerol used as plasticizer for the starch was pumped into the extruder in zone 1. All blends were plasticized with 35 wt% glycerol

with regards to the starch. In order to ease the processing, an extra 10% water was pumped with the glycerol. Starch and plasticizer were then subjected to intensive mixing in zones 2-3 using kneading elements, leading to starch gelatinization. Complete gelatinization was assumed at the end of zone 3 where the extruder was left open for water devolatilization. The addition of 10% water was done in order to help the starch gelatinization but did not increase the total plasticizer content since it was removed through devolatilization in zones 4 and 5. A dry blend of LDPE and compatibilizer was introduced through a side feeder in zone 6 and blended with the TPS in zones 7-8 using kneading elements. At the end of the extruder, the produced strands of TPS/LDPE were cooled down in air and stored in closed PE bags.

The temperature of the extruder was kept at 80°C in the two first zones for the introduction of the starch and the plasticizer. It was increased to 140°C in zones 2-5 for the gelatinization and devolatilization steps. The second half of the extruder, starting in zone 6, was kept at 160°C. This temperature was selected because it was high enough to enable LDPE melting but low enough to minimize starch thermal degradation.

4.3 Multilayer Film extrusion

The film preparation was performed on a multilayer Lab Tech blown film extrusion line using two 20mm single-screw extruders in an ABA configuration. The extruders had a L/D=30 and were used to feed the material into a co-extrusion die with a 50 mm outer diameter and a gap of 1.5 mm. The present work aimed at producing symmetric 3-layer films consisting of a TPS/PE blend as inner layer between two identical pure LDPE outer layers. The operating temperature of the extruder feeding the TPS/PE blend was set to 145°C in the feeding zone and increased gradually to 165°C at the end of the extruder. The LDPE outer layers were extruded at 210°C. The two extruders were set at 80 RPM for an expected thickness ratio between the layers of 1:2:1. Figure 4.1 shows a photo of the blowing of the 3-layer film. All blends used to prepare films were produced with the one-step blending process described in the previous section.

Figure 4.1: Example of film blowing of the 3-layer system

The aim was to produce 50 µm thick films. Two different processing strategies were used to produce the films. For films without clay, the aim was to produce films with a thickness as close as possible to the 50 µm regardless of the stretching ratio. The films containing the higher TPS content (in the inner layer) exhibited bubble stability issues and were particularly difficult to produce. To facilitate processing, 5 wt% water was added to the blends containing 70 and 80 wt% TPS, before film blowing. This improved film strechability as water acts as an additional plasticizer during processing. The continuous LDPE outer layers were made out of LDPE with a MFI of 4. As the TPS content increased, the maximum blow up ratio decreased. Therefore, to achieve the thinnest possible films, the forming ratio was progressively decreased from 11 to 4 when increasing TPS content from 50 to 80 wt%.

For films containing clay, the second processing strategy was used. In this approach, the forming ratio was kept constant and equal to 3. The continuous LDPE outer layers were made out of LDPE with a MFI of 2.5. After film blowing, produced samples were stored in closed PE bags until further testing.

4.4 Characterization techniques

4.4.1 X-ray diffraction

In order to monitor the transformation of starch into TPS as well as the level of exfoliation of clay particles, Wide Angle X-ray Diffraction (WAXD) was used. It was carried out directly on pure TPS extrudates one day after extrusion in order to assess gelatinization or on blends containing clay. The samples of approximately 1 mm^3 were glued with silicon on a goniometer head and mounted at room temperature on a Bruker APEX DUO X-Ray diffractometer. These runs were then treated and integrated with the XRW2 Eval Bruker software to produce WAXD diffraction pattern from 3.5 to 40 degrees 2θ and 3.5 to 15 degrees 2θ in the case of pure TPS and samples with clay respectively. The pattern was then treated with Diffrac Eva (v 2.0) software from Bruker.

In order to investigate the orientation of the clay particles in the film, two dimensions Small Angle X-ray Diffraction (2D-SAXS) was performed. SAXS images on films were collected with a Bruker AXS Nanostar system equipped with a Microfocus Copper Anode at 45 kV / 0.65 mA, MONTAL OPTICS and a VANTEC 2000 2D detector. The detector to sample distance was calibrated with a Silver Behenate standard at 28.20 cm. The films were positioned vertically on the sample holder with the X-ray beam hitting the cross-section of the film. Since the films were very thin compared to the beam size, four films were stacked to each other to increase the signal. All SAXS measurements are from 0.5 to 10.5 degrees 2θ. In order to see preferential orientation, an azimuthal integration around the expected peak was calculated for γ=0 to 360°.

4.4.2 Moisture content

The TPS moisture content was measured on a Mettler Toledo V20 volumetric Karl Fisher titrator using an oven temperature of 180°C. Samples were heated for 1000 s to extract humidity, then nitrogen carried the water to the titrator until measurement was complete. Prior to testing, extruded samples were placed in closed polyethylene bags to maintain their humidity level.

4.4.3 Viscosity measurements

Capillary rheometry was carried out using an Instron CEAST SR20 rheometer. A 1 mm capillary die with a die length of 40 mm was used. The shear rate was varied from 10 s^{-1} to 10000 s^{-1}. TPS/LDPE blends were characterized at a temperature of 160°C. To minimize degradation, measurement temperature for pure TPS was set to 130°C. Rabinovitch corrections were applied to correct the results for non-Newtonian effects. Since the L/D ratio of the die was 40, the entry and exit effects (Bagley correction) were neglected.

In order to assess the effect of the humidity level and the rheological response of the materials, selected TPS samples were conditioned for three weeks at room temperature. The residual humidity in TPS samples after extrusion was around 10 wt%. For low humidity levels, samples were placed in a closed container with desiccant (Dierite $CaSO_4$ from Anachemia, VWR) while for high humidity level, the samples were subjected to saturated humidity. Final moisture content of 5 and 25 wt% were attained respectively.

4.4.4 Scanning Electron Microscopy (SEM)

The blend morphology was assessed using a Scanning Electron Microscopy (Hitachi S-3000 N) in secondary electron mode. Observations were made on extruded strands that were microtomed under liquid nitrogen using a glass knife. Film samples first needed to be casted in epoxy before microtoming. In order to ensure proper characterization, all cuts were done perpendicularly to the film's surface and the morphology in both machine (MD) and transverse (TD) directions were displayed. The samples were then subjected to HCl 6N for 3 hr to selectively remove the TPS

phase, thus improving the contrast for imaging. Samples were sputtered with gold-palladium coating prior to SEM observation.

For blends where the TPS was the matrix or blends close to phase inversion, the acid-etching technique described above could not be used. In these cases, observations were made using a S-4700 FEG SEM from Hitachi in secondary electron mode because of its higher sensitivity compared to the previous microscope.

To determine average diameters, image analysis was performed using Sigma Scan Pro 5 software from Systat. For every sample, more than 300 diameter measurements were made from which the volume and number average diameters, namely d_v and d_n, were calculated using the formula reminded in Equation (4.1). The factor n_i represent the number of occurrences for the diameter d_i.

$$d_n = \frac{\sum_{i=1}^{n} n_i d_i}{\sum_{i=1}^{n} n_i};\ \ d_v = \frac{\sum_{i=1}^{n} n_i d_i^4}{\sum_{i=1}^{n} n_i d_i^3} \tag{4.1}$$

Equivalent diameters based on surface area of the measured domains were used to calculate the averages. The dispersity defined by the ratio d_v/d_n was calculated for selected samples.

4.4.5 Continuity analysis

The extent of continuity of the TPS phase was calculated using a gravimetric method. Four to six segments of extruded strands with a length of around 1 cm were immersed in HCl, 6N, and stirred for 24 h. Weight loss measurements were then carried out on dried samples in order to determine the percentage of continuity using Equation (4.2):

$$\%continuity = \left(\frac{W_{initial} - W_{final}}{W_{initial}}\right) * 100 \tag{4.2}$$

4.4.6 Mechanical properties

Mechanical testing on films were performed according to ASTM D882 on an Instron Electropuls E3000 for the determination of Young's modulus and on an Instron 3365 for the other mechanical properties. The sensitivity of the first equipment was adapted to the measurement of the Young's modulus whereas the second equipment was ideal for the measurement of large elongations. Tensile specimens of 4 inches in length and 1 inch in width were cut from the blown films. Since the film thickness varied from one formulation to another, all results were normalized with thickness. The tests were carried out at room temperature and the samples were stored in closed polyethylene bags prior to testing.

Since pure LDPE possess the required mechanical properties for food packaging applications, the film produced in this project aims at conserving the mechanical properties compared to pure LDPE. The standard ASTM D4635 could be used as reference.

4.4.7 Oxygen permeability

Oxygen permeability measurements were done on an Oxtran 2/21 device (Mocon, USA). In such a device, the membrane is placed in a diffusion cell separated into two chambers as illustrated in Figure 4.2. The inner chamber is flushed with nitrogen as the carrier gas whereas the flow of permeant, i.e. oxygen in this case, goes through the outer chamber. As the oxygen molecules permeates through the film, they are carried away by the nitrogen to the sensor. The tests described in this thesis used a mixture of N_2/H_2 (98/2%) as carrier gas and the test gas was oxygen (purity 99.9%).

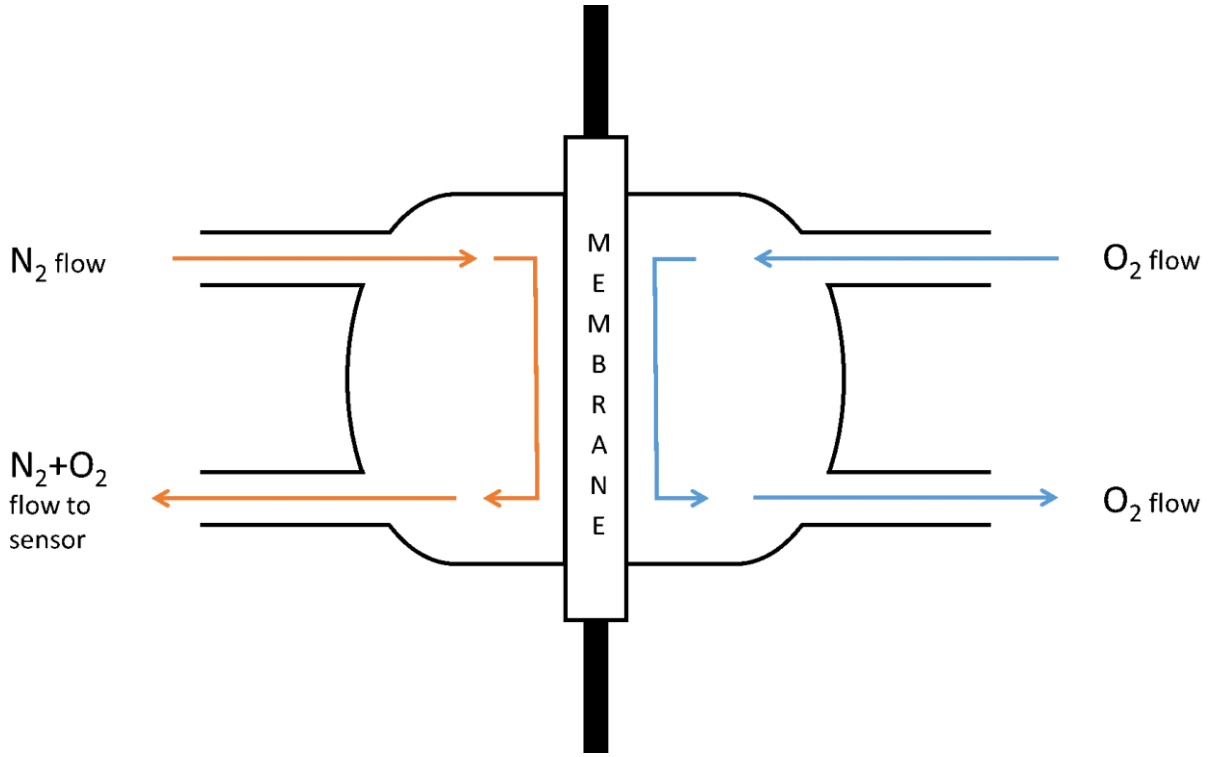

Figure 4.2 : Schematic of the side view in an oxygen transmission rate test

In the case of this test, the sensor is a fuel cell. When exposed to oxygen, the sensor generates an electrical current which is proportional to the amount of oxygen that gets to the sensor. The sensor has cadmium anode and a graphite cathode. The reactions that happen in the sensor are detailed in Equation (4.3):

$$\begin{aligned} &\text{(anode) } \tfrac{1}{2}\, O_2 + H_2O + 2\acute{e} \rightarrow 2\, HO^- \\ &\text{(cathode) } Cd + 2\, HO^- - 2\acute{e} \rightarrow Cd(OH)_2 \end{aligned} \qquad (4.3)$$

Film samples with a measuring area of 100 cm^2 were prepared. All tests were performed with a dry gas flux and at room temperature. All produced samples were kept in sealed PE bags until testing. Since the film thickness varied upon formulation, all measured values have been normalized to 100 µm thick film.

4.4.8 Transparency

Transparency was measured on a Lambda 1050 spectrometer (Perkin-Elmer, USA) within wavelengths from 350 to 800 nm, covering the visible range. The results in transmission are presented at three selected wavelengths: 400, 600 and 800 nm. These values stand for the total light transmitted through the films. For selected samples, a measurement of the diffusion component of the transmitted light was done to assess their haze. All measurements were normalized for a thickness of 100 μm.

CHAPTER 5 DEVELOPMENT OF CO-CONTINUOUS MORPHOLOGY IN BLENDS OF THERMOPLASTIC STARCH AND LOW-DENSITY POLYETHYLENE

5.1 Forewords

Auteurs et affiliations:

Thomas Mazerolles: Université de Sherbrooke, Département de génie chimique et biotechnologique, 2500 boulevard de l'Université, Sherbrooke, QC, Canada.

Marie-Claude Heuzey: Département de génie chimique, Centre de recherche sur les systèmes polymères et composites (CREPEC), Polytechnique Montréal, 2500 chemin de Polytechnique, Montréal, QC, Canada.

Maria Soliman: SABIC Global technologies B.V., T&I STC Geleen, Pays Bas.

Ralf Kleppinger: SABIC Global technologies B.V., T&I STC Geleen, Pays Bas.

Hans Martens: SABIC Global technologies B.V., T&I STC Geleen, Pays Bas.

Michel A. Huneault : Université de Sherbrooke, Département de génie chimique et biotechnologique, 2500 boulevard de l'Université, Sherbrooke, QC, Canada.

Statut: version finale publiée

Date accepté: 11 novembre 2018

Journal: Carbohydrate Polymers

Référence: Carbohydrate Polymers, 206 (2019), 757–766.

Titre en français: Développement de morphologie co-continue dans les mélanges d'amidon thermoplastique et de polyethylène basse densité.

Résumé en français:

L'étude se concentre sur le développement de la morphologie des mélanges d'amidon thermoplastique (TPS) avec du polyéthylène basse densité (LDPE) autour du point d'inversion de phase. L'effet de la concentration en glycérol et en eau sur la rhéologie du TPS et sur le développement de morphologie qui en découle après le mélange avec des polyéthylènes de différentes densités a été examiné. Les mélanges ont été préparés grâce à une extrudeuse bi-vis pour former des filaments. Le niveau de plastifiant a varié de 30 à 40% en masse pour le glycérol et jusqu'à 10% d'eau ajouté dans la phase de TPS. Une gamme de fraction de TPS dans le mélange allant de 40 à 80% en masse a été étudiée. Le ratio de viscosité TPS/LDPE a été modifié soit en augmentant la plastification du TPS soit en utilisant différents grades de LDPE. L'analyse de la morphologie de mélange a été effectuée par microscopie électronique à balayage sur des échantillons microtomés après que la phase de TPS ait été retirée par attaque acide pour améliorer le contraste des images. L'utilisation d'un rhéomètre capillaire sur des échantillons de TPS et de mélanges a permis de caractériser leur comportement viscoélastique. Une attention particulière a été portée sur l'effet de l'humidité sur la viscosité du TPS, ainsi des mesures d'humidité ont été effectuées sur les échantillons en utilisant la méthode de Karl Fisher. Différents types de morphologies de mélanges ont été observés depuis des gouttelettes jusqu'à la co-continuité. La relation entre la transition de phase dans le mélange et le ratio de viscosité des phases a été établie.

Contribution au document:

Cet article présente le développement de morphologie co-continue dans les mélanges TPS/LDPE. Il traite de l'évolution de la viscosité du TPS en fonction du type et de la concentration en plastifiants comme l'eau et le glycérol. La relation entre structure et propriétés des mélanges TPS/LDPE contenant une importante fraction de TPS est également abordée.

Mots-clés : amidon de pomme de terre, amidon thermoplastique, polyéthylène, co-continuité, mélange polymère.

5.2 Abstract

This study focuses on the morphology development in blends of thermoplastic starch (TPS) with Low Density Polyethylene (LDPE) in the 40 to 80 TPS wt% concentration range. The effect of glycerol and water content on TPS rheology and the subsequent morphology development after blending with LDPE of various viscosity levels was investigated. The TPS/LDPE viscosity ratio was modified either by increasing the TPS plasticization or by proper selection of the LDPE grade. Particular attention was given to the effect of TPS humidity on viscosity and therefore humidity levels were carefully measured by Karl Fisher titration prior to rheometry. It was found that the viscosity of the TPS was highly dependent on the plasticizer level and that the flow activation energy of TPS was around 3 times higher than that of LDPE. Different types of blend morphologies were achieved from dispersed to co-continuous. It was found that the co-continuous structure appeared at higher TPS concentration when increasing the TPS/LDPE viscosity ratio.

Keywords: potato starch, thermoplastic starch, polyethylene, co-continuous, polymer blend.

5.3 Introduction

Over the past few years, many research activities were focused on substituting fossil-based polymers by polymers produced from renewable resources. Among biobased materials, thermoplastic starch has shown to be very promising. Thermoplastic starch is produced by plasticizing and destructuring natural starch under shear and heat. Since starch is abundant and available from a wide variety of botanical sources, materials based on starch promise to be cost-competitive.

The microstructure of starch is complex but has been widely investigated (Buleon et al., 1998; Jane, 2009; Pérez et al., 2009; Van Soest et al., 1996b). Starch comprises two polysaccharides, amylose and amylopectin, and exhibit different crystalline structures depending on the botanical source. Cereals like corn and wheat display A-type structure, tubers like potato exhibit B-type structures and legumes are a mix between the two (Van Soest et al., 1996b). The microstructural characteristics of starch differ widely according to the botanical source. For example, the molecular weight of potato amylose is around five times that of corn. In terms of granule diameter, potato starch typically exhibits 75-100 micron granules which is around three times the diameter of corn starch granules (Grommers & Van der Krogt, 2009).

Thermoplastic starch is a destructured and plasticized version of starch. This can be achieved industrially by adding a plasticizer such as water or other hydrophilic chemicals and by mechanically shearing starch under heat. In these conditions, native starch granules lose their integrity and the starch crystalline structure is destroyed (Rodriguez-Gonzalez, Ramsay, & Favis, 2004; Van Soest et al., 1996b). The botanical source and thus the microstructure of the starch has an effect on final TPS properties. For example, higher amylose and higher molecular weight starches such as potato starches will lead to more viscous materials and to larger processing energy requirement compared to corn-based ones (Della Valle et al., 1995).

Thermoplastic starch is highly hydrophilic and must be blended with other synthetic polymers to produce materials that can be attractive for common packaging or industrial applications. Moreover, humidity affects the structure of pure TPS leading to recrystallization through a process called retrogradation. This evolution is highly detrimental as it leads to a drastic decrease in mechanical performance (Van Soest et al., 1996a). The common solution to overcome this issue is to blend TPS with a hydrophobic polymer in order to protect the TPS phase from environmental humidity. In all investigated blends with synthetic polymers, the blends are immiscible with clear phase separation. Blend of TPS have been produced with biodegradable materials such as polycaprolactone (Li & Favis, 2010), polybutyrate adipate terephthalate (Raquez et al., 2008) and polylactide (Huneault et Li 2007, 2012) as well as with non-biodegradable polymers such as polystyrene (Vaidya & Bhattacharya, 1994) and polyethylene (Rodriguez-Gonzalez, Ramsay, & Favis, 2003; Taguet et al., 2009).

Different methods for blending TPS and polyethylene have been reported. Aburto et al. produced a 35 wt% glycerol plasticized octanoated potato starch in an internal mixer prior to the addition of the LDPE (Aburto et al., 1997). St-Pierre et al. used a twin-screw extruder with the starch fed as a slurry through a side feeder positioned at mid extruder (St-Pierre et al., 1997). The reverse process was then proposed by Rodriguez-Gonzalez where the starch slurry was introduced in the primary feed hopper while LDPE was added in molten form at mid-extruder through a side single-screw extruder (Rodriguez-Gonzalez et al., 2004; Rodriguez-Gonzalez, Ramsay, et al., 2003; Rodriguez-Gonzalez, Virgilio, et al., 2003). Huneault et al. proposed a variation of the previous method where starch was fed in dry form instead of a slurry and where the second polymer was fed in solid form rather than in melt form at mid-extruder (Huneault & Li, 2012). Another simpler processing technique involved the prior mixing of potato starch and glycerol followed by the direct feeding in the twin-screw extruder, along with the LDPE (Gupta et al., 2008).

One of the main characteristics of immiscible polymer blends is their phase morphology. Early work on blending TPS and LDPE showed matrix-droplets morphology for blends up to 36 wt% wheat-based TPS in LDPE. When increasing the TPS content up to 53 wt%, the blend displayed fiber-like structures due to an increased coalescence (St-Pierre et al., 1997). Phase inversion was found to occur in the range 45-50 wt% TPS (Rodriguez-Gonzalez, Ramsay, et al., 2003). Later work by the same research group showed that, increasing the plasticizer level in TPS increased the deformability of the TPS phase when subjected to stretching (Rodriguez-Gonzalez, Virgilio, et al., 2003). Very coarse morphology was observed with symmetric blends of TPS and LDPE yet with a high level of interconnexion (Li et al., 2011).

With TPS being very polar and LDPE apolar, the blend is characterized by a very high interfacial tension of 16.4 $mJ.m^{-2}$ (Wu, 1982). Compatibilizers are typically used to reduce the interfacial tension, prevent coalescence and stabilize blend structures. Chemical modification of starch has been investigated in literature in order to increase its compatibility with apolar polymers however it requires more reaction steps before the blending itself. Adding a third component, the compatibilizer, was found to be easier. Various compatibilizers for starch/PE have been investigated such as ethylene-co-acrylic acid copolymer (EAA) (Otey et al., 1980; Willett, 1994) or ethylene-vinyl alcohol (EVA) (Bikiaris et al., 1998). Later work suggested a simple and cheaper way

by using polyethylene grafted maleic anhydride (PE-g-MA) either by in situ reactive extrusion (Wang et al., 2005) or adding as a separate component (Chandra & Rustgi, 1997; Gupta et al., 2008; Huneault & Li, 2012). Over the esterification reaction between maleic anhydride groups and starch and interactions between the long PE chains, compatibility will be enhanced. With blend composition up to 30 wt% corn-based TPS, the use of PE-g-MA led to a finer and more uniform dispersion of the starch phase (Bikiaris & Panayiotou, 1998; Huneault & Li, 2012). When it comes to high wheat TPS content in such blend, dispersed TPS droplets in PE matrix were observed even at 60 wt% TPS, co-continuity was only achieved around 75 wt% TPS (Mortazavi et al., 2013, 2014).

Earlier work have shown the crucial impact of material rheology over morphology development: material viscosities would determine blend morphology and give indications on the range of composition in which phase inversion can be expected (Avgeropoulos et al., 1976; Paul & Barlow, 1980). Rheology measurement of starch materials, however, is not straightforward. For most TPS, the viscosity shows a power-law behavior without Newtonian plateau. However, empiric models have shown that consistency and power law index depend on many inherent and experimental factors such as botanical source, processing (N. Singh et al., 2003), testing conditions as well as plasticizer type and content (Liu et al., 2009; Xie et al., 2012). Potato starch in particular was found to be harder to process due to its higher melt viscosity compared to other starch types (Della Valle et al., 1995). The most common way to study starch rheology is capillary rheometry. This method allows the measurement of viscosity over a wide range of shear rate and limits the evaporation of plasticizer compared to rotational rheometers (Xie et al., 2012).

Even though TPS and TPS blends have been studied in the past years, potato starch-based TPS and its blend with LDPE has not been investigated and even less for blends around the inversion point. This article examines the structure and development of co-continuous blends of potato starch-based TPS with LDPE, processed by twin-screw extruder. In particular the effect of plasticizer type and content on the TPS rheology, studied by capillary rheometer, and the blend morphology development. All studied blends were compatibilized to stabilize the morphology. Starch destructuration was verified using X-ray diffraction while blend morphology was monitored through Scanning Electron Microscopy (SEM).

5.4 Experimental

5.4.1 Materials

Industrial grade potato and corn starch were used. The potato starch was supplied by Emsland Group (Germany) while the industrial corn starch was supplied by Ingredion (Canada). Karl Fisher titration was used to measure the water content of granular and thermoplastic starch. The native potato and corn starch exhibited initial water contents of 16 and 9 wt% respectively. Distilled water and glycerol were used as plasticizers, the latter being a 99.5% pure grade supplied by Mat Laboratories (Canada).

Three different grades of LDPE (2101TN, 2404TN and 2008TN) supplied by Sabic were used. The grades had melt flow indices of 1, 4 and 8 g/10 min respectively and will be referred to as PE1, PE4 and PE8. A random terpolymer of ethylene, acrylic ester and maleic anhydride, Lotader 3410, supplied by Arkema, was used as compatibilizer for the TPS/LDPE blends.

5.4.2 Processing

Pure TPS material and blends of TPS with LDPE were prepared on a Leistriz 18 mm co-rotating Twin-Screw Extruder (TSE) operated at a screw rotation speed of 150 rpm. The process configuration is presented in Figure 5.1. Prior to extrusion, the starch and plasticizer were mixed manually and let to stand for 24 hours enabling complete absorption of the plasticizer in the granular starch. This mixture was then fed in zone 1 of the extruder and starch gelatinization was carried out in barrel section 1-3 by subjecting the mixture to intensive mixing at 130°C using kneading elements. The starch was assumed to be fully gelatinized at the end of barrel section 3. The LDPE and the compatibilizer were dry-blended and then introduced in the process in barrel section 4 using a side feeder. The TPS and LDPE were melt blended in the second half of the process mainly using two sets of kneading elements placed in barrel section 5 and 7. Temperature was set to 160°C in section 4-8. It is noteworthy that since section 4 was open to atmospheric pressure, excess water was able to devolatilize through the side-feeder.

For selected experiments, pure TPS was produced through the same process but using lower temperature of 130°C in section 4-6 and around 100°C in section 7-8 to prevent bubble formation at die exit.

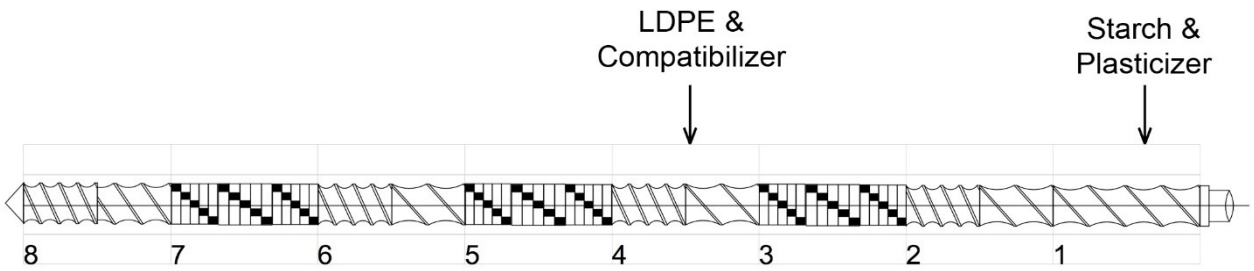

Figure 5.1: Screw configuration used to process TPS and TPS/LDPE blends.

The nomenclature used to describe the composition of the different TPS prepared in this study will be TPS30 and TPS40 for a starch plasticizer mixture fed to the extruder of 30 and 40 wt% glycerol respectively. In selected cases, W5 and W10 refer to added water of 5 and 10 wt% respectively, in addition to the water already naturally present in the native starch.

5.4.3 Wide angle X-ray diffraction

Wide angle X-ray diffraction (WAXD) measurements were carried out on TPS strands to assess their gelatinization one day after extrusion. The sample was glued with paratone oil on a sample holder of approximately 1 mm diameter and mounted at room temperature on a Bruker APEX DUO X-Ray diffractometer. The runs were integrated with the XRW^2 Eval Bruker software to produce WAXD diffraction pattern and then treated with Diffrac Eva (v 2.0) software from Bruker.

5.4.4 Moisture content

The TPS moisture content was measured on a Mettler Toledo V20 volumetric Karl Fisher titrator using an oven temperature of 180°C. Samples were heated for 1000 s to extract humidity, then

nitrogen carried the water to the titrator until measurement was complete. Prior to testing, extruded samples were placed in closed polyethylene bags to maintain their humidity level.

5.4.5 Rheological measurements

Capillary rheometry was carried out using an Instron CEAST SR20 rheometer. A 1 mm capillary die with a die length of 40 mm was used. The shear rate was varied from 10 s^{-1} to 10000 s^{-1}. TPS LDPE blends were characterized at a temperature of 160°C. To minimize degradation, measurement temperature for pure TPS was set to 130°C. Rabinovitch corrections were applied to correct the results for non-Newtonian effects. Since the L/D ratio of the die was 40, the entry and exit effects (Bagley correction) were neglected.

In order to assess the effect of the humidity level and the rheological response of the materials, selected TPS samples were conditioned for three weeks. The residual humidity in TPS samples after extrusion was around 10 wt%. For low humidity levels, samples were placed in a closed container with desiccant (Dierite $CaSO_4$ from Anachemia, VWR) while for high humidity level, the samples were subjected to saturated humidity. Final moisture content of 5 and 25 wt% were attained respectively.

5.4.6 Scanning Electron Microscopy (SEM)

The blend morphology was assessed using a Scanning Electron Microscopy (Hitachi S-3000 N) in secondary electron mode. Observations were made on extruded strands that were microtomed under liquid nitrogen using a glass knife. The samples were then subjected to HCl 6N for 3 hr to selectively remove the TPS phase, thus improving the contrast for imaging. Samples were sputtered with gold-palladium coating prior to SEM observation.

For blends where the TPS was the matrix or blends close to phase inversion, the acid-etching technique described above could not be used. In these cases, observations were made using a S-

4700 FEG SEM from Hitachi in secondary electron mode because of its higher sensitivity compared to the previous microscope.

To determine average diameters, image analysis was performed using Sigma Scan Pro 5 software from Systat. For every sample, more than 500 diameter measurements were made from which the volume and number average diameters, namely d_v and d_n, were calculated. Equivalent diameters based on surface area of the measured domains were used to calculate the averages.

5.4.7 Continuity analysis

The extent of continuity of the TPS phase was calculated using a gravimetric method. Four to six segments of extruded strands with a length of around 1 cm were immersed in HCl, 6N, and stirred for 24 h. Weight loss measurements were then carried out on dried samples in order to determine the percentage of continuity using Equation ((5.1):

$$\%continuity = \left(\frac{W_{initial} - W_{final}}{W_{initial}}\right) * 100 \quad (5.1)$$

where $W_{initial}$ corresponds to the weight of the sample before acid etching and W_{final} the one after the removal of the TPS phase.

5.5 Results and discussion

5.5.1 Thermoplastic starch production

Figure 5.2 presents X-ray diffractometry results for native potato starch and for corresponding extruded TPS one day after processing. The native potato starch showed all characteristic peaks of B-type starch, especially the strong signal at 2θ=5.5° which is very different from A and C-type starches. For the TPS30 (i.e. 30 wt% glycerol as plasticizer), a large amorphous hump was observed. The peaks associated to the original crystalline structure were absent, indicating that the crystalline structure was destroyed during processing. The loss of starch crystallinity is a

confirmation of its successful gelatinization. This can be followed by X-ray diffraction and is valid for every botanical source (Van Soest, Hulleman, et al., 1996b). The small remaining signals at 2θ=17.2; 18.4; 20° can be interpreted as process-induced crystallinity: the new V-type crystalline structure is formed after processing and should increase upon aging (Van Soest, Hulleman, et al., 1996a, 1996b).

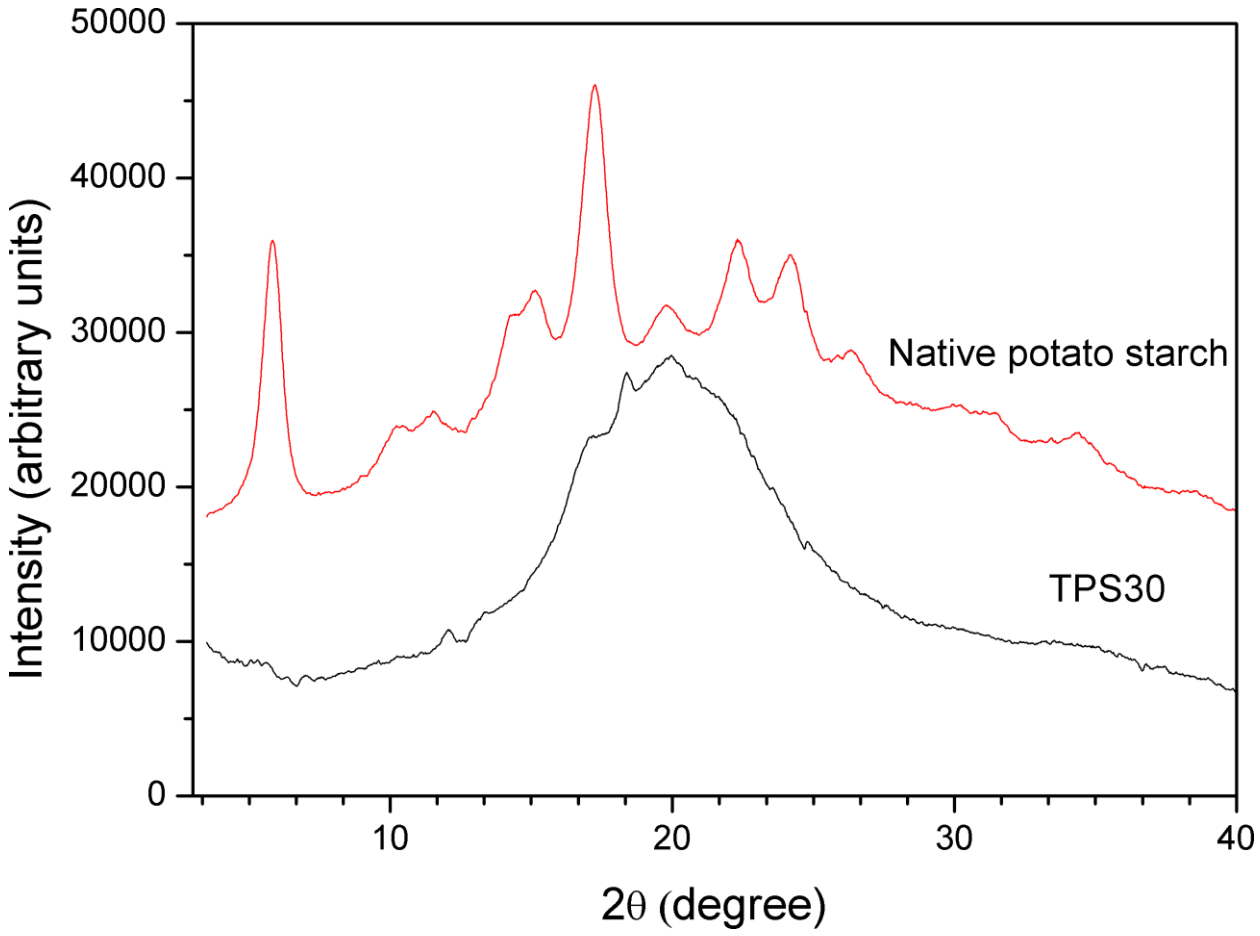

Figure 5.2: WAXD patterns for native potato starch and corresponding TPS with 30 wt% glycerol.

5.5.2 Thermoplastic starch rheology

When blending two immiscible polymers, the dispersed phase size and phase inversion point are known to be dependent on the viscosity ratio between the blend's components. Figure 5.3

displays the viscosity of potato and corn-based TPS, plasticized with 30 and 40 wt% glycerol, as a function of shear rate as well as the Arrhenius plot for LDPE and potato TPS at the two different glycerol levels aforementioned. The humidity level in the TPS was 7 wt%. In the investigated shear rate range presented in Figure 5.3a, a shear-thinning behavior was observed with no indication of a Newtonian plateau at low shear rate. For both TPS, the increase in plasticizer level from 30 to 40 wt% led to a 2-fold decrease in viscosity. It is noteworthy that potato-based TPS was always more viscous than corn-based samples for a given plasticization level. The experimental data were used to determine the consistency, *K*, and power-law index, *n*, of the well-known power-law viscosity model shown in Equation (5.2):

$$\eta = K\dot{\gamma}^{n-1} \tag{5.2}$$

where η is the viscosity and $\dot{\gamma}$ the shear rate. The power-law index value for potato TPS was around 0.37 whereas for corn TPS, the value was 0.57. Increasing the glycerol content from 30 to 40 wt% divided the consistency by a factor 2 for both starch types. The higher potato TPS viscosity relative to corn is consistent with past observations reported by Grommers and Van der Krogt. One common measurement method of starch slurry viscosity in industry is based on the torque measured on the shaft of an internal mixer. With this method, they reported a potato/corn viscosity ratio of 5 (Grommers & Van der Krogt, 2009). The difference in viscosity between starches can be explained by inherent differences in molecular weight and in molecular chain interactions. Potato and corn starches have relatively close ratios of amylose/amylopectin, however the amylose of potato starch is known to display higher molecular weight than the one found in cereals like corn (Bertoft & Blennow, 2016). Similar observations have been made with TPS: Della Valle et al. reported a power-law index of 0.46 for potato-based TPS plasticized with 32% water (Della Valle et al., 1995), whereas Rodriguez-Gonzalez et al. mentioned a power-law index of 0.66 for corn-based TPS plasticized with 32% glycerol and 20% water (Rodriguez-Gonzalez et al., 2004).

One way to present the effect of temperature on polymer viscosity is to plot the natural logarithm of the temperature shift factor as a function of the reciprocal temperature, i.e. the Arrhenius plot. The shift factor is the ratio between the viscosity at a given temperature and a reference

temperature at constant stress. For a power-law fluid, the shift factor is independent of the stress level if the power-law index is independent of temperature. That was the case for TPS in the current investigation. In such a plot, the slope has an important significance since it is a direct measure of the flow activation energy *E* (divided by *R*, the ideal gas constant).

Figure 5.3b presents the Arrhenius plot for LDPE and potato TPS at two different glycerol levels. The activation energy (i.e. slope) of TPS is much greater to that of LDPE. Increasing the glycerol content from 30 to 40 wt% did not have much effect on the TPS activation energy. Activation energy of 103 and 98 kJ/mol were calculated for potato-based TPS30 and TPS40 respectively, whereas LDPE showed an activation energy of 37 kJ/mol. This value is slightly lower than the ones generally reported in the literature, between 45-60 kJ/mol (Delgadillo-Velázquez, Hatzikiriakos, & Sentmanat, 2008). It is noteworthy that the activation energy is very dependent on the branching level of the material.

Values of activation energy for TPS reported in literature vary widely upon processing conditions, starch type and plasticizer content. Corn starch TPS plasticized with water in the range 15-35% yielded activation energy around 32-51 kJ/mol (Cervone & Harper, 1978; Della Valle, Colonna, Patria, & Vergnes, 1996; Fletcher, McMaster, Richmond, & Smith, 1985), potato TPS plasticized with 26-32% water was reported with an activation energy of 47 kJ/mol, whereas wheat starch TPS plasticized with a combination of glycerol and water showed an activation energy of 120 kJ/mol (Della Valle, Vergnes, & Lourdin, 2007).

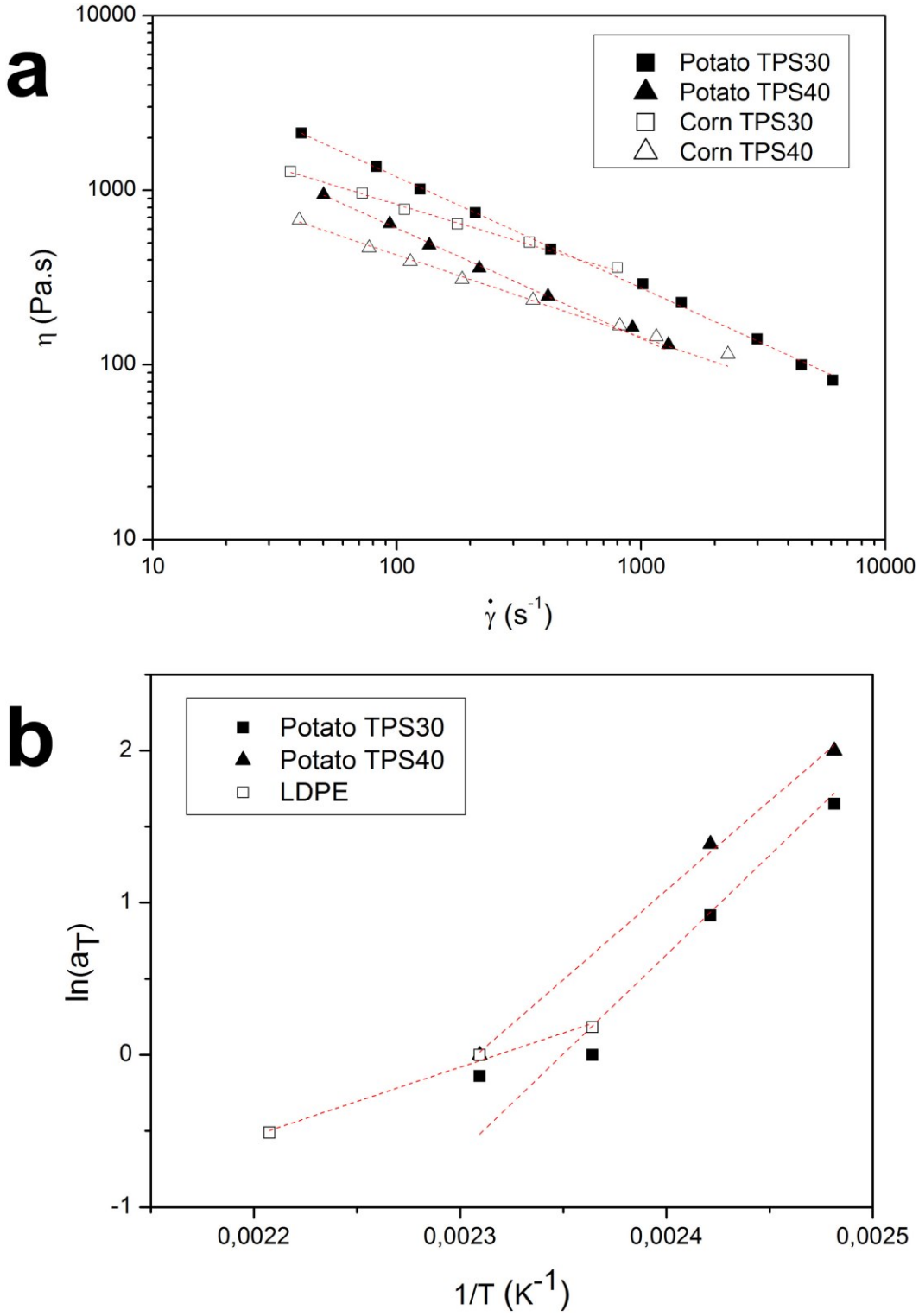

Figure 5.3 : (a) viscosity as a function of shear rate at 130°C for potato and corn-based TPS plasticized with 30 and 40 wt% glycerol and (b) evolution of the shift factor as a function of the reciprocal of temperature for potato TPS plasticized with 30 and 40 wt% glycerol and LDPE (dash lines are drawn to guide the eye)

The data presented in Figure 5.3a were obtained for TPS comprising 7 wt% moisture. This value was varied to investigate the plasticizing effect of water on TPS. The viscosity was measured over the same shear rate range as in Figure 5.3a but since the humidity level did not change the level of shear-thinning, i.e. power-law index, it was possible to summarize the effect of moisture content by showing its effect on consistency *K* as shown in Figure 5.4. The consistency dropped by one order of magnitude when moisture level was increased from 5 to 25 wt%. Similar viscosity drops were observed for the 30 and 40 wt% glycerol levels. It is noteworthy that a linear behavior was found on a log-linear scale.

An Arrhenius type equation can be used to describe the impact of plasticizer content on consistency: $K=K_0 exp(E/RT-\alpha MC)$ where *MC* is the moisture content. A review of such models applied to different TPS can be found in the literature (Della Valle, Buleon, Carreau, Lavoie, & Vergnes, 1998; Vergnes & Villemaire, 1987; Xie et al., 2012). In some of these studies, the Specific Mechanical Energy (SME) was taken into account in the consistency model. In the current study, the processing conditions (screw rotation speed, temperature, etc.) were kept constant for all produced blends. This leads to variations in SME but enabled minimization of thermal and mechanical degradation. SME was not taken into account however another term was added in order to take into account the glycerol content *GC* as shown in Equation (5.3):

$$K = K_0 \exp\left(\frac{E}{RT} - \alpha * MC - \beta * GC\right) \quad (5.3)$$

where α, β and K_0 are the model coefficients. The parameters that led to the best fitting of the experimental data were: K_0=2.17x10^{-9} Pa.s^n, α=15.5, β=-2.4. The lines on Figure 5.4 are the calculated consistencies using Equation (5.3), the power law index *n* was kept constant at the value calculated from data in Figure 5.3a. Della Valle et al. analyzed potato starch TPS plasticized only with water (up to 30 wt%) processed in a twin-screw extruder and obtained a value of 18.6 for α (Della Valle et al., 1995). Previous work on maize starch yielded values about a hundred times lower for α (Cervone & Harper, 1978; Fletcher et al., 1985; Sandoval & Barreiro, 2007). Other work showed the same trend for α being two to three times higher than β (Martin et al., 2003; Tajuddin et al., 2011). It emphasizes the stronger effect of water on TPS consistency compared to glycerol. The constant K_0 was found to be a few orders of magnitude different from

data collected in literature, however this depends greatly on experimental conditions, starch type and other constants taken into account in the model.

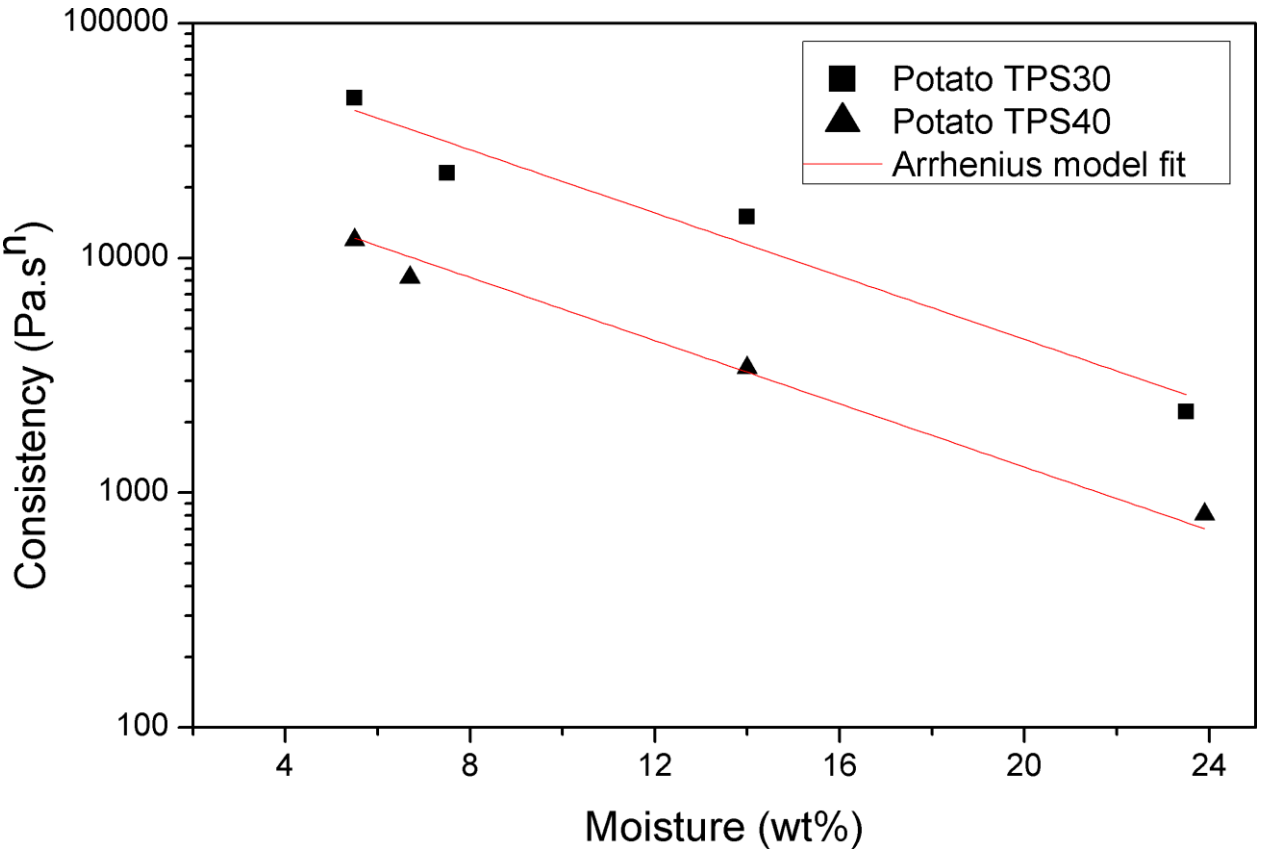

Figure 5.4: Effect of moisture on the consistency of potato TPS plasticized with 30 and 40 wt% glycerol at 130°C.

5.5.3 Blending TPS and LDPE

Figure 5.5 presents the viscosity as a function of shear rate for the pure components and the corresponding compatibilized and non-compatibilized blends. Figure 5.5a compares the experimental viscosity as a function of shear rate for all studied LDPE, as well as the compatibilizer at 160°C. Viscosity predictions for TPS30 and TPS40 at that temperature were obtained by shifting results from Figure 5.3a using the activation energy calculated from Figure 5.3b. The predictions

are shown as lines on the figure. The TPS was always less viscous than LDPE no matter the plasticization. The power-law index, in the high shear rate range for LDPE was around n=0.23, while the ones for TPS30 and TPS40 were 0.4 and 0.45 respectively, from the power-law regression. The viscosity of the compatibilizer was close to PE4 but its Newtonian plateau appeared earlier.

Blending two immiscible polymers with high interfacial tension, such as TPS and LDPE, may lead to coarse morphologies, poor adhesion in the solid state and thus to poor mechanical properties. A commercial random terpolymer comprising of ethylene, acrylic ester and maleic anhydride was then used to compatibilize TPS and LDPE. Figure 5.5b shows the viscosity of TPS/LDPE blends at 160°C as a function of shear rate for formulations with and without compatibilizer, when increasing the amount of TPS in the blend from 50 to 70 wt%. Prediction of viscosity for TPS30 is presented with lines.

Uncompatibilized formulations were found to be less viscous than the individual components while the compatibilized blends were more viscous. Globally, the TPS concentration did not affect significantly the viscosity of the blends. Since the neat components had similar viscosities, the blend ratio was not expected to have a significant effect on the blend viscosity. The fact that the compatibilized blends have a higher viscosity than the pure components is a sign of interfacial reaction that lead to the formation of high molecular weight structure composed of the compatibilizer backbone grafted with starch macromolecules.

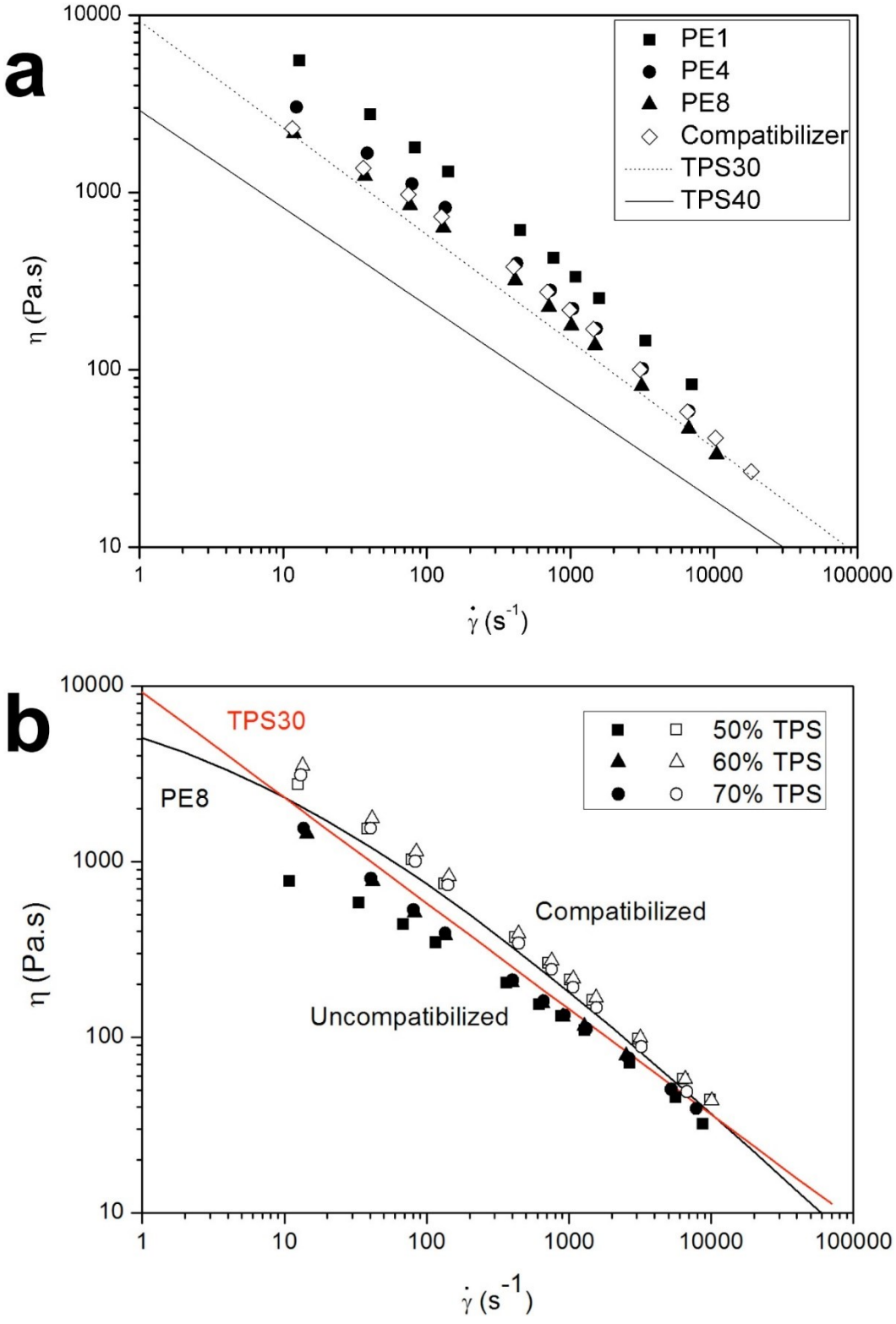

Figure 5.5: Viscosity as a function of shear rate at 160°C for: (a) various LDPEs and compatibilizer and (b) PE8, TPS30 and various corresponding compatibilized (open symbols) and non-compatibilized (filled symbols) blends. The dotted and plain lines are predicted viscosity values.

5.5.4 Morphology of the blend

The mechanical and optical properties of immiscible polymer blends are intimately linked to the blend microstructure. Figure 5.6 shows scanning electron micrographs of microtomed surfaces of TPS30/PE1 blends for TPS30 content varying from 50 to 80 wt%. All blends presented in the following sections were compatibilized with 20 wt% compatibilizer on a PE basis, i.e. from 10 to 4 wt% in the overall composition. The TPS phase had been selectively removed in order to increase contrast for the microscopy observation, therefore appears as cavities, except for the blend at 80 wt% where phase inversion occurred. At 50 wt% the TPS phase was dispersed in PE with traces of coalesced particles. The measured TPS continuity was 19% for this blend. When increasing TPS content to 60 and 70 wt%, the morphology changed to a co-continuous one, even if smaller drops remained. This was confirmed with TPS continuity measurement around 90% for the two blends. When reaching 80 wt% TPS, phase inversion occurred and the TPS phase became the matrix. This was confirmed by the acid-etching treatment used to remove the TPS. When trying to apply this treatment to 80 wt% TPS samples, the latter lost their integrity since the TPS matrix was removed and the acid-etching media was left only with the remaining PE fragments. Therefore, for concentration of 80 wt% TPS30 and higher, TPS was considered continuous.

The 80 wt% TPS level corresponds approximately to 72 vol%. The phase inversion therefore occurs at a volume fraction much greater than 50% even though the blend viscosity ratio was close to one. High phase inversion points were also found in literature. Mortazavi et al. reported co-continuous blends at 75 wt% TPS for blends compatibilized with 1.5 wt% LDPE-g-MA. The TPS was prepared from wheat starch plasticized with 36 wt% glycerol. They concluded that phase inversion would occur beyond 75 wt% TPS (Mortazavi et al., 2013). In the case of blends of TPS with polycaprolactone, the phase inversion point was found to be in the 70-80 wt% TPS range (G. Li & Favis, 2010). Blends with lower TPS content were reported to lead to matrix-droplets structure in many other works (Huneault & Li, 2012; Mortazavi et al., 2014).

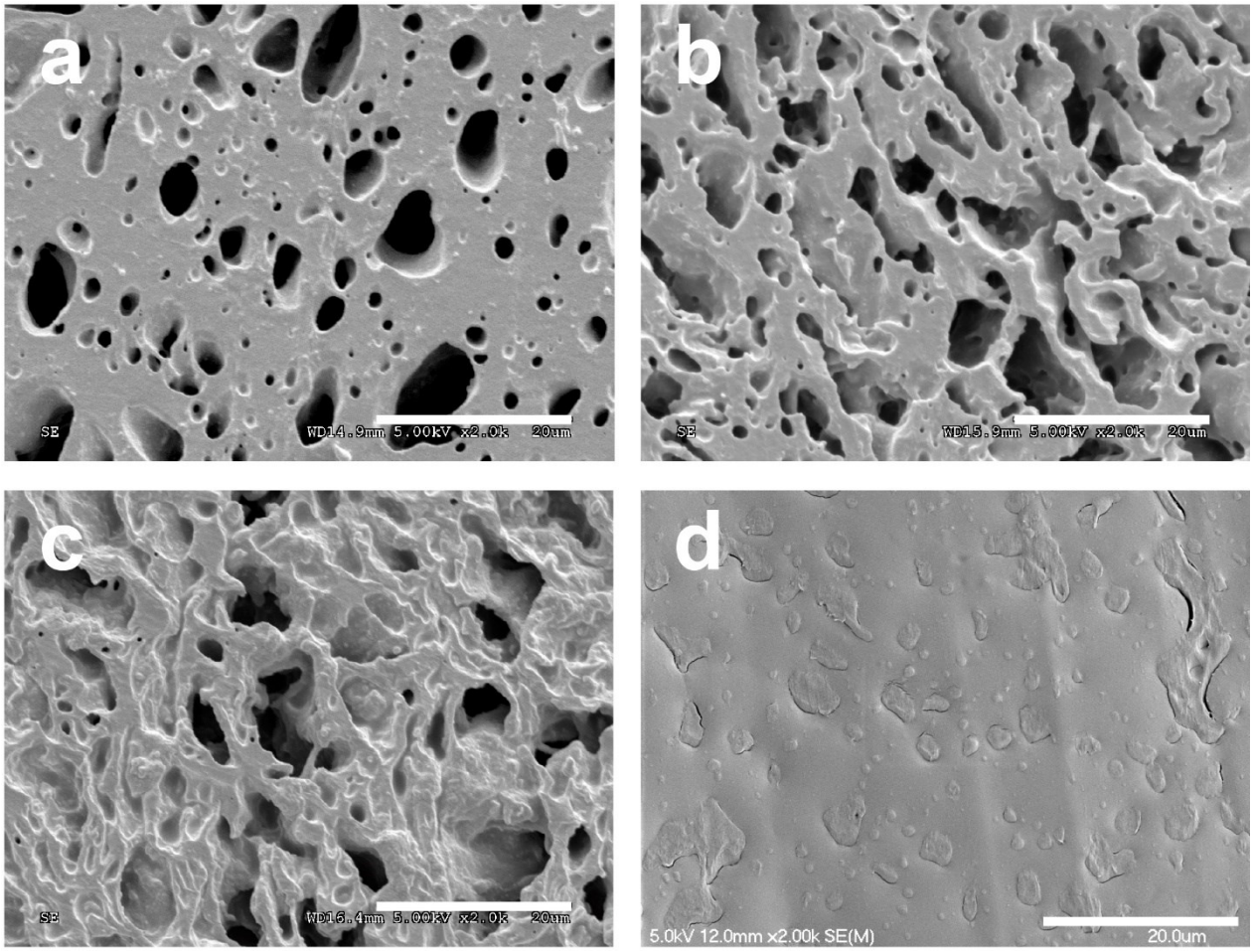

Figure 5.6: SEM micrograph of compatibilized blends of potato TPS30 with PE1: (a) 50 wt% TPS c=19%, (b) 60 wt% TPS c=95%, (c) 70 wt% TPS c=89% and (d) 80 wt% TPS c=100%. The "c" value corresponds to the percentage of continuity. The scale bar represents 20 µm.

Using a more viscous minor phase will typically increase the phase inversion concentration as the minor component becomes less prone to encapsulate the major one. Figure 5.7 displays the morphology for compatibilized 60 wt% TPS30 with LDPEs of various viscosity, namely PE4 and PE8. These are to be compared to Figure 5.6b obtained in the same conditions but with PE1. Both blends showed very fine dispersed TPS drops in LDPE matrix while the blend with PE1 was co-continuous. Image analysis on micrographs displayed in Figure 5.7 indicated very similar number-average diameters, 0.66 and 0.72 µm, and volume-average diameters: 0.84 and 0.85 µm, for the blend with PE4 and PE8 respectively.

The TPS/PE viscosity ratios were calculated at a shear rate of 100 s^{-1}, representative of the conditions that the material may undergo in the extruder. When the blend was close to co-continuity at 60 wt% TPS30 with PE1, the viscosity ratio was of 0.38 whereas values of 0.60 and 0.83 were found for blends with PE4 and PE8 respectively. In the case of the last two blends, the very close number and volume-average diameters showed that above a certain viscosity ratio and under the studied shear conditions, the viscosity ratio had no influence over the diameter of the dispersed phase. This shows that the compatibilizer was able to stabilize the blend morphology even if the viscosity of the matrix varies.

Previous studies showed that the size of the dispersed phase was affected by changes in the viscosity ratio in a non-compatibilized immiscible blend (Favis & Chalifoux, 1987) whereas using a compatibilizer often leads to significantly less dependence (Favis & Willis, 1990). Moreover, Willemse et al. reported for blends of similar interfacial tensions with different viscosity ratios that increasing the viscosity ratio yielded a smaller range of composition where co-continuity was possible (Willemse, Posthuma De Boer, Van Dam, & Gotsis, 1998). Therefore, in the current study, a narrower range of co-continuity should be expected for blends with the less viscous LDPE.

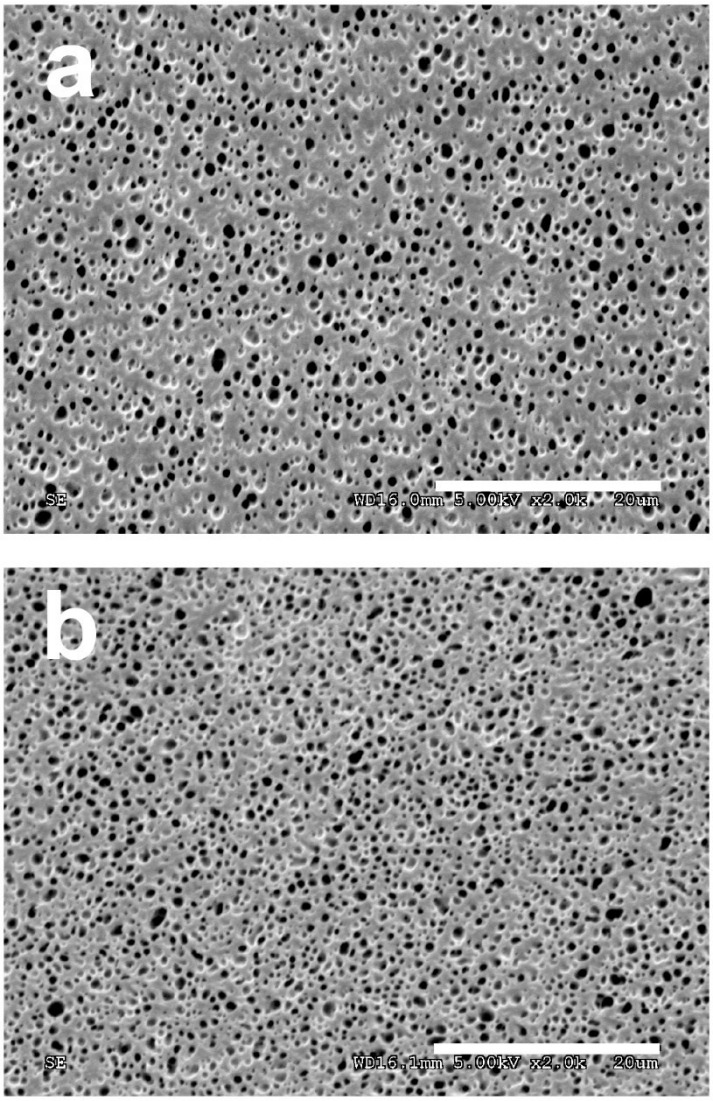

Figure 5.7: SEM micrograph of compatibilized blends of potato TPS30 with 40 wt% of (a) PE4 and (b) PE8. The scale bar represents 20 µm.

In order to evaluate the impact of the plasticizer level on the morphology development, a similar blend series with a higher glycerol content was investigated. Figure 5.8 shows the morphology of compatibilized TPS40/PE1 blend series for 40-70 wt% TPS. Samples presented in pictures (a) and (b) underwent acid-etching. For (c) and (d) the samples lost their integrity during acid-etching indicative that phase inversion has occurred. SEM was there performed on un-etched surfaces. At 40 wt%, the TPS phase was deformed into elongated particles exhibiting already some continuity. The percentage continuity was 20% at 40 wt% TPS. This value jumped to 77% at 50

wt% TPS. The micrograph showed continuity in plane but also in the depth of the etched sample, supporting the high continuity value. Above 60 wt% TPS, the micrographs showed LDPE particles dispersed in a continuous TPS phase, thus confirming that phase inversion had occurred.

The TPS40/PE1 viscosity ratio was 0.15, which is below the value of 0.38 obtained between TPS30 and PE1. Decreasing the viscosity of TPS by increasing the plasticizer content has shifted the co-continuity region towards lower TPS content.

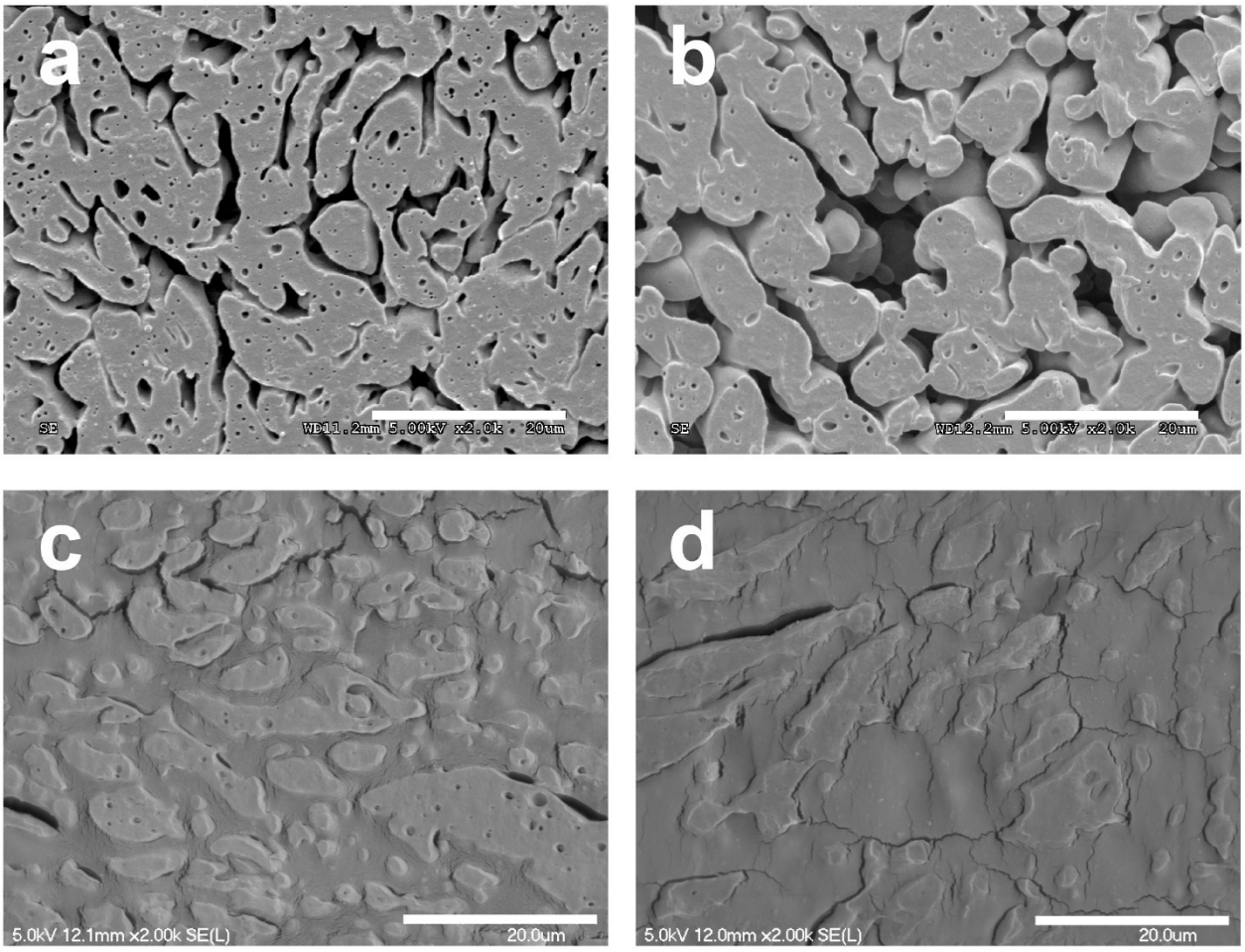

Figure 5.8: SEM micrograph of compatibilized potato TPS40/PE1: (a) 40 wt% TPS c=19%, (b) 50 wt% TPS c=77%, (c) 60 wt% TPS c=100% and (d) 70 wt% TPS c=100%. The "c" value corresponds to the percentage continuity. The scale bar represents 20 µm.

It was shown, in light of the rheological results, that water is more effective than glycerol for starch plasticization. The effect of substituting some glycerol by water on the blend morphology has therefore been investigated. Figure 5.9 shows the morphology for compatibilized 60 wt% TPS blends with PE1 and PE8 respectively. The added amount of plasticizer was kept constant at 40 wt% for all formulations. Pictures (a) to (c) present the series with PE1 where 0, 5 and 10 wt% glycerol was substituted by water, whereas pictures (d) to (f) show the same but with PE8. In the case of the blend series with PE1, the 0% water (40% glycerol) blend was phase inverted with PE acting as dispersed phase.

Substituting glycerol with 5 and 10% water changed the morphology from phase inverted to co-continuous. This was confirmed with measured continuity values around 70%. On the other hand, the substitution did not change the morphology as dramatically in the PE8 series. All micrographs showed elongated TPS phases with measured continuity levels in the range 40-60%.

For blends with PE1, the phase inversion difference may be explained by the loss of water at mid-extruder, leading to a lower plasticizer level and thus higher TPS viscosity at the point where PE is mixed with the TPS in the second half of the extrusion process.

The morphology of TPS30/PE1 with 10% added water (Figure 5.9c) was very close to the one of the TPS30 with PE1 presented in Figure 5.6, both being close to co-continuity. The extra water could still be of use since it accelerates the gelatinization of starch and gets a more homogeneous TPS melt. Moreover, this substitution can be an interesting process aid since it reduces the viscosity of the TPS in the first step of the process, hence being especially helpful with higher viscosity starches like potato.

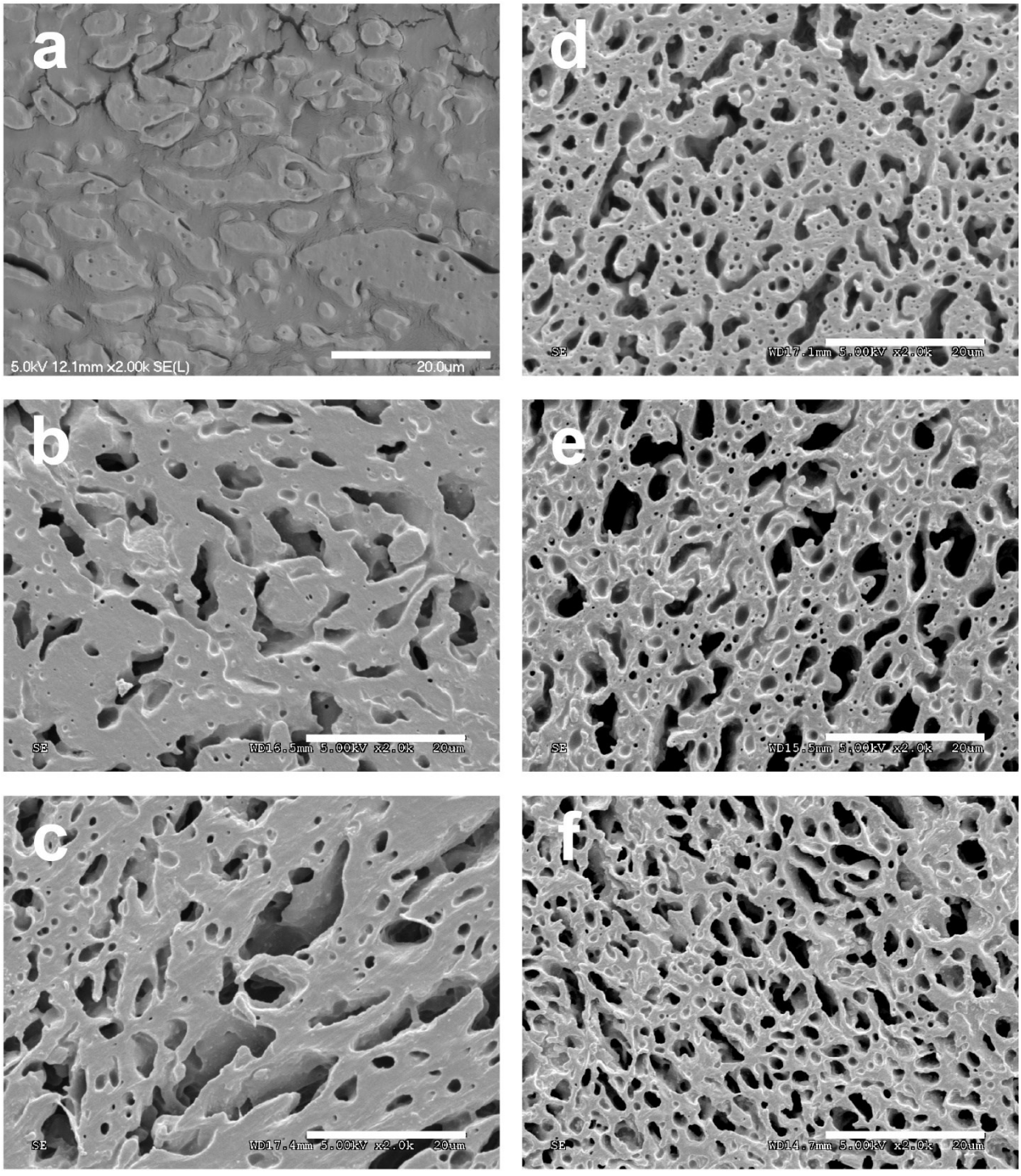

Figure 5.9: SEM micrograph of compatibilized blends of potato TPS with PE1: (a) TPS40 c=100%, (b) TPS35 W5 c=71%, (c) TPS30 W10 c=72% and for blends with PE8: (e) TPS40 c=41%, (f) TPS35 W5 c=56%, (g) TPS30 W10 c=62%. The “c” value corresponds to the percentage continuity and the scale bar represents 20 µm.

Corn starch has been abundantly investigated in the literature and it is therefore interesting to compare the results above with similar formulations made with corn starch. Figure 5.10 presents the morphology of compatibilized 60 wt% corn TPS/PE blends. Again, glycerol levels of 30 and 40 wt% were used to plasticize the starch, each formulation then being blended with PE1 and PE8 respectively. The TPS30/PE1 (Figure 5.10a) blend showed emerging co-continuity supported with a measured 39% continuity value. By contrast, when blended with PE8, TPS30 formed a clearly defined dispersed phase in the LDPE matrix (Figure 5.10b). When increasing the glycerol content to 40 wt% (Figure 5.10c), the TPS/PE1 blend samples lost their integrity during acid-etching, showing once again that phase inversion had occurred. The same TPS40 blended with the more fluid PE8 (Figure 5.10d) led to a TPS dispersion, interconnected at a measured continuity level of 36%. This again illustrates that the phase inversion concentration can be lowered by the use of a less viscous TPS.

Calculation of the viscosity ratios were made using an activation energy for corn based TPS of 54 kJ/mol in order to get the viscosity at 160°C (Kaseem, Hamad, & Deri, 2013). For the only blend presenting matrix-droplets structure, namely the corn based TPS30/PE8, the viscosity ratio was around 0.59. It correlates with the results from Figure 5.7 where viscosity ratios above 0.6 led to that kind of morphology. The size of the dispersed phase was similar to that obtained with the potato starch. With a number-average diameter of 0.83 µm and a volume-average diameter of 1.06 µm, the dispersity was found to be slightly higher in the case of corn starch blends compared to the same formulation with the potato. The difference in viscosity of the TPS phase between potato and corn could explain this result.

Co-continuous TPS30/PE1 and TPS40/PE8 had viscosity ratios of 0.27 and 0.32, similar to what was found for potato TPS (cf Figure 5.6). Finally the corn-based TPS40/PE1, with a viscosity ratio of 0.15, underwent phase inversion such as the potato based blends presented in Figure 5.8c. As for the potato starch, corn-based blend morphology with LDPE was controlled by the viscosity ratio between components of the blend. No matter the type of starch, controlling the viscosity of the TPS through the plasticization or varying LDPE's MFI enables the displacement of the co-continuous region.

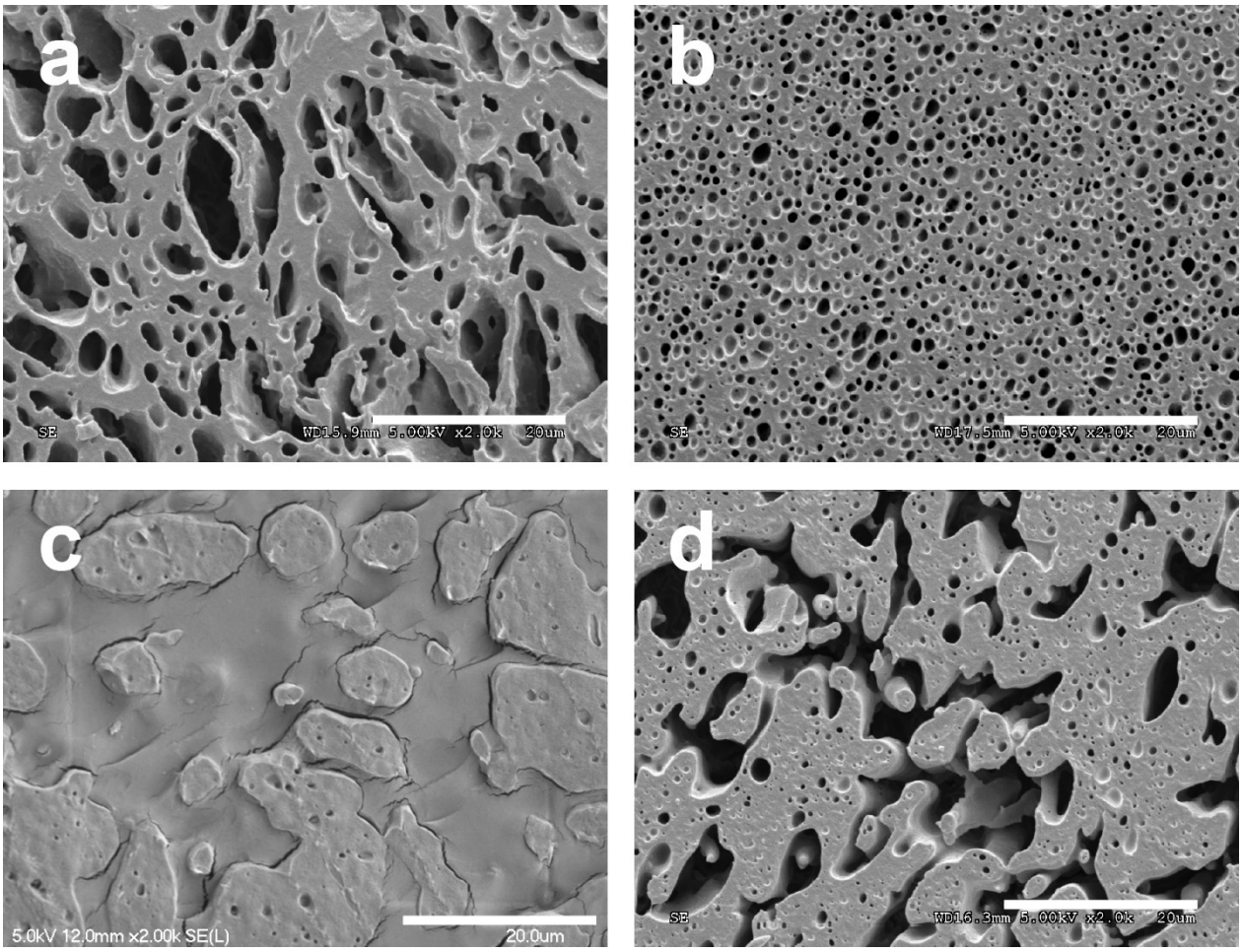

Figure 5.10: SEM micrograph of compatibilized blends of corn TPS with LDPE: (a) TPS30/PE1 c=39%, (b) TPS30/PE8, (c) TPS40/PE1 c=100% and (d) TPS40/PE8 c=36%. The “c” value corresponds to the percentage continuity when applicable and the scale bar represents 20 µm.

5.6 Conclusions

This paper examined the influence of water and glycerol plasticization on the rheological behavior of potato-based thermoplastic starch and on TPS/LDPE blend morphology development around the co-continuity region.

A modified Arrhenius-type model was successfully used to characterize the effect of water and glycerol plasticization on potato TPS viscosity. The model can be used to predict the power-law consistency parameter of TPS as a function of temperature, water content and glycerol content. It was found that the power-law index, indicative of shear-thinning, was unaffected by temperature and TPS composition. Water was shown to have a stronger effect than glycerol on starch plasticization.

A commercial random terpolymer comprising of ethylene, acrylic ester and maleic anhydride was shown to be effective for the compatibilization of the TPS/LDPE blend. The compatibilizer increased the blend viscosity compared to the neat components and provided finer blend structures.

The viscosity ratio was shown to have a striking effect on blend morphology and on the development of a co-continuous structure. When lowering the TPS/LDPE viscosity ratio, the co-continuity concentration range was shifted toward lower TPS content. This leads to two options for displacing the co-continuity concentration range: varying the LDPE viscosity or modifying plasticizer type and/or amount. This will enable the development of co-continuous blends of varying absolute viscosity as long as the viscosity ratio is carefully controlled.

CHAPTER 6 DEVELOPMENT OF MULTILAYER BARRIER FILMS OF THERMOPLASTIC STARCH AND LOW-DENSITY POLYETHYLENE

6.1 Forewords

Auteurs et affiliations:

Thomas Mazerolles: Université de Sherbrooke, Département de génie chimique et biotechnologique, 2500 boulevard de l'Université, Sherbrooke, QC, Canada.

Marie-Claude Heuzey: Département de génie chimique, Centre de recherche sur les systèmes polymères et composites (CREPEC), Polytechnique Montréal, 2500 chemin de Polytechnique, Montréal, QC, Canada.

Maria Soliman: SABIC Global technologies B.V., T&I STC Geleen, Pays Bas.

Ralf Kleppinger: SABIC Global technologies B.V., T&I STC Geleen, Pays Bas.

Hans Martens: SABIC Global technologies B.V., T&I STC Geleen, Pays Bas.

Michel A. Huneault : Université de Sherbrooke, Département de génie chimique et biotechnologique, 2500 boulevard de l'Université, Sherbrooke, QC, Canada.

Statut: article soumis

Date soumission: 28 juin 2019

Journal: Journal of Polymer Research

Titre en français: développement de film barrière multicouche à base d'amidon thermoplastique et de polyéthylène basse densité

Résumé en français:

L'étude se concentre sur la production de film 3 couches à base de polyéthylène basse densité (LDPE) et d'amidon thermoplastique (TPS) où ce dernier est utilisé pour améliorer les propriétés barrières à l'oxygène. Des TPS à base de pomme de terre et de maïs, plastifiés avec du glycérol, ont été préparés et mélangés au LDPE grâce à une extrudeuse bi-vis. La concentration en TPS a évolué entre 50 et 80% en masse. L'effet d'un copolymère maléique comme compatibilisant du mélange a été exploré grâce à l'étude de la morphologie de mélange réalisée par microscopie électronique à balayage. Le mélange TPS/LDPE a été utilisé comme couche centrale dans un film de 3 couches avec des couches externes constituées de LDPE pur. Jusqu'à 5% en masse d'argile naturelle ou modifiée ont été ajoutés à la phase TPS pour explorer leur effet sur la morphologie du mélange, la mise en forme ainsi que sur les propriétés physiques du film. Une exfoliation significative ainsi qu'une orientation privilégiée des argiles parallèles au film ont été confirmées par diffraction des rayons X. L'addition d'argile naturelle au TPS a amélioré drastiquement la mise en forme et la qualité des films. Des films transparents, présentant une perméabilité à l'oxygène 20 fois plus basse que celle du LDPE tout en maintenant des propriétés mécaniques similaires ont été produits. Les films multicouches à base de TPS et de LDPE pourraient donc présenter une alternative peu chère pour des applications d'emballage alimentaires demandant une meilleure protection à l'oxygène.

Contribution au document:

Cet article présente la mise en forme du film soufflé 3 couches dont le mélange TPS/LDPE constitue la couche centrale. De plus, il décrit la relation entre la morphologie de mélange, la morphologie de film et les propriétés du film (mécaniques, transparence et perméabilité à l'oxygène).

Mots-clés : amidon thermoplastique, polyéthylène, argile, multicouche, film soufflé, barrière.

6.2 Abstract

This study focuses on producing 3-layer films out of Low-Density Polyethylene (LDPE) and Thermoplastic Starch (TPS) using the latter to improve the film oxygen barrier properties. Potato and corn-based TPS, plasticized with glycerol, have been prepared and blended with LDPE using a twin-screw extruder. The TPS fraction was varied from 50 to 80 wt%. The effect of a maleated copolymer as blend compatibilizer was assessed by examining blend morphology using scanning electron microscopy. The aforementioned TPS/LDPE blend was used as a core layer in a 3-layer blown film with pure LDPE as outer layers. Natural and organo-modified clays were added to the TPS phase at concentrations up to 5 wt% to investigate their effect on blend morphology as well as on processability and physical properties of the film. X-ray diffraction experiments indicated significant exfoliation and a general orientation of non-exfoliated clay parallel to the film surface. Adding natural clay to the TPS was also found to improve processing and quality of the films. Highly transparent films with oxygen barrier 20 times higher than pure LDPE films were achieved while maintaining similar mechanical properties relative to pure LDPE. The multilayer TPS/LDPE films could therefore represent a low-cost bio-based alternative for food packaging requiring better oxygen protection in order to increase shelf-life.

Keywords: thermoplastic starch, polyethylene, clay, multilayer, blown film, barrier.

6.3 Introduction

Packaging plays a crucial role in the protection of goods. In order to increase shelf life and limit product waste, food packaging has very high standards regarding gas barrier properties. Moisture level, on one hand, should be kept constant to avoid product's dryness and on the other hand, oxygen permeation must be limited to prevent oxidation and therefore degradation of the food. With their high hydrophobicity, most of the polyolefins such as polyethylene and polypropylene display low vapor permeability and are therefore good humidity barriers. However, the low oxygen permeability required to provide an oxygen barrier is generally achieved with highly polar

polymers such as polyvinyl alcohol or polyamides. For example, ethylene - vinyl alcohol copolymers (EVOH) have an oxygen permeability around 0.01 $cm^3.mm.m^{-2}.day^{-1}.atm^{-1}$. This is 4 orders of magnitude lower than the oxygen permeability of low-density polyethylene (LDPE). The permeability of EVOH is highly dependent on moisture content (Muramatsu et al., 2003; Zhang et al., 2001). Therefore, barrier films are typically a multilayer assembly of a polyolefin, tie layers and of the EVOH or polyamide barrier layer. The polyolefin provides water vapor protection to the EVOH or polyamide layer. The tie layers, placed between the polyolefin and the oxygen barrier layers are typically functionalized polyolefins that improve interlayer adhesion and thus prevent film delamination.

Starch is also known to have low oxygen permeability and therefore it could be an interesting material for the preparation of oxygen barrier films. Starch is a semi-crystalline polysaccharide consisting of linear and branched polymers, namely amylose and amylopectin. It can be found in various crops such as potato, corn or rice for example, each of which having slightly different properties. In its native form, starch is a solid powder with particle size in the 5-100 µm range. Dry-starch particles can be dispersed into polymers but would not provide much help in reducing oxygen permeability in a dispersed state. However, starch's crystalline structure can be destroyed through a process called gelatinization leading to a thermoplastic material called thermoplastic starch or TPS (Rodriguez-Gonzalez et al., 2004; Van Soest, Hulleman, et al., 1996a). In its thermoplastic state, starch could be processed into a lamellar form that would be better suited for oxygen permeability reduction. Thermoplastic starch can be produced industrially by adding a plasticizer such as water or glycerol and by applying shear and heat to the mixture. The obtained material can be processed by conventional polymer processing techniques. The oxygen barrier properties of various TPS have been reported. For example, potato-based amylose and amylopectin films made with 40 wt% glycerol showed an oxygen permeability of 0.7 and 1.4 $cm^3.mm.m^{-2}.day^{-1}.atm^{-1}$ respectively at 50%RH (Rindlav-Westling et al., 1998). This is not as low as the values reported for EVOH but starch could qualify as an interesting material for medium oxygen barrier materials. It would also offer the advantages of being a low-cost and bio-based alternative to currently used materials.

Different techniques have been developed to produce films out of TPS. First, the starch can be dispersed in its plasticizer such as water or glycerol, heated and then casted or compression molded. Rice-based and corn-based starch films, both plasticized with 30 wt% glycerol and cast-filmed presented an oxygen permeability of 1.0 $cm^3.mm.m^{-2}.day^{-1}.atm^{-1}$ at a humidity ratio of 0% and 3.8 $cm^3.mm.m^{-2}.day^{-1}.atm^{-1}$ at 70 %RH respectively (Jost & Stramm, 2016; Laohakunjit & Noomhorm, 2004). The film casting process is not industrially appealing since it involves a long drying time. In an industrial context, melt based techniques are generally preferred. This was shown to be possible using two steps: gelatinization of the starch with a plasticizer in an extruder followed by film production through a casting or blown film process. For example, potato starch plasticized and gelatinized using a high glycerol content was successfully extruded into films using a blown film process. However, the resulting films were not fully transparent and were sticky which could severely hinder their use (Thunwall et al., 2008). Also in this unprotected form, the TPS film properties are very sensitive to moisture thus further limiting their use.

To protect the TPS, reduce its moisture sensitivity and facilitate its handling, it is necessary to blend it with a less hygroscopic material. TPS blends with both bio-based (Avérous, 2004; Huneault & Li, 2007; G. Li & Favis, 2010) and synthetic polymers have been studied (Taguet, Huneault, & Favis, 2009; Vaidya & Bhattacharya, 1994). Among the polymers to blend with TPS, low-density polyethylene (LDPE) is a very interesting option for its low-cost and easy processing. TPS and LDPE are immiscible and exhibit a very high interfacial tension, around of 16.4 $mJ.m^{-2}$ (Schwach & Avérous, 2004). The TPS/LDPE blend microstructure has been investigated over a wide range of concentration and was shown to exhibit a variety of morphological structures from dispersed nodules to highly elongated structures (St-Pierre et al., 1997). For example, Rodriguez-Gonzales et al. reported droplets of the minor phase in TPS/LDPE blends (30/70) with starch plasticized with 29% glycerol. However, increasing the glycerol content to 40% lead to elongated TPS structures (Rodriguez-Gonzalez, Ramsay, et al., 2003). Due to the high interfacial tension between TPS and LDPE, the blend properties tend to decrease relative to those of pure LDPE. The material homogeneity and properties can be improved by adding a compatibilizer that will reduce the dispersed phase size (by reducing the interfacial tension and suppression of coalescence) and improve the solid-state interfacial adhesion. Bikiaris et al. noted a 45% increase in tensile strength

for TPS/LDPE blends with maleic anhydride grafted polyethylene (PE-g-MA) as compatibilizer (Bikiaris & Panayiotou, 1998). It was also reported that for blends in which the TPS was the dispersed phase, a finer and more uniform dispersion of the TPS phase can be achieved when adding PE-g-MA as compatibilizer. Huneault et al. reported a 10-fold decrease in TPS phase size in a 25 wt% TPS blend with HDPE with the addition of PE-g-MA (Huneault & Li, 2012).

Most of the literature on the TPS/polyethylene blends has focused on blends where the TPS was the minor phase and was dispersed in polyethylene. By contrast, Mortazavi and al. investigated high TPS concentration range and showed that it was possible to achieve a co-continuous morphology at 75 wt% TPS (Mortazavi et al., 2013). Recent work has also highlighted that a co-continuous structure was achievable. The transition from dispersed to co-continuous appeared at concentration as low as 50 wt% TPS but this transition was pushed to higher concentration when the TPS/LDPE viscosity ratio was increased (Mazerolles et al., 2019).

Early work on producing films out of TPS/LDPE reported the mixing of water-plasticized starch with LDPE and ethylene co-acrylic acid prior to blown film extrusion (Otey et al., 1980). The process was carried out at laboratory scale for formulations up to 40% starch and lead to poor transparency and mechanical properties at high starch content. Arvanitoyannis et al. have compression-molded LDPE/TPS blends into films. The TPS was plasticized with up to 20 wt% water and was used at concentrations up to 40%. The TPS phase was not continuous at this concentration level and lead to oxygen permeability that was greater than that of pure polyethylene. They also noticed an increase in water vapour permeability at high starch content (Arvanitoyannis et al., 1998). One way to limit the water sorption in films is to use multilayer systems. Dole et al. produced 5-layer films by a laboratory-scale combination of solution casting and compression molding. They reported the conservation of starch's oxygen barrier performances at high humidity ratio when using a 5-layer film (LDPE/PE-g-MA/TPS/PE-g-MA/LDPE) where PE-g-MA was the tie layer (Dole et al., 2004). These results showed the potential of a multilayer approach for improving oxygen barrier properties and prompted the need for the development of a continuous process for the production of such films.

To further reduce the permeability of TPS, platy minerals could be added. For example, layered silicates such as clays are low cost minerals extensively used in polymers in order to improve mechanical or flame retardancy properties. Since clay platelets are essentially made out of inorganic crystals, they are impermeable to gases thus being an asset in creating barrier materials. In films, exfoliated clay platelets with high surface area and aspect ratio like montmorillonite can create a tortuous path in the polymer matrix thus reducing the diffusion of gases through the film. Clays have been used in TPS casted films up to 5% to enhance mechanical properties (Avella et al., 2005) and reduce water uptake through improved intercalation (Cyras et al., 2008). Later work by Sabetzadeh and al. also investigated compatibilized blends of LDPE with 15 wt% corn-based TPS blown into a film with various amount of organo-modified montmorillonite. The clay exhibited partial exfoliation and lead to improved mechanical properties and conservation of the films transparency (Sabetzadeh et al., 2016).

Multilayer films were shown to be a valid route to produce barrier films with TPS acting as an oxygen barrier. However, these films have not yet been produced by a continuous process that could be used at an industrial scale. In this study, we have investigated a novel approach for the production of 3-layer film using a blown film process. The films were made of LDPE outer layers and of a middle layer composed of a co-continuous TPS/LDPE blend. The idea of using a blend rather than pure TPS as the inner layer was based on the fact that pure TPS cannot be handled easily since it tends to stick together and it does not adhere well to LDPE. The main objective was to investigate if oxygen barrier properties of the film can be improved while keeping film properties such as transparency and mechanical performance close to those of a pure LDPE. The effect of starch type and content on film morphology development and the subsequent properties were investigated. The crucial role of the compatibilizer in stabilizing the blend as well as the film structure was also studied. Finally, the effect of natural and modified clays addition on film processing and final properties was assessed.

6.4 Experimental

6.4.1 Materials

Industrial grade potato starch was supplied by Emsland group (Germany) while corn starch was obtained from Ingredion (Canada). Karl Fisher titration measurements were carried out in order to evaluate the water content in both starches. Native potato and corn starch exhibited initial water content of 16 and 9 wt% respectively. Glycerol 99.5% pure grade supplied by Mat Laboratories (Canada) was used as starch plasticizer.

Two different grades of LDPE were used: 2101TN and 2102N0W supplied by SABIC Global Technologies (The Netherlands). These grades had melt flow indices of 0.85 and 2.5 g/10min at 190°C respectively and will be referred to as PE1 and PE2. A random terpolymer of ethylene, acrylic and maleic anhydride, namely Lotader 3410 supplied by Arkema (France), was used as compatibilizer for the TPS/PE blends. Natural clay was Cloisite Na whereas organically modified clay was Cloisite 15A, both supplied by Byk (Germany).

6.4.2 Extrusion

The TPS/PE blends were prepared on a co-rotating 34 mm Leistritz Twin-Screw Extruder (TSE) with L/D=42 using a screw rotation speed of 160 RPM. Process and detailed screw configuration are presented in Figure 6.1. The starch was gravimetrically introduced as a powder in the hopper in zone 0. In specific formulations containing clays, the clay powder was dry-mixed with the starch and introduced in zone 0 as well. The glycerol used as plasticizer for the starch was pumped into the extruder in zone 1. All blends were plasticized with 35 wt% glycerol with regards to the starch content. Starch and plasticizer were then subjected to intensive mixing in zones 2-3 using kneading elements, leading to starch gelatinization. Complete gelatinization was presumed at the end of zone 3 where the extruder was left open for water devolatilization. A dry blend of LDPE and compatibilizer was introduced through a side feeder in zone 6 and blended with the TPS in zones 7-8 using kneading elements. At the end of the extruder, the produced strands of TPS/LDPE were cooled down in air and stored in closed PE bags.

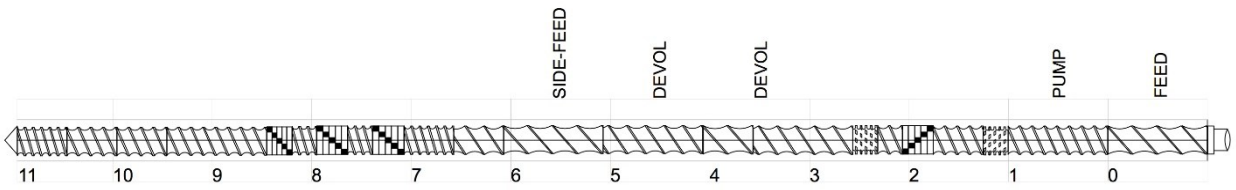

Figure 6.1: Screw configuration used to process TPS/LDPE blends

The temperature of the extruder was kept at 80°C in the two first zones for the introduction of the starch and the plasticizer. It was increased to 140°C in zones 2-5 for the gelatinization and devolatilization steps. The second half of the extruder, starting in zone 6, was kept at 160°C. This temperature was selected because it was high enough to enable LDPE melting but low enough to minimize starch thermal degradation. For all formulations described in this paper, the amount of starch plasticizer is indicated with regard to the starch phase and the percentage of compatibilizer with regard to the LDPE phase.

6.4.3 Film blowing

The film preparation was performed on a multilayer Lab Tech blown film extrusion line using two 20 mm single-screw extruders in an ABA configuration. The extruders had a L/D=30 and were used to feed the material into a co-extrusion die with a 50 mm outer diameter and a gap of 1.5 mm. The present work aimed at producing symmetric 3-layer films consisting of a TPS/PE blend as inner layer between two identical pure LDPE outer layers. The operating temperature of the extruder feeding the TPS/PE blend was set at 145°C in the feeding zone and increased gradually to 165°C at the end of the extruder. The LDPE outer layers were extruded at 210°C. The two extruders rotating speed was set at 80 RPM for an expected thickness ratio of 1:2:1. Processing parameters such as blow-up (BUR) and take-up ratios (TUR) were calculated. The BUR is the ratio of bubble diameter to the die diameter whereas the TUR is the ratio of film velocity to melt velocity. In order to calculate the TUR, the TPS density has been considered equal to 1.4 g/cm^3. The forming ratio, defined as the ratio TUR/BUR, indicates the balance of stretching between machine (MD) and transverse (TD) direction.

Two different processing strategies were used. For films without clay, the aim was to produce the thinnest film regardless of the stretching ratio. The films containing the higher TPS content (in the inner layer) exhibited bubble stability issues and were particularly difficult to produce. To facilitate processing, 5 wt% water was added to the blends containing 70 and 80 wt% TPS, before film blowing. This improved film strechability was due to water that acts as an additional plasticizer during processing. As the TPS content increased, the maximum blow up ratio decreased. Therefore, to achieve the thinnest possible films, the forming ratio was progressively decreased from 11 to 4 when increasing TPS content from 50 to 80 wt%. For films containing clay, the second processing strategy was used. In this approach, the forming ratio was kept constant and equal to 3. After film blowing, produced samples were stored in closed PE bags until further testing.

6.4.4 Scanning Electron Microscopy (SEM)

The blend morphology was assessed using a Scanning Electron Microscopy (Hitachi S-3000 N) in secondary electron mode. Extruded strands after melt blending were microtomed under liquid nitrogen using a glass knife. Film samples first needed to be casted in epoxy before microtoming. In order to ensure proper characterization, all cuts were done perpendicularly to the film's surface and the morphology in both machine (MD) and transverse (TD) directions was displayed. The samples were then subjected to HCl 6N for 3 hours to selectively remove the TPS phase, in order to improve the contrast for imaging. Finally, samples were sputtered with gold-palladium coating prior to SEM observation. The determination of average diameters was done through image analysis using Sigma Scan Pro 5 software from Systat. For every sample, more than 300 diameter measurements were made from which the volume and number average diameters, namely d_v and d_n, were calculated. Equivalent diameters based on surface area of the measured domains were used to calculate the averages. The dispersity defined by the ratio d_v/d_n was calculated as well.

6.4.5 Viscosity measurements

Rheology assessment was carried out on an Instron CEAST SR20 capillary rheometer at a testing temperature of 160°C. A 1 mm capillary die with a die length of 40 mm was used. The shear rate was varied from 10 s-1 to 10000 s-1. In order to correct the results for non-Newtonian effects, Rabinovitch corrections were applied. Since the L/D ratio of the capillary was large (i.e. L/D=40), end-effect were neglected.

6.4.6 Mechanical properties

Mechanical testing was performed according to ASTM D882 on an Instron Electropuls E3000 for the determination of Young's modulus and on an Instron 3365 for the other mechanical properties. Tensile specimens of 4 inches in length and 1 inch in width were cut from the blown films. Since the film thickness varied from one formulation to another, all results were normalized with thickness. The tests were carried out at room temperature and the samples were stored in closed polyethylene bags prior to testing.

6.4.7 X-ray diffraction

Wide angle X-ray diffraction (WAXD) measurements were carried out directly on blend extrudates. The samples of approximately 1 mm^3 were glued with silicon on a goniometer head and mounted at room temperature on a Bruker APEX DUO X-Ray diffractometer. These runs were then treated and integrated with the XRW^2 Eval Bruker software to produce WAXD diffraction pattern from 3.5 to 15 degrees 2θ. The pattern was then treated with Diffrac Eva (v 2.0) software from Bruker. SAXS images on films were collected with a Bruker AXS Nanostar system equipped with a Microfocus Copper Anode at 45 kV / 0.65 mA, MONTAL OPTICS and a VANTEC 2000 2D detector. The detector to sample distance was calibrated with a Silver Behenate standard at 28.20 cm. The films were positioned vertically on the sample holder with the X-ray beam hitting the cross-section of the film. Since the films were very thin compared to the beam size, four films

were stacked to each other to increase the signal. All SAXS measurements are from 0.5 to 10.5 degrees 2θ. In order to see preferential orientation, an azimuthal integration around the expected peak was calculated from 0 to 360°.

6.4.8 Oxygen permeability

Oxygen permeability measurements were performed on an Oxtran 2/21 device (Mocon, USA). Film samples with a measuring area of 100 cm^2 were prepared. All tests were performed with a dry gas flux and at room temperature. All produced samples were kept in sealed PE bags until testing. Since the film thickness varied upon formulation, all measured values have been normalized to 100 µm thick film.

6.4.9 Transparency measurements

Transparency was measured on a Lambda 1050 spectrometer (Perkin-Elmer, USA) within wavelengths from 350 to 800 nm, covering the visible range. The results in transmission are presented at three selected wavelengths: 400, 600 and 800 nm. These values stand for the total light transmitted through the films. For selected samples, a measurement of the diffusion component of the transmitted light was done to assess their haze. All measurements were normalized for a thickness of 100 µm.

6.5 Results and discussion

6.5.1 Potato-based TPS/PE multilayer films – effect of compatibilizer

Mechanical and optical properties of polymer blends are highly dependent on the blend's microstructure. Figure 6.2 shows scanning electron micrographs of TPS/PE1 blends with a varying potato-based TPS content from 50 to 80 wt%. All blends in Figure 6.2a to Figure 6.2d were modified with 20 wt% of the maleated compatibilizer on a PE basis, i.e. from 10 to 4 wt% on the global composition. As detailed in the experimental section, the TPS phase was selectively

removed and therefore appears as holes on the micrographs. For a TPS content of 50 wt%, the blend displays a typical dispersed morphology: small TPS drops in a PE matrix. The droplet size increased at 60 wt%. The volume-average diameter d_v increased from 1.17 to 1.52 µm when increasing the TPS content from 50 to 60 wt%, the dispersity being constant. Interconnected particles appeared at 70 wt% TPS. Finally at 80 wt% TPS, a more continuous TPS phase was achieved.

Mortazavi et al. also reported continuity at high TPS content when working with blends of 36 wt% glycerol plasticized starch and polyethylene compatibilized with 1.5 wt% PE-g-MA. They noticed that the phase inversion occurred for a TPS fraction beyond 75 wt% (Mortazavi et al., 2013). In previous work using different processing conditions, co-continuity was observed at lower TPS content, around 60 and 50 wt% TPS for 30 and 40 wt% glycerol levels respectively (Mazerolles et al., 2019). This showed that the blend morphology was sensitive to the processing conditions. In this previous study, starch and plasticizer were mixed together prior to being fed in the twin-screw extruder. Moreover, there was no vent zone at mid-extruder to devolatilize humidity prior to the introduction of polyethylene. This lead to a higher water content in the TPS phase thus shifting the phase inversion towards lower TPS content.

In immiscible polymer blends, the compatibilizer plays a crucial role in stabilizing the blend morphology as well as improving interfacial adhesion. Figure 6.2e to Figure 6.2g show the morphology of 60 wt% TPS potato-based blends with PE1 for compatibilizer content varying from 0 to 10 wt% with regard to the PE phase. The same blend with 20 wt% compatibilizer can be found in Figure 6.2b. Without compatibilizer, the blend displayed a very coarse morphology with a majority of large and irregular structures. Adding 5 wt% compatibilizer drastically changed the morphology with the TPS phase now dispersed as fine spherical droplets. Similar morphology was found for higher compatibilizer content yet with smaller TPS drops. Volume-average diameters of 2.81, 2.10 and 1.52 µm were measured for 5, 10 and 20 wt% compatibilizer respectively. This showed that a compatibilizer concentration as low as 5 wt% was sufficient to significantly reduce the dispersed phase size.

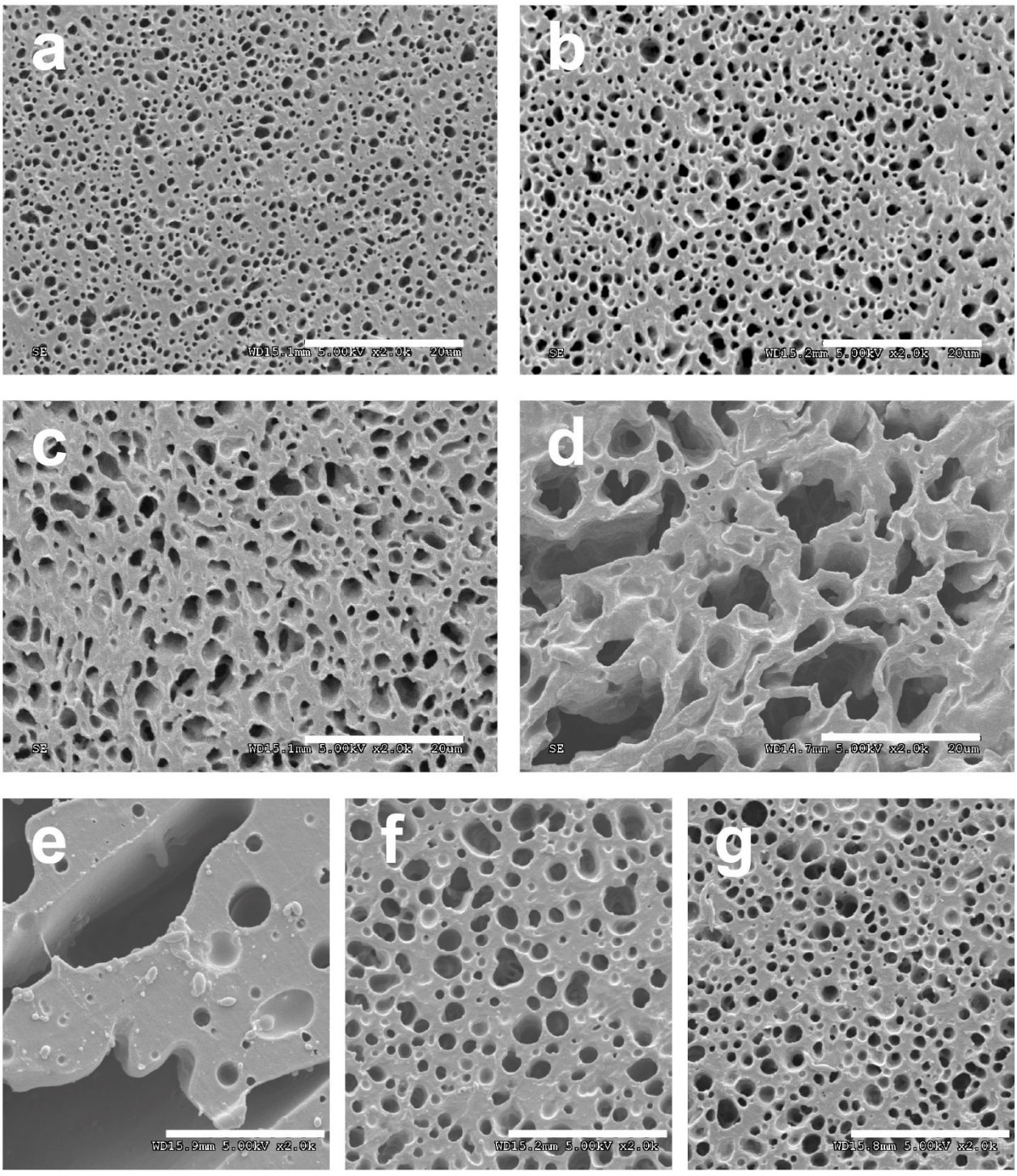

Figure 6.2: Micrographs of 20wt% compatibilized blends of PE1 with: (a) 50 wt% TPS, (b) 60 wt% TPS, (c) 70 wt% TPS and (d) 80 wt% TPS as well as micrographs of blends of 60 wt% potato TPS with PE1: (e) without compatibilizer, (f) with 5 wt% and (g) with 10 wt% compatibilizer. The bar represents 20 µm.

The next step was to investigate the morphology after subsequent film processing. Figure 6.3 presents SEM micrographs of 3-layer films consisting of PE2 outer layers and a TPS/PE1 inner layer. The TPS was made with potato starch and the TPS content was varied from 50 to 80 wt%. The compatibilizer content in the inner layer was 20 wt%. For 50 wt% TPS blends, the TPS phase appeared as drops in the inner layer no matter the direction of observation. When increasing the TPS content to 60 wt%, more elongated structures were found along MD leading to small lamellas of TPS oriented along MD. Further elongated and larger particles were found at 70 wt% TPS. At 80 wt% TPS, the TPS phase was deformed into long continuous particles oriented along MD. It is noteworthy that films produced with 70 and 80 wt% TPS were difficult to process into films and led to thicker films with poor TPS dispersion compared to formulations with lower TPS content. All films showed good adhesion between the layers except for the 80 wt% TPS formulation. The loss of adhesion in this case may be due to phase inversion, which causes direct contact between the TPS inner layer and the PE outer layer. Using 20 wt% compatibilizer in the inner layer was required to get both blend stabilization and layer adhesion. It allowed an easy processing without delamination for a TPS content up to 60 wt%.

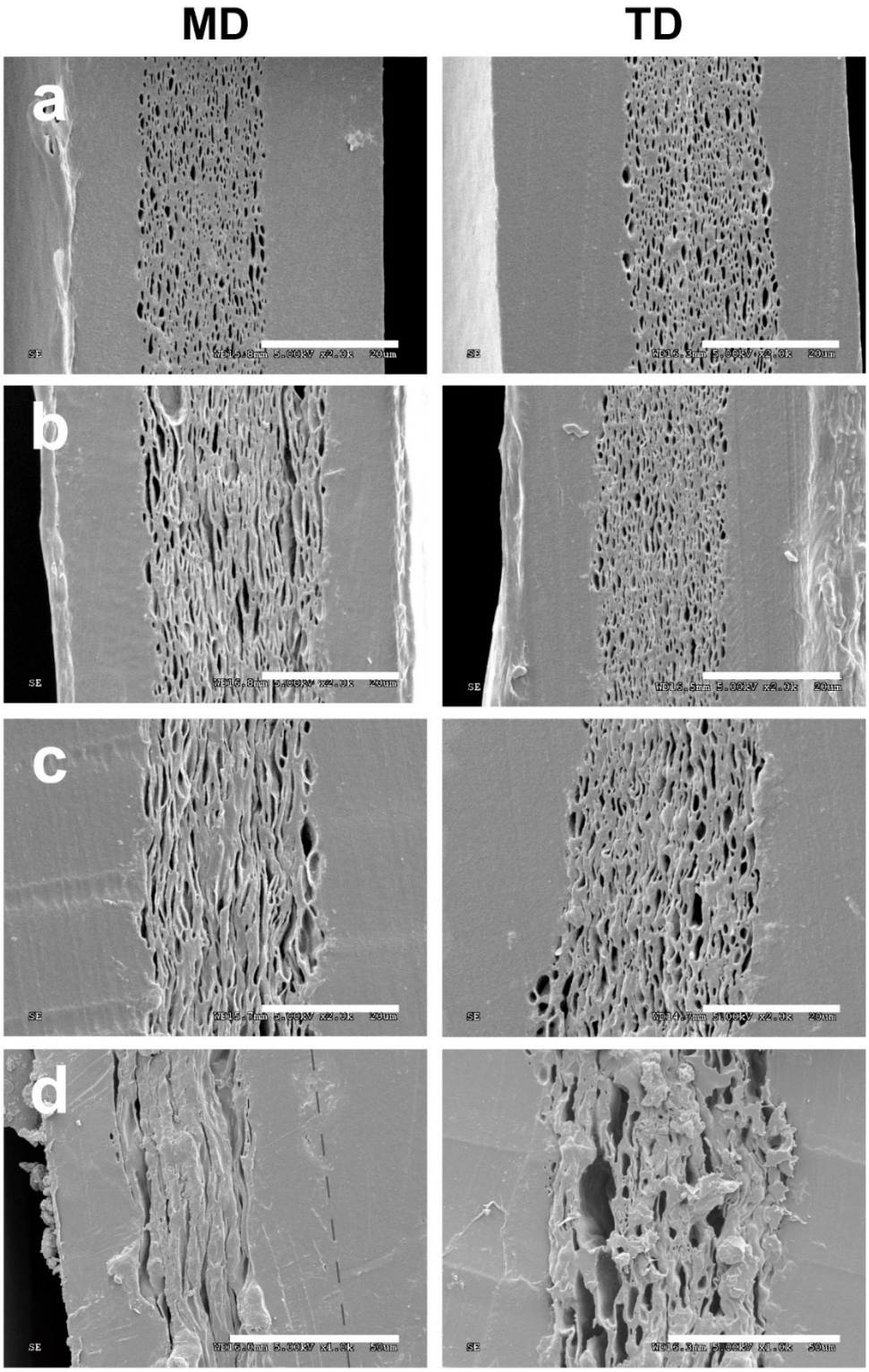

Figure 6.3: Micrographs of 3-layer films in both machine (MD) and transverse (TD) directions consisting of PE2 outer layers and inner layer containing a 20 wt% compatibilized blend of PE1 with: (a) 50 wt%, (b) 60 wt%, (c) 70 wt% and (d) 80 wt% TPS. The dash lines indicate the limit of the outer layer. The bar represents 20 µm except for (d) where it stands for 50 µm.

As explained previously, the compatibilizer is essential for blend stabilization and layer adhesion. It is interesting to investigate the effect of the compatibilizer content in the inner layer on the film structure and properties and also to determine if the addition of the compatibilizer in the LDPE outer layer could provide a more efficient path to minimize compatibilizer usage. To this purpose, the blends with 5 and 10 wt% compatibilizer were extruded into 3-layer films. Surprisingly, even though the blend morphology was relatively similar for the 5, 10 and 20 wt% compatibilizer, the film properties were strikingly different with the 5 and 10% compatibilizer blends exhibiting generalized delamination. In a subsequent experiment, the compatibilizer was added to the LDPE outer layer to see if this could reduce the delamination problem. Figure 6.4 shows micrographs of these 3-layer films. The film comprised an inner layer containing 60 wt% TPS in PE1 with 5 and 10 wt% compatibilizer respectively. A level of 20 wt% compatibilizer was added to the PE2 outer layers. Again, both films showed poor interlayer adhesion and were easy to delaminate. The morphology was found to be highly continuous with 5 wt% compatibilizer whereas PE fiber-like structures were observed at 10 wt% compatibilizer. It is interesting to reflect on the compatibilization mechanism in the current processing sequence. The compatibilizer is a reactive terpolymer comprising maleic anhydride units. The terpolymer is expected to provide compatibilization between the LDPE and starch macromolecules through the creation of a covalent link between the maleic anhydride moieties and the hydroxyl moieties of starch. The end-result of this reaction is a branched copolymer of starch with ethyl - ethyl acrylate branches that will be produced in situ at the interface. This branched copolymer is ultimately the molecule that will modify the interfacial tension of the blend. How can a 5 wt% level be seemingly sufficient to compatibilize the blend at the end of the twin-screw compounding step but be clearly insufficient to produce good interlayer adhesion after the blown film production step? The answer may lie in the generation of new interface during the film blowing process. In fact, to obtain high aspect ratio structures such as those observed in Figure 6.3, the TPS droplets present at the end of the compounding step must be deformed and possibly coalesced into lamellas and fiber-like structures during the flow in the film extrusion die and during the subsequent stretching after die exit. If this new interfacial surface is created at a rate or to an extent where it cannot be covered by the compatibilizer, the result will be that un-compatibilized interface will be produced.

This will lead to a weaker LDPE/TPS interface and the film will delaminate either within the inner TPS/LDPE layer or at the layer interface. This could explain why seemingly correct compatibilizer levels at the end of the compounding step are not sufficient after film formation. The addition of the reactive terpolymer in the outer layer could have alleviated this effect but in this case, the problem is that the terpolymer is diluted in the bulk of the LDPE layer and is therefore not as readily available for reaction at the interface. Also, compared to a twin-screw compounding step, the contact time between the compatibilizer and the TPS phase is much smaller since the contact between the materials occurs only at the end of the extrusion die. The compatibilizer used in this way was therefore totally ineffective. Based on the observations above, the reactive terpolymer level was kept at 20 wt% (of the LDPE content) and was introduced in the twin-screw compounding step for the remainder of the study.

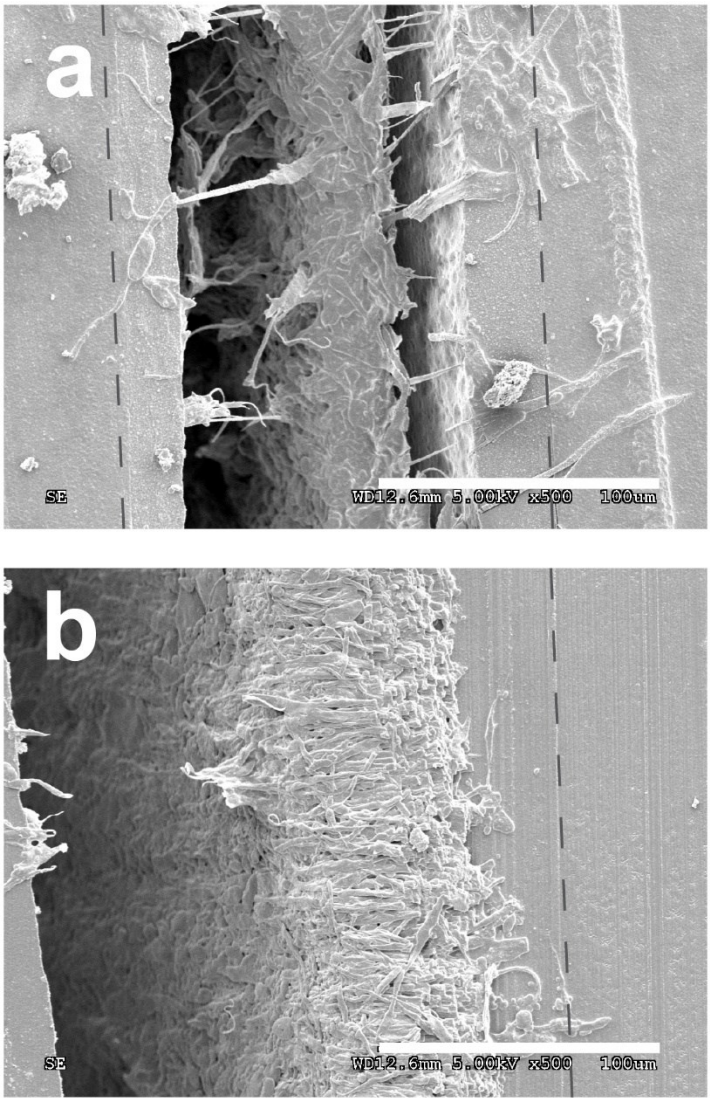

Figure 6.4: Micrographs of 3-layer films consisting of a mix of PE2 with 20 wt% compatibilizer as outer layers and an inner layer containing a blend of TPS/PE1 (ratio 60/40 in weight) with: (a) 5 wt% and (b) 10 wt% compatibilizer with regard to the PE phase. The dash lines are drawn to guide the eye to see the limit of the outer layer. The bar represents 100 µm.

6.5.2 Effect of clays on film structure

Using minerals with a very high aspect ratio such as clay can be an asset for gas barrier enhancement because it creates a more tortuous path for the diffusion of molecules through the film. In the following section, the effect of adding natural and modified clay will be reviewed. Table 6.1 presents a qualitative description of all produced films. The minimum achievable film

thickness was reported. Other criteria such as gels frequency in the film, bubble stability during the process and final film quality were rated from 1 (poor) to 4 (excellent) for each formulation with pure LDPE being the reference. Gels can be defined as non-gelatinized starch particles. The film quality assessment included its general aspect, smoothness and the distribution of the TPS phase in the inner layer. The PE reference was easily extruded into gel-free, high quality, 50 µm 3-layer films. Small gels appeared with the use of TPS, giving a cloudy aspect to the film. Corn-based samples were found to have less gels than potato ones. Moreover, corn-based films showed a better bubble stability and therefore were easier to process than potato-based films. Previous works highlighted the difference in viscosity from corn to potato starch TPS in such system. Potato-based TPS was found to be more viscous than corn (Mazerolles et al., 2019). This may explain why corn starch formulations were easier to process.

Using natural clay led to an improved bubble stability and much smoother films with a homogeneous distribution of the TPS, no matter the starch type. For example, the films with a high potato TPS content of 70 wt% in the inner layer were rated poor in terms of gel content but were easy to process and much clearer than the films described in Figure 6.3c when adding 1 wt% natural clay. Adding 1 wt% natural clay to potato-based films also reduced the number of gels. However, the organo-modified clay did not improve the film processability and appearance for any of the two starches. Furthermore, the materials with 1 wt% organo-modified clay in potato TPS could not be formed into films thinner than 160 µm and were highly textured. It is noteworthy that the same proportion of compatibilizer was used in all films and that the final layer adhesion was very good in all cases except for the sample with modified clay. The reduction of interlayer adhesion in the case of modified clay may result from their migration to the interface. The modification of clays is obtained by the intercalation of organic molecules such as quaternary ammonium surfactant that have a greater affinity towards the non-polar LDPE phase. In the course of the intense mixing during twin screw compounding, the modified clay may preferentially locate at the interface between TPS and LDPE. Since the surfactant are low molecular weight chemicals, they cannot entangle with the LDPE chains and therefore cannot contribute to interlayer adhesion in the solid state. In the case of natural clay, improvement in blown film processing has been reported for polyester/TPS blend. The authors attributed the

improvement to better retention of the plasticizer in the TPS phase due to limited plasticizer migration and evaporation. This led to a lowering of the TPS viscosity and an improvement of processability (McGlashan & Halley, 2003).

Table 6.1: Qualitative description of all produced films

Sample ID	Inner layer composition	Minimum film thickness achievable (μm)	Gels	Bubble stability	Quality of the film
Corn S60	Corn 60wt%	75	3	4	3
Corn S60 C1	Corn 60wt%, natural clay 1wt%	64	3	4	4
Corn S60 C3	Corn 60wt%, natural clay 3wt%	95	3	4	4
Corn S60 C5	Corn 60wt%, natural clay 5wt%	86	3	3	2
Corn S60 C1M	Corn 60wt%, modified clay 1wt%	80	3	2	2
Corn S60 C3M	Corn 60wt%, modified clay 3wt%	100	3	1	2
Potato S60	Potato 60wt%	82	1	1	2
Potato S60 C1	Potato 60wt%, natural clay 1wt%	75	2	4	4
Potato S60 C3	Potato 60wt%, natural clay 3wt%	78	2	4	4
Potato S70 C1	Potato 70wt%, natural clay 1wt%	80	1	3	3
Potato S60 C1M	Potato 60wt%, modified clay 1wt%	160	1	1	1
PE2		50	4	4	4

The blend rheology and morphology were investigated to understand the origin of the processability and appearence improvement in the presence of clay. Figure 6.5 presents the viscosity as a function of shear rate for PE1 and its blends with potato-based TPS at 160°C. The clay content was varied from 1 to 3 wt%. All formulations were highly shear-thinning (power-law index around 0.3) and showed no sign of a Newtonian plateau in the investigated shear rate

range. The viscosity curves were found to be in a narrow range for all formulations with the most viscous material being PE1. The blend comprising 60 wt% TPS was only around 5% less viscous compared to the reference polyethylene. Addition of natural clay led to a viscosity that was intermediate between those of the TPS/PE blend and PE1 while the addition of the modified clay led to a slight reduction of the blend viscosity. The slight viscosity increase was expected since the viscosity of suspensions is known to increase with the solid particulate concentration. The slight decrease in the case of the modified clay may be due to degradation or plasticization effect related with the organic portion of modified clay. Regardless of the particular sequence leading to the slight rheological differences, it seems clear that the important processing improvement observed in the presence of the natural clay (or *a contrario*, the poorer performance observed with organo-modified clay) cannot be explained by some radical changes in rheological behavior.

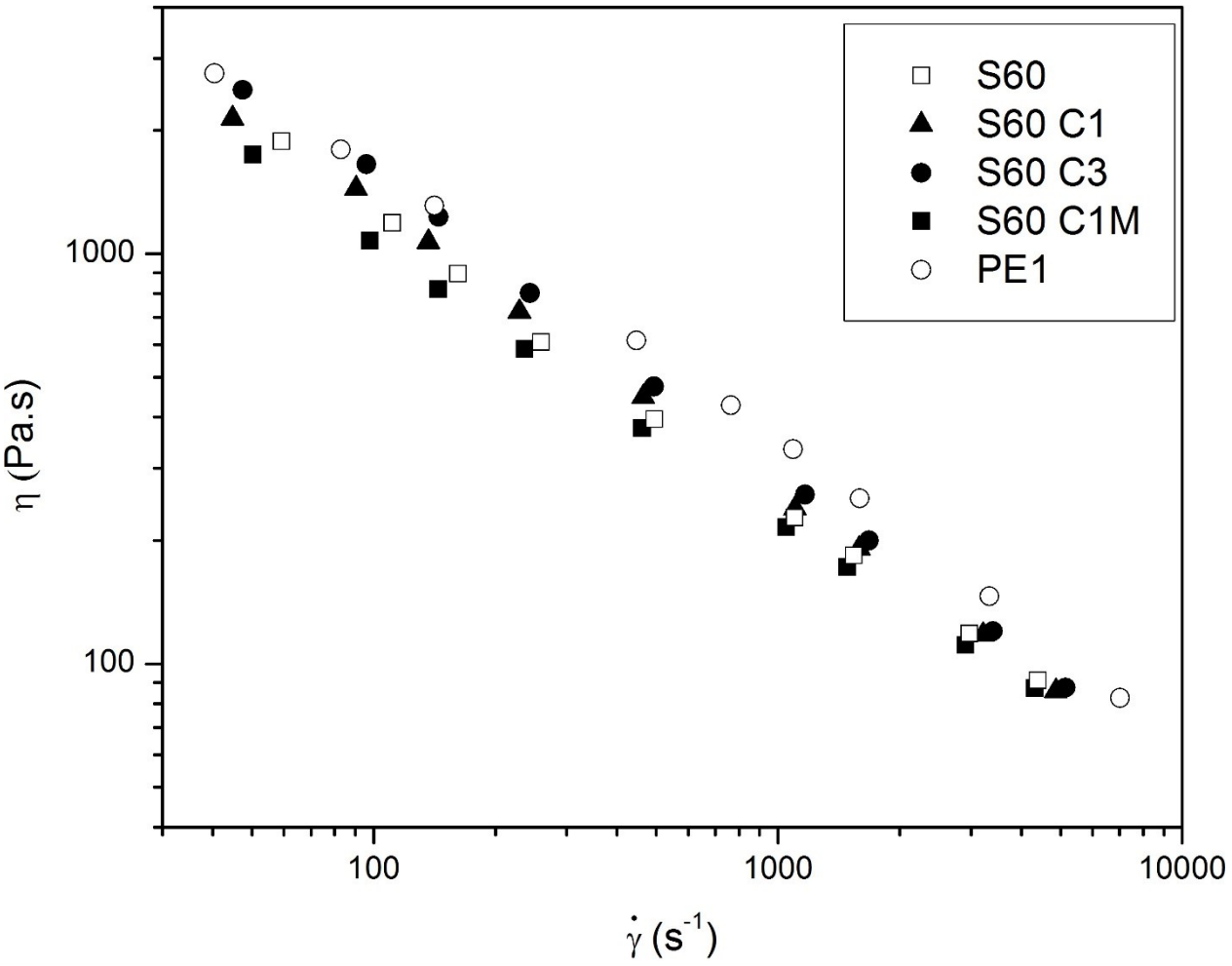

Figure 6.5: Viscosity as a function of shear rate at 160°C for PE1 and the corresponding blends with potato-based TPS and increasing content of natural and modified clays (see Table 6.1 for nomenclature)

Figure 6.6 presents scanning electron micrographs of microtomed surfaces of TPS/PE1 samples with various contents of natural and modified clays. All blends contained 60 wt% potato TPS compatibilized with 20 wt% compatibilizer on a PE basis. Figure 6.6a shows the reference blend without any clay whereas Figure 6.6b and Figure 6.6c show blends with respectively 1 and 3 wt% natural clays with regards to the TPS phase. Finally, Figure 6.6d displays blends with 1 wt% organically modified clays. All blends showed dispersed TPS droplets in PE. Smaller TPS droplet size were found with the addition of clay. The volume average diameter was 2.75 µm for the TPS/PE blend reference. The d_v dropped to 1.84 and 1.24 µm respectively for 1 and 3 wt% natural

clay. For the blend comprising modified clay, d_v was equal to 1.35 µm. The dispersity index was between 1.5 and 2.0 in all cases. The effect of clay therefore seemed to be more important on the dispersed phase size than on the rheological characteristics of the blend. This points to an additional compatibilization effect between the blend components. One potential explanation is that despite its affinity for the TPS phase, a small fraction of natural clay may be positioned at the interface. This effect has been found in blends of PE and PBT where clay was found to locate at the interface regardless of its greater affinity for the PBT phase and acted as a compatibilizer (Hong, Kim, Ahn, Lee, & Kim, 2007). In immiscible blends of corn-based TPS with polypropylene (Ferreira, Khalili, Figueira, & Andrade, 2014) and polyethylene (Sabetzadeh et al., 2016), enhanced compatibility between blend components was also found with the addition of clays. A potential interpretation of this result may be that, when properly exfoliated, the clay leaflets can position at the interface and effectively decrease the blend's interfacial tension. This apparent reduction in interfacial tension and potential barrier to coalescence may therefore explain the significant TPS phase size reduction.

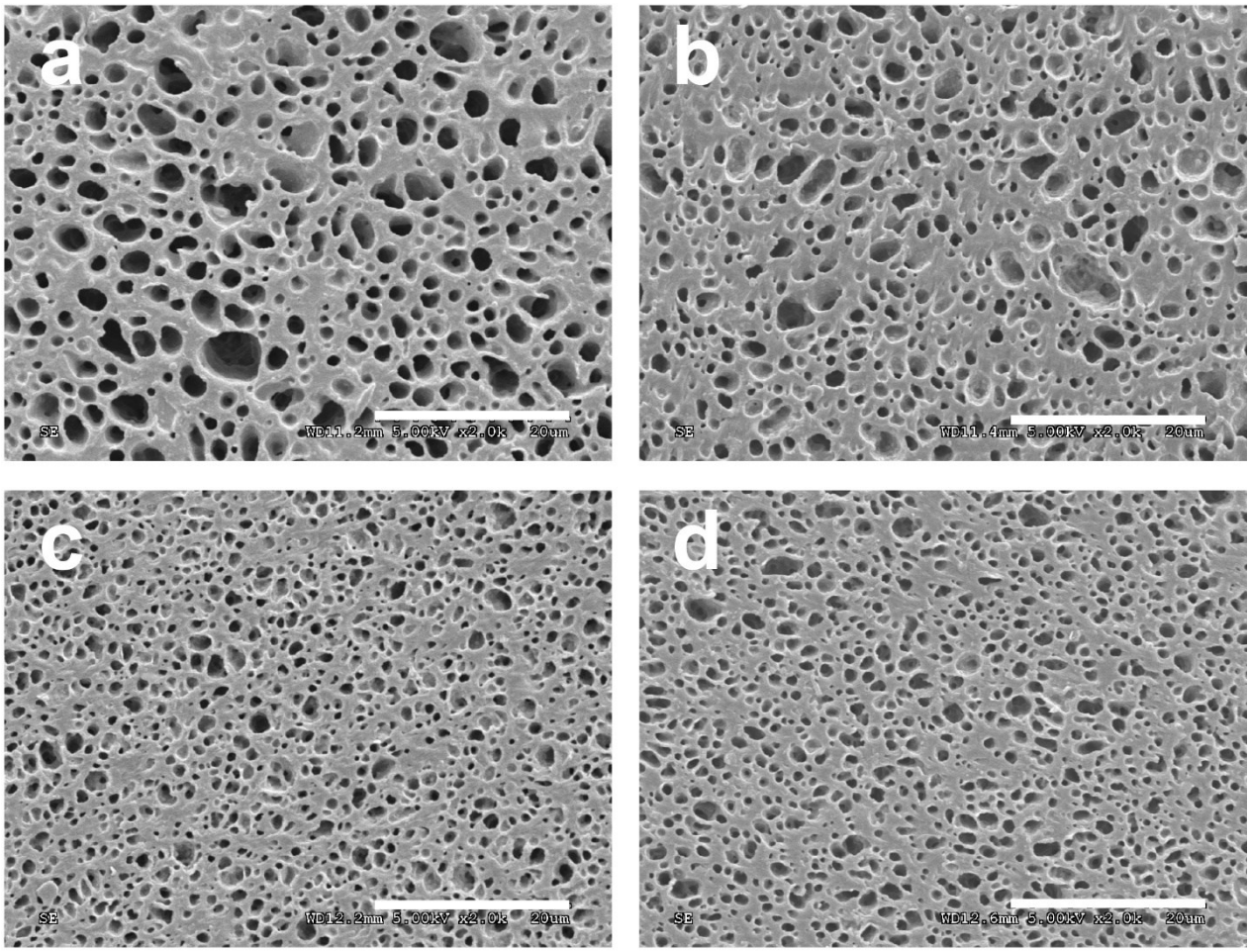

Figure 6.6: SEM micrographs of 60 wt% potato TPS in PE1: (a) reference, (b) with 1 w% natural clay, (c) with 3 wt% natural clay and (d) with 1 wt% modified clay. The bar represents 20 µm.

In order to evaluate the impact of clay on the film processing and the development of blend morphology, the blown films were produced at a fixed forming ratio of 3. Figure 6.7 presents SEM micrographs of key formulations in both MD and TD. Figure 6.7a shows the reference formulation with 60 wt% TPS in the blend whereas Figure 6.7b and Figure 6.7c display the same blend with 1 wt% natural and organically modified clays respectively. Figure 6.7d presents the morphology of a film with 70 wt% TPS and 1 wt% natural clay in the core.

SEM images for the reference 60 wt% potato TPS sample and the same formulation with 1 wt% natural clay showed similar small elongated TPS lamellas. These lamellas were slightly more elongated along MD due to the fact that stretching was three times higher in that direction. In

the case of the films with modified clay and high TPS loading, the extraction was not as successful thus making the observation difficult. It seems that the increased continuity in the TPS phase lead to a collapse of the film structure after acid-etching. However, a close observation showed the presence of lamellar structures. At 70 wt% TPS with natural clay, the film displayed large holes and a rough surface. On the other hand, the smaller TPS phase size observed in Figure 6.6d when adding modified clay may have led to very thin elongated TPS domains in the film.

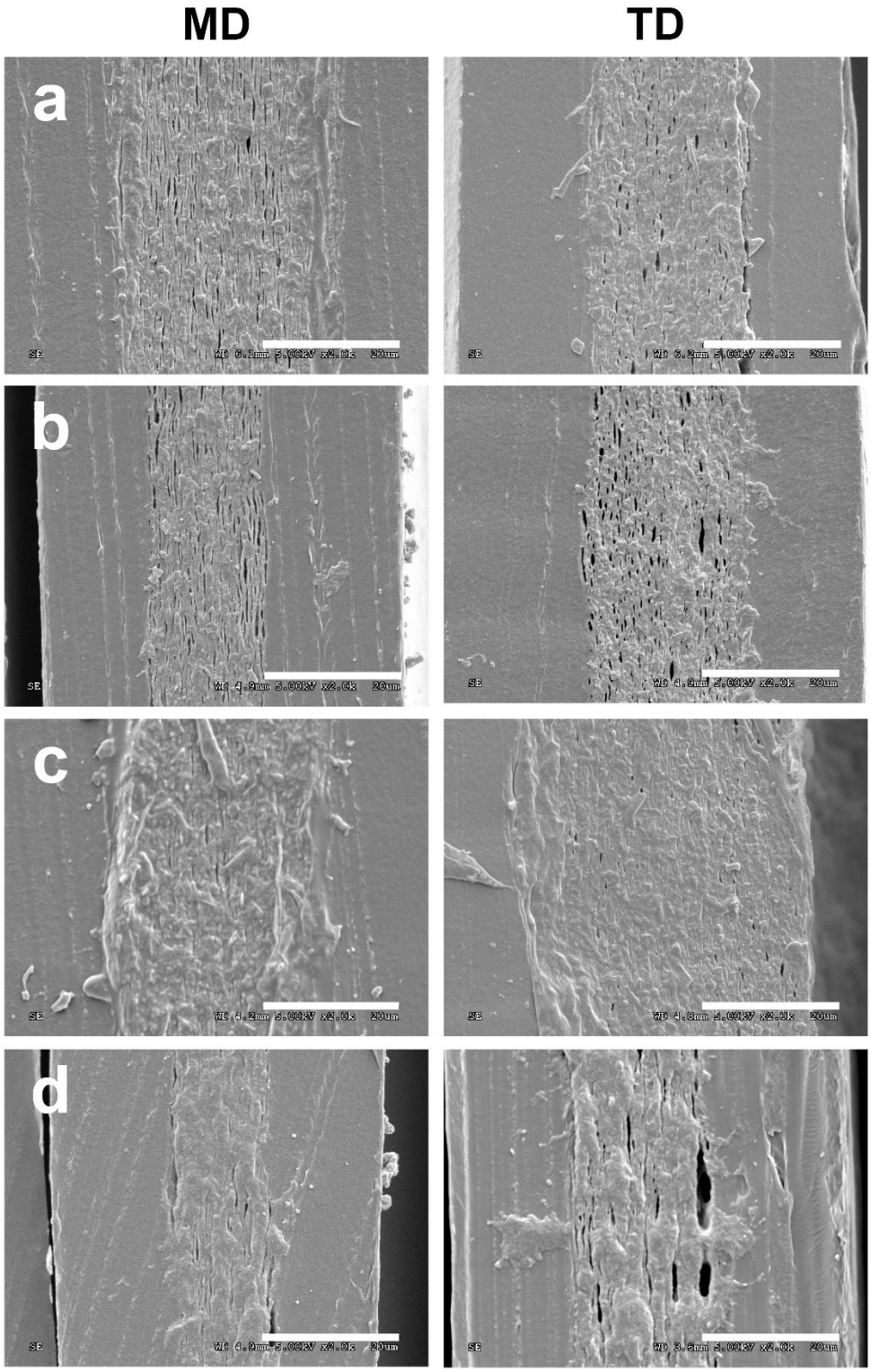

Figure 6.7: SEM micrographs of 3-layer films in both machine (MD) and transverse (TD) directions consisting of PE2 outer layers and inner layer containing a blend of PE1 with (a) Potato S60, (b) Potato S60 C1, (c) Potato S60 C1M and (d) Potato S70 C1. The bar represents 20 µm.

Figure 6.8 shows SEM images of the morphology of 3-layer films produced using the same blown film process as described previously yet with corn starch based TPS. In Figure 6.8a, the inner layers was made out of 60 wt% corn-based TPS. Figure 6.8b and Figure 6.8c present the same blend but with the addition of 1 and 3 wt% natural clays respectively. All the corn TPS films presented in Figure 6.8 showed lamellar morphology, more elongated along MD. Adding 1 wt% clay decreased slightly the TPS phase size, leading to thinner elongated plates. The reference without clay and the formulation with 3 wt% natural clay were found to have very similar morphologies. This highlights that a small concentration of clay, i.e. 1 wt%, is sufficient to cause the compatibilization effect. Globally, the effect of clay on film morphology was the same for potato and corn-based samples.

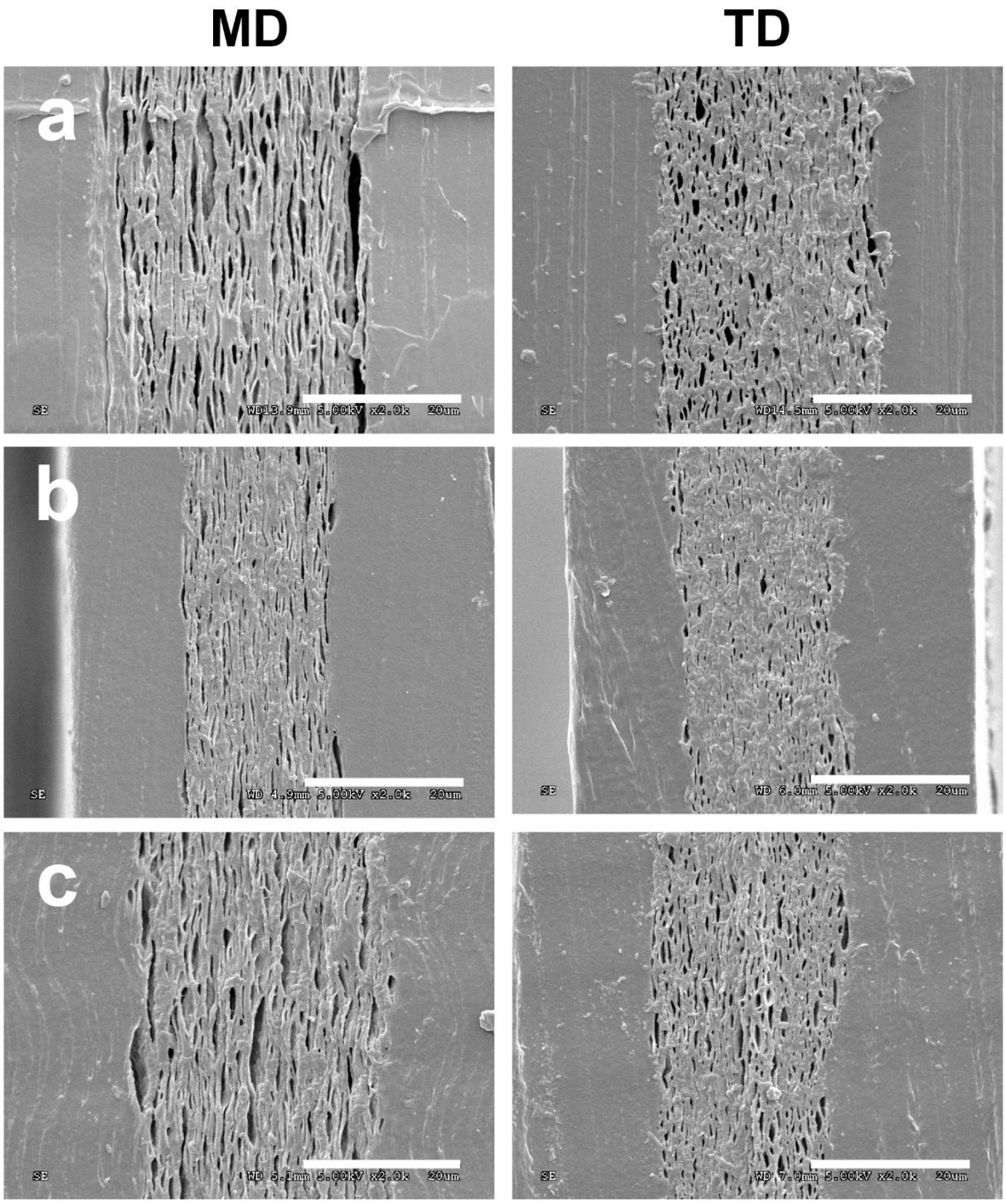

Figure 6.8 : SEM micrographs of 3-layer films in both machine (MD) and transverse (TD) directions consisting of PE2 outer layers and inner layer containing a blend of PE1 with (a) Corn S60 (b) Corn S60 C1 and (c) Corn S60 C3. The bar represents 20 µm.

Exfoliation of clay particles would be an asset for gas barrier properties since it leads to a more tortuous path for the gas molecules thus reducing permeability. The level of exfoliation of clay particles was investigated using wide-angle X-ray diffraction. Figure 6.9a presents X-ray diffractometry results for the natural clay as well as corresponding blends of potato and corn-based with LDPE containing 1 and 3 wt% clay.

Natural clay showed an intense diffraction peak at 2θ=7.5° corresponding to a spacing between the platelets of 11.8 Å. All blends showed a diffraction peak of various intensities around 2θ=5° corresponding to the clay particles. This means that the spacing between the clay platelets was increased to 17.6 Å and therefore indicates that intercalation of polymer molecules between the clay platelets has occurred. The presence of the diffraction peak corresponding to the clay was very clear in corn-based blends and its intensity increased when increasing clay content. This also confirmed the increase in the fraction of non-exfoliated particles at high clay loading. However, a very weak signal was observed for potato-based blends. For both blends with 60 and 70 wt% potato TPS, the peak intensity was very low with 1 wt% clay. Increasing clay content to 3 wt% increased the peak intensity. This indicates that for the same clay content, the fraction of exfoliated particles is higher in potato-based blends compared to corn-based ones. Native potato starch naturally contains more moisture than corn starch. This extra moisture may be responsible for the extra clay exfoliation since both starch powder and clay particles are mixed together in the extruder.

Complete exfoliation of clay would maximize the tortuous path around clay platelets especially if all the platelets were positioned parallel to the axis of the film. 2D X-ray diffraction figures can be very useful in determining particle orientation. Intensity peaks at specific values of the azimuthal angle gamma (γ) on the diffraction circle will show any preferential orientation. Figure 6.9b to Figure 6.9g present 2D-SAXS diffraction figures for the 3-layer films for potato and corn starch-based TPS inner layers with various amount and type of clays. Figure 6.9b is the reference formulation with potato TPS whereas Figure 6.9c and Figure 6.9d show potato-based films with 1 and 3 wt% natural clays respectively. Figure 6.9e present the potato-based film with 1 wt% modified clays. Finally Figure 6.9f displays corn-based TPS with 3 wt% natural clays and Figure 6.9g 3 wt% modified clays, for comparison purposes.

According to the X-ray measurements made on blends before film blowing, the peak corresponding to the clay in the film was expected at 2θ=5° for the natural clays and 2θ=2.3° for the modified ones. As explained in the experimental section, in order to see the orientation when the signal is weak, an azimuthal integration of the signal for γ=0 to 360° in the range 2θ=4.4-5.5° for natural clays and 2θ=1.8-2.8° for modified clays is presented beside every SAXS image. In the case of the reference formulation in Figure 6.9b, no variation in intensity was measured at both studied zones. When adding 1 and 3 wt% natural clays, only a very weak signal appeared in the 2θ=5° area. The weak intensity of the signal confirmed that only a small fraction of non-exfoliated clay particles remained. Moreover, the radial integration showed a stronger intensity at γ=90° and γ=180° of about 15 and 40% for 1 and 3 wt% added clays respectively. This means that non-exfoliated particles showed a preferential orientation parallel to the film i.e. along the stretching direction. It was not surprising since blown film processing allows a higher orientation comparing to other processes like cast film due to the high stretching when blowing the bubble. The same behavior was observed with modified clays (c.f. Figure 6.9e) with a very weak oriented signal in the 2θ=2.3° region. A striking difference was observed with the corn-based samples. The diffraction patterns were much more intense meaning a much higher fraction of non-exfoliated particles in the film. An increase of around 30% in peak intensity was observed between the potato-based film with 3 wt% natural clay (Figure 6.9d) and the same formulation with corn starch (Figure 6.9f). This confirms the extra exfoliation of clay in potato-based TPS observed in the blends in Figure 6.9a. However the same preferential orientation was observed with a stronger intensity around γ=90° and γ=180°.

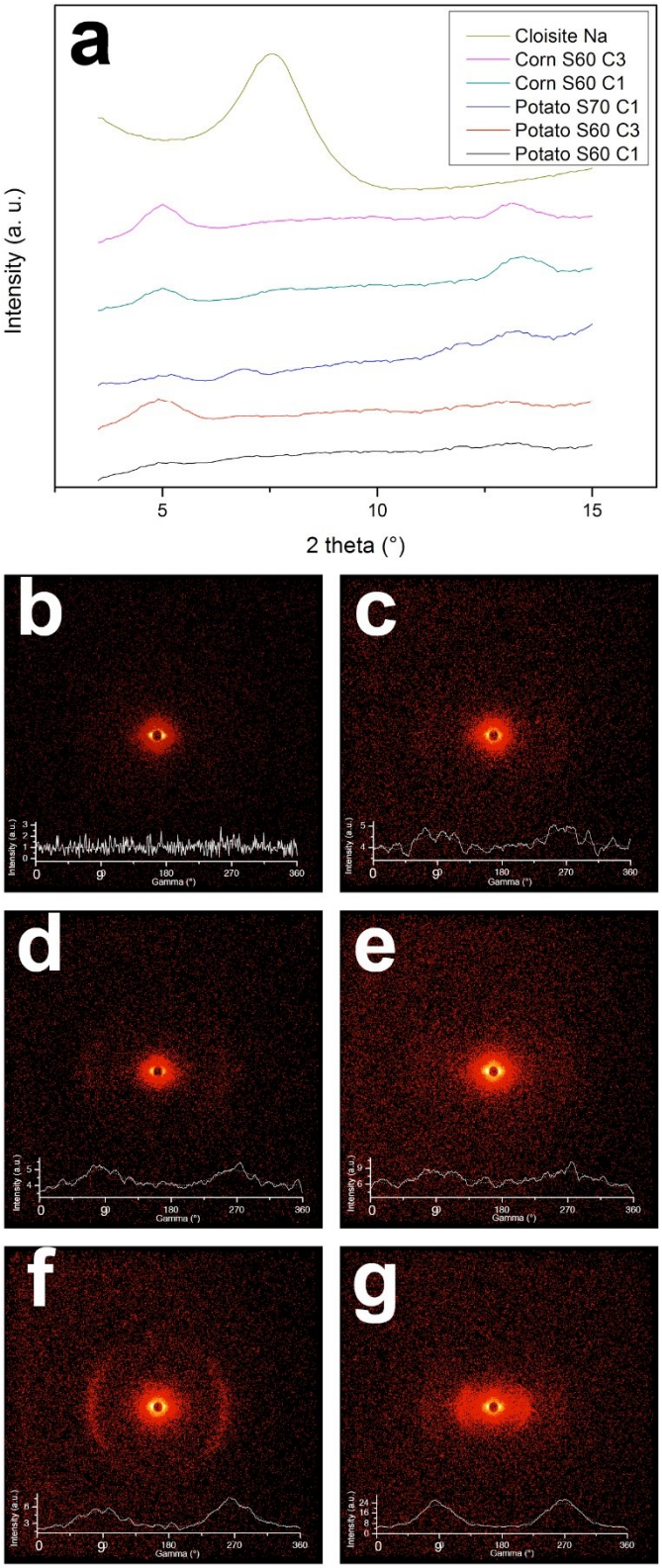

Figure 6.9: (a) WAXD pattern of pure clay as well as potato and corn-based blends with different clay content. SAXS photographs of multilayer films with: (b) Potato S60, (c) Potato S60 C1, (d) Potato S60 C3, (e) Potato S60 C1M, (f) Corn S60 C3 and (g) Corn S60 C3M.

6.5.3 Effect of clay on film properties

Table 6.2 presents an overview of the studied physical properties of the film, namely mechanical, oxygen permeability and transparency. The results are presented for multilayer films comprising both potato and corn-based inner layer blends with increasing amounts of natural and modified clays. A 3-layer system consisting of pure LDPE is used as a reference. This reference showed a Young's modulus of 201 MPa in MD and 174 MPa in TD as well as an elongation at break of 506% in MD and 690% in TD. The maximum tensile stress was of 22 MPa in both directions. The difference between MD and TD is related to the difference in stretching during processing. Globally, the incorporation of 60 wt% potato TPS in the inner layer decreased the mechanical properties. Young's modulus decreased by 40% along MD yet stayed constant along TD compared to LDPE. Moreover, the elongation at break dropped by around 30% and the maximum tensile stress dropped by a factor 2. Corn-based films showed similar results yet the elongation at break decreased only by around 25%. The addition of clays did not change this tendency. The lowest mechanical properties were obtained with the modified clays in potato-based samples. In that case, the samples exhibited around half the Young's modulus and only 15% of the elongation at break compared to LDPE. It is noteworthy that extensive delamination was observed in the case of the material comprising organo-modified clay (i.e. Potato S60 C1M) during testing. The decrease in mechanical properties when adding TPS was expected since TPS's modulus is around 10 times lower than that of pure LDPE (Van Soest, Hulleman, et al., 1996a). A similar decrease in mechanical properties of TPS/LDPE blends at high TPS content was reported in the literature. Mortazavi et al. reported around half the tensile strength and two thirds of the modulus for LDPE/TPS blends containing 60% TPS compared to pure LDPE (Mortazavi et al., 2013). Sabetzadeh et al. mentioned that the use of organo-modified clay in LLDPE/LDPE/TPS films increased mechanical properties yet with a much smaller TPS amount of 15 wt% (Sabetzadeh et al., 2016).

The investigated films showed high transparency with a percentage of transmitted light over 87% for all samples at the studied wavelengths. Adding TPS or clay did not significantly alter the transparency. It is noteworthy that in order to characterize the amount of light scattered by the film, diffusion measurements were carried out on selected samples. As a reference, pure LDPE

showed 18% transmitted light lost in diffusion at λ=400nm and 8% at λ=800nm, whereas films with potato TPS and potato TPS with 1 wt% natural clay showed 19 and 25% at λ=400nm as well as 11 and 16% at λ=400nm respectively. This latter aspect showed that the addition of TPS and clay with this procedure did not alter significantly the haze of the film as well. As a comparison, Sabetzadeh et al. reported percentages of transmitted light between 51 and 68 % for films of LLDPE/LDPE/TPS with up to 5 wt% modified clay (Sabetzadeh et al., 2016).

As expected, a high permeability value of 1845 $cm^3.m^{-2}.day^{-1}.atm^{-1}$ for a 100 µm thick LDPE film was found. Adding TPS lead to a significant reduction in permeability. Adding 60 wt% potato-based TPS was found to decrease the permeability by a factor 10 compared to LDPE. Corn starch samples at the same concentration showed the same tendency yet with a permeability value twice as high as with potato starch. The best results in terms of permeability reduction were achieved with the higher potato TPS content of 70 wt% (with 1 wt% clay): the oxygen permeability was found to be 20 times lower than that of pure LDPE. The improved barrier can be explained by the high level of continuity of the blend. At 60 wt% TPS, the blend morphology in the inner layer was lamellar but not fully co-continuous, as observed in Figure 6.7. Increasing the TPS content to 70 wt% pushed the blend morphology toward a co-continuous lamellar morphology and thus dramatically improved the gas barrier effect.

At 60 wt% TPS, the addition of natural clay did not lower the oxygen permeability. In fact, the reported values were found to be two to three times higher than those of the corresponding 60 wt% TPS films, no matter the starch type. Modified clays yielded a very high permeability in the case of potato-based sample, even higher than pure LDPE. This is consistent with the low quality of the films possibly associated to non-homogeneous distribution of the TPS and high number of gel defects. The addition of modified clay in corn-based samples led to a slight reduction in permeability. This suggests that the effect of the clay on permeability may be indirect, through differences in the TPS/LDPE blend morphology, rather than through the classical tortuous path explanation. In the case of the 60 wt%TPS blends with natural clay, the smaller dispersed phase size found at the end of the compounding steps may lead to smaller lamellas or a less continuous

morphology after film formation. Thus, the potential benefit of a longer tortuous path due to the presence of clay may be overwhelmed by the change in the overall blend morphology. The usefulness of clay in this context lies in the fact that it enables the formation of films at higher TPS content. For example, the 70 wt% TPS film which showed the best overall permeability reduction was not achievable without the stabilizing effect that clay brings for the film processing. Even though unexpected, this effect may prove to be a precious contribution in the preparation of quality multilayer LDPE/TPS films for packaging applications.

Table 6.2: Mechanical properties, oxygen permeability and transparency of all studied films

	Young's modulus (MPa)		Elongation at break (%)		Maximum tensile stress (MPa)		Oxygen permeability ($cm^3*m^{-2}*day^{-1}*atm^{-1}*[100\mu m]$)	Transparency for 100µm (%T)		
	MD	TD	MD	TD	MD	TD		λ=400 nm	λ=600 nm	λ=800 nm
Corn S60	126 ± 6	125 ± 3	400 ± 14	424 ± 8	12,0 ± 0,6	10,0 ± 0,3	273 ± 17	88,1	89,6	90,2
Corn S60 C1	136 ± 8	156 ± 3	300 ± 28	329 ± 73	13,0 ± 1,0	10,0 ± 0,4	316 ± 10	87,46	88,46	88,76
Corn S60 C3	139 ± 3	159 ± 5	251 ± 51	392 ± 23	12,0 ± 0,8	10,0 ± 0,6	372 ± 9	87,5	89,2	89,8
Corn S60 C5	134 ± 7	152 ± 5	269 ± 48	420 ± 33	13,0 ± 0,7	11,0 ± 0,7	447 ± 11	87,44	89,14	89,74
Corn S60 C1M	141 ± 14	154 ± 11	254 ± 32	271 ± 92	10,0 ± 0,5	8,0 ± 1,0	202 ± 5	87,3	88,7	89,3
Corn S60 C3M	138 ± 12	154 ± 6	281 ± 34	299 ± 67	10,0 ± 1,0	8,0 ± 1,0	140 ± 3	88,4	89,7	90,2
Potato S60	144 ± 14	172 ± 25	159 ± 39	258 ± 35	12,0 ± 1,0	10,0 ± 1,0	167 ± 4	88,08	89,08	89,68
Potato S60 C1	145 ± 6	163 ± 8	181 ± 17	219 ± 56	13,0 ± 1,0	9,0 ± 0,4	334 ± 9	88,22	89,22	89,82
Potato S60 C3	172 ± 8	185 ± 6	165 ± 25	130 ± 20	13,0 ± 1,0	9,0 ± 0,3	414 ± 13	87,7	88,8	89,4
Potato S60 C1M	98 ± 5	114 ± 4	109 ± 26	74 ± 41	9,0 ± 1,0	7,0 ± 0,4	5130 ± 71	89,5	90,5	91
Potato S70 C1	136 ± 9	158 ± 5	110 ± 14	116 ± 22	11,0 ± 0,4	8,0 ± 0,3	100 ± 3	87,6	88,5	88,9
PE2	201 ± 21	174 ± 14	506 ± 84	690 ± 35	22,0 ± 5,0	22,0 ± 2,0	1845 ± 50	89,28	88,98	88,38

6.6 Conclusion

This paper describes the successful development of a 3-layer film with an inner layer composed of a TPS/LDPE blend and of LDPE outer layers that exhibits good oxygen and water vapor barrier. The originality of the approach resides in the fabrication of the TPS/LDPE blend as a first step and in the continuous blown film production of the 3-layer film without the use of a tie layer. One key in the development of the multilayer film was the incorporation of a sufficient amount of a reactive terpolymer (i.e. 20 wt% based on the LDPE fraction) as compatibilizer during the blend compounding step. The compatibilizer is necessary to obtain proper dispersion but it was shown that the necessary amount to obtain good film quality and prevent film delamination is much higher that the concentration required to get proper emulsification. This was attributed to the fact that a large interfacial area is created during the film blowing process and that sufficient interfacial agent must be present to cover this area and prevent loss of interlayer adhesion. It was found that the compatibilizer is much more effective for layer adhesion when used directly during blend compounding than when mixed to the LDPE layers.

A second key finding in this study is that the addition of natural clay into the TPS/LDPE blend improves drastically the processing of the 3-layer film. Producing a stable and thin film containing up to 70 wt% TPS was made possible by adding 1 wt% natural clay. The clay platelets were found to be partially exfoliated in the blend. Non-exfoliated particles showed a preferential orientation parallel to the blown films.

Overall, it was shown that multilayer films produced with the method described above have adequate mechanical properties and a transparency equivalent to that of pure LDPE while exhibiting interesting oxygen permeability reduction. Films with an inner layer comprising 60 wt% TPS can exhibit a 10-fold permeability decrease compared to the LDPE reference while films with a 70 wt% TPS level can reach a 20-fold decrease.

CHAPTER 7 CONCLUSIONS AND RECOMMENDATIONS

7.1 Conclusions

7.1.1 French version

Dans cette thèse, le développement de la morphologie de mélanges d'amidon thermoplastique et de polyéthylène basse densité autour de l'inversion de phase a été étudié et ce à la suite du malaxage du mélange et après une étape de mise en forme par soufflage de pellicules. Deux sources d'amidon sont pour cela étudiées : amidons de pomme de terre et de maïs. Les conditions menant à la production de films soufflés 3 couches de bonne qualité ont été élucidées et ceci a mené à la réalisation de pellicules aux propriétés barrières aux gaz améliorées.

La première partie de la thèse se concentre sur l'influence de l'eau et du glycérol comme plastifiants de l'amidon sur le comportement rhéologique de ce dernier. Pour caractériser l'effet de ces plastifiants sur la viscosité du TPS, un modèle d'Arhenius modifié a été développé. Ce modèle permet ainsi une prédiction du paramètre de consistance de la loi de puissance en fonction de la température, de la quantité d'eau et de glycérol. Ce travail a permis de conclure que l'indice de loi de puissance qui caractérise la rhéo-épaississance du matériau, n'est pas affecté par la température et la composition du TPS. L'eau reste cependant le plastifiant le plus efficace de l'amidon comparé au glycérol. Le mélange TPS/LDPE est ensuite réalisé en deux étapes : l'amidon et son plastifiant sont mélangés manuellement avant d'être introduit dans une extrudeuse bi-vis pour y rencontrer le LDPE. Une autre conclusion importante du travail est que l'ajout d'un compatibilisant pour stabiliser la morphologie du mélange TPS/LDPE est absolument nécessaire à la stabilité du procédé de fabrication des pellicules. Dans le cas présent, le compatibilisant était un terpolymère commercial d'éthylène, acrylique ester et anhydride maléique. Ce compatibilisant a augmenté la viscosité du mélange comparativement aux composants purs et a entrainé la formation de structures plus fines dans le mélange. Ensuite, il a été mis en évidence que le rapport de viscosité entre les phases a un impact crucial sur la morphologie de mélange et le développement de la co-continuité. La transition d'une morphologie de phase dispersée à la co-continuité est apparue pour des concentrations en TPS

aussi basses que 50% en masse. Cependant, cette transition s'est trouvée déplacée vers des valeurs de concentration plus élevées quand le rapport de viscosité TPS/LDPE augmentait. Déplacer la zone de valeurs de concentrations dans laquelle la co-continuité se produit est donc rendu possible de deux façons différentes : changer la viscosité du LDPE ou modifier le type et/ou la quantité de plastifiant du TPS.

La seconde partie de cette thèse décrit la production de film soufflé à trois couches dont la couche centrale est un mélange TPS/LDPE. Le mélange était produit en une seule étape dans une extrudeuse bi-vis : l'amidon était introduit sec et le plastifiant était pompé directement dans l'extrudeuse. L'élément clé dans le développement de ce film multicouche est l'ajout d'une concentration critique de compatibilisant (i.e. 20% en masse de terpolymère réactif dans la fraction de LDPE) dans le mélange TPS/LDPE durant la phase de malaxage bivis. Il a été mis en évidence que cet ajout est nécessaire à la stabilité du procédé d'extrusion soufflage et à l'obtention d'une pellicule qui ne délamine pas. Il a été également démontré que cette concentration critique est plus importante que le minimum nécessaire pour obtenir une bonne émulsion. Ceci a été attribué au fait qu'une large surface interfaciale est créée pendant la mise en forme du film et que cela nécessite une quantité suffisante d'agent interfacial pour couvrir cette surface et éviter la perte d'adhésion entre les couches. De plus, le compatibilisant est utilisé de façon plus efficace lorsqu'il est introduit dans le mélange plutôt que dans les couches externes de LDPE.

L'impact de l'ajout d'argile naturelle et modifiée sur la mise en forme du film et ses propriétés finales a également été exploré. Une autre découverte clé de cette thèse est que l'ajout d'argile naturelle a facilité significativement la mise en forme du film 3 couches. La production d'un film stable et fin contenant jusqu'à 70% en masse de TPS en couche centrale a été rendu possible grâce à l'ajout de 1% d'agile naturelle. L'ajout d'argile à des concentrations supérieures à 1% n'a pas entraîné de changement significatif. On peut alors conclure qu'une concentration de 1% est suffisante pour améliorer la stabilité du procédé de soufflage. Basé sur l'analyse par diffraction de rayons X, il est possible de conclure à l'obtention d'une exfoliation partielle des argiles dans le mélange avec une fraction en particules exfoliées encore plus importante dans le cas des mélanges à base de pomme de terre. De plus, il a été mis en évidence que les particules d'argile

non exfoliées montrent une orientation préférentielle parallèle au film soufflé. L'addition d'argiles n'a pas eu d'effet sur la transparence du film ni altéré significativement les propriétés mécaniques.

Globalement, la méthode développée dans cette thèse permet la production de film multicouche présentant des propriétés mécaniques et une transparence équivalentes à celles du LDPE pur tout en réduisant drastiquement la perméabilité à l'oxygène. Le film 3 couches avec une couche centrale constituée à 60% en masse de TPS présentait une réduction d'un facteur 10 de la perméabilité à l'oxygène comparé au LDPE tandis que l'incorporation de 70% en masse de TPS entraînait une réduction d'un facteur 20.

7.1.2 English version

In this thesis, the morphology of blends of thermoplastic starch and low-density polyethylene around the phase inversion range has been studied after the blending step as well as after the film blowing process. Two starches from different botanical sources have been investigated: potato and corn starch. Moreover, this blend has been successfully used in a 3-layer blown film with improved gas barrier properties.

The first part of this thesis focused on the influence of water and glycerol as starch plasticizers on the rheological behavior of thermoplastic starch and on TPS/LDPE blend morphology development around the co-continuity range. In order to characterize the effect of water and glycerol plasticization on potato TPS viscosity, a modified Arrhenius-type model was developed. The model can be used to predict the power-law consistency parameter of TPS as a function of temperature, water content and glycerol content. It was found that the power-law index, indicative of shear-thinning, is unaffected by temperature and TPS composition. Water was found to have a stronger effect than glycerol on starch plasticization. The TPS/LDPE blends are produced in two steps: starch and plasticizer are manually mixed together before the introduction in the twin-screw extruder where the slurry meets the LDPE. Another important conclusion of this thesis is that adding a compatibilizer to stabilize the TPS/LDPE blend morphology is absolutely necessary

to obtain a stable film production process. In this case, the compatibilizer used was a random terpolymer comprising of ethylene, acrylic ester and maleic anhydride. The compatibilizer increases the blend viscosity compared to the neat components and provided finer blend structures. Moreover, the viscosity ratio of the blend was found to have a crucial impact on the blend morphology and the development of co-continuity. The transition from dispersed to co-continuous blend morphology appeared at concentration as low as 50 wt% TPS but this transition was pushed to higher concentration when the TPS/LDPE viscosity ratio was increased. Displacing the co-continuity concentration range is therefore made possible through two different ways: varying the LDPE viscosity or modifying starch's plasticizer type and/or amount.

The second part of this thesis dealt with the multilayer blown film extrusion of the TPS/LDPE blend. The blend was produced through a one-step process in a twin-screw extruder and then pelletized before film blowing. Instead of a slurry, dry starch was introduced directly in the twin-screw extruder where the plasticizer is being pumped. A 3-layer blown film consisting of the compatibilized TPS-LDPE blend as inner layer and two continuous LDPE outer layers was successfully produced. One key finding in the development of the multilayer film is the incorporation of a critical amount of compatibilizer (i.e. 20 wt% of a reactive terpolymer based on the LDPE fraction) in the TPS/LDPE blend during the twin-screw compounding. It was found to be necessary to achieve good film processing stability and avoid delamination. This critical concentration was found to be much higher than the minimum necessary for a good emulsification. This was attributed to the fact that a large interfacial area is created during the film blowing process and that sufficient interfacial agent must be present to cover this area and prevent loss of interlayer adhesion. Moreover, the compatibilizer is more effective when used directly in the blend and not in the outer layers.

The impact of both natural and modified clays on processing and final film properties of the multilayer film was also investigated. The second key finding of this thesis is that using natural clay improved drastically the processing of the 3-layer film. Producing a stable and thin film containing up to 70 wt% TPS in the inner layer was made possible by adding 1 wt% natural clay. Adding clay at concentrations higher than 1% did not significantly change film properties. It is then possible to conclude that 1% clay is sufficient to improve film processing stability. Based on

the X-ray diffraction results, it is also possible to conclude to a partial exfoliation of the clay particles in the blend with an even higher fraction of exfoliated platelets in potato-based blends. Moreover, non-exfoliated particles show a preferential orientation parallel to the blown film. The addition of natural clay did not alter the transparency nor decreased significantly the mechanical properties of the films.

Globally, the method developed in this thesis allows the production of multilayer films with adequate mechanical properties and transparency equivalent to that of pure LDPE while reducing tremendously the oxygen permeability. The 3-layer film with an inner layer consisting of 60 wt% TPS can exhibit a 10 times decrease in oxygen permeability compared to LDPE while 70 wt% TPS in the inner layer lead to a 20-fold decrease.

7.2 Recommendations

The following topics could be of interest for further investigation:

1) Starch is a biological material and is not as stable as synthetic polymers. In the 3-layer film, the TPS phase is protected from humidity by the LDPE. However, few studies have shown that the crystalline structure of TPS evolves in time thus modifying slightly its thermal and mechanical properties. For commercial development, it would be essential to study the aging of the 3-layer film. Applications in the food packaging require the conservation of properties such as permeability for a duration varying from weeks to months. It would therefore be important to measure the evolution of mechanical and permeability properties as a function of time in order to evaluate the commercial viability of the film.

2) Starch limited stability can be seen as downside in the recyclability of the 3-layer film. It would be important to explore the recyclability of the system and see to what extend the material could be recycled. For internal recycling, the recycling of off-spec multilayer films into the central layer would also be critical for the commercial viability.

3) Regarding the final application in food packaging, it would be important to explore the microwavability and sealing properties of the film as well as finding out about the conservation of mechanical and permeability properties after such treatments. For specific food applications, the conservation of aromas could be investigated as well.

REFERENCES

Aburto, J., Thiebaud, S., Alric, I., Borredon, E., Bikiaris, D., Prinos, J., & Panayiotou, C. (1997). Properties of octanoated starch and its blends with polyethylene. *Carbohydrate Polymers*, *34*(1–2), 101–112. https://doi.org/10.1016/S0144-8617(97)00053-2

Alexandre, M., & Dubois, P. (2000). Polymer-layered silicate nanocomposites: Preparation, properties and uses of a new class of materials. *Materials Science and Engineering R: Reports*, *28*(March), 1–63. https://doi.org/10.1016/S0927-796X(00)00012-7

Arvanitoyannis, I., Biliaderis, C. G., Ogawa, H., & Kawasaki, N. (1998). Biodegradable films made from low-density polyethylene (LDPE), rice starch and potato starch for food packaging applications: Part 1. *Carbohydrate Polymers*, *36*, 89–104. https://doi.org/10.1016/S0144-8617(98)00016-2

Avella, M., De Vlieger, J. J., Errico, M. E., Fischer, S., Vacca, P., & Volpe, M. G. (2005). Biodegradable starch/clay nanocomposite films for food packaging applications. *Food Chemistry*, *93*, 467–474. https://doi.org/10.1016/j.foodchem.2004.10.024

Avérous, L. (2004). Biodegradable Multiphase Systems Based on Plasticized Starch: A Review. *Journal of Macromolecular Science, Part C: Polymer Reviews*, *44*(July 2014), 231–274. https://doi.org/10.1081/MC-200029326

Avgeropoulos, G. N., Weissert, F. C., Biddison, P. H., & Böhm, G. G. A. (1976). Heterogeneous Blends of Polymers. Rheology and Morphology. *Rubber Chemistry and Technology*, *49*(1), 93–104. https://doi.org/10.5254/1.3534954

Ayana, B., Suin, S., & Khatua, B. B. (2014). Highly exfoliated eco-friendly thermoplastic starch (TPS)/poly (lactic acid)(PLA)/clay nanocomposites using unmodified nanoclay. *Carbohydrate Polymers*, *110*, 430–439. https://doi.org/10.1016/j.carbpol.2014.04.024

Bertoft, E., & Blennow, A. (2016). Structure of Potato Starch. In J. Singh & L. Kaur (Eds.), *Advances in Potato Chemistry and Technology* (2nd ed., pp. 57–73). Elsevier. https://doi.org/10.1016/B978-0-12-800002-1.00003-0

Bikiaris, D., & Panayiotou, C. (1998). LDPE / Starch Blends Compatibilized with PE-g-MA copolymers. *Journal of Applied Polymer Science*, *70*(8), 1503–1521. https://doi.org/papers://590F92D9-0B76-4B88-8729-9AF064BE5AC8/Paper/p5365

Bikiaris, D., Theologidis, S., & Panayiotou, C. (1998). Preparation and Characterization of LDPE/Starch Blends Containing Ethylene/vinyl Acetate Copolymer as Compatibilizer. *Polymer Engineering and Science*, *38*(6), 954–964. https://doi.org/Doi 10.1002/Pen.10263

Biliaderis, C. G. (2009). *Structural Transitions and Related Physical Properties of Starch*. *Starch: Chemistry and Technology*. Elsevier. https://doi.org/10.1016/B978-0-12-746275-2.00008-2

Buleon, A., Colonna, P., Planchot, V., & Ball, S. (1998). Starch granules: Structure and biosynthesis. *International Journal of Biological Macromolecules*, *23*(2), 85–112.

https://doi.org/10.1016/S0141-8130(98)00040-3

Cantor, K. (2011). Processing. In *Blown Film Extrusion* (pp. 91–100). München: Carl Hanser Verlag GmbH & Co. KG. https://doi.org/10.3139/9783446428195.004

Carraher, C. E. (2013). *Introduction to polymer chemistry*. (CRC Press Taylor & Francis Group, Ed.) (3rd ed.). Boca Raton, FL.

Cervone, N. W., & Harper, J. M. (1978). Viscosity of an intermediate moisture dough. *Journal of Food Process Engineering*, *2*(1), 83–95. https://doi.org/10.1111/j.1745-4530.1978.tb00196.x

Chandra, R., & Rustgi, R. (1997). Biodegradation of maleated linear low-density polyethylene and starch blends. *Polymer Degradation and Stability*, *56*, 185–202. https://doi.org/10.1016/S0141-3910(96)00212-1

Chiou, B. S., Yee, E., Glenn, G. M., & Orts, W. J. (2005). Rheology of starch-clay nanocomposites. *Carbohydrate Polymers*, *59*, 467–475. https://doi.org/10.1016/j.carbpol.2004.11.001

Chivrac, F., Pollet, E., & Avérous, L. (2009). Progress in nano-biocomposites based on polysaccharides and nanoclays. *Materials Science and Engineering R: Reports*, *67*(1), 1–17. https://doi.org/10.1016/j.mser.2009.09.002

Chivrac, F., Pollet, E., Dole, P., & Avérous, L. (2010). Starch-based nano-biocomposites: Plasticizer impact on the montmorillonite exfoliation process. *Carbohydrate Polymers*, *79*(4), 941–947. https://doi.org/10.1016/j.carbpol.2009.10.018

Chomon, P. (2005). Emballages plastiques souples et semi-rigides - Polymères techniques - Procédés de transformation. *Techniques de l'ingénieur*, *33*, 1–12.

Cros, S. (2007). Propriétés barrières des polymères utilisés en emballage. In *Technique de l'ingénieur*. Techniques de l'ingénieur.

Cyras, V. P., Manfredi, L. B., Ton-That, M.-T., & Vázquez, A. (2008). Physical and mechanical properties of thermoplastic starch/montmorillonite nanocomposite films. *Carbohydrate Polymers*, *73*, 55–63. https://doi.org/10.1016/j.carbpol.2007.11.014

Dai, L., Zhang, J., & Cheng, F. (2019). Effects of starches from different botanical sources and modification methods on physicochemical properties of starch-based edible films. *International Journal of Biological Macromolecules*, *132*, 897–905. https://doi.org/10.1016/j.ijbiomac.2019.03.197

Delgadillo-Velázquez, O., Hatzikiriakos, S. G., & Sentmanat, M. (2008). Thermorheological properties of LLDPE/LDPE blends: Effects of production technology of LLDPE. *Journal of Polymer Science, Part B: Polymer Physics*, *46*(16), 1669–1683. https://doi.org/10.1002/polb.21504

Della Valle, G., Boché, Y., Colonna, P., & Vergnes, B. (1995). The extrusion behaviour of potato starch. *Carbohydrate Polymers*, *28*(3), 255–264. https://doi.org/10.1016/0144-8617(95)00111-5

Della Valle, G., Buleon, A., Carreau, P. J., Lavoie, P.-A., & Vergnes, B. (1998). Relationship between structure and viscoelastic behavior of plasticized starch. *Journal of Rheology*, *42*(3), 507–525. https://doi.org/10.1122/1.550900

Della Valle, G., Colonna, P., Patria, A., & Vergnes, B. (1996). Influence of amylose content on the viscous behavior of low hydrated molten starches. *Journal of Rheology*, *40*(3), 347–362. https://doi.org/10.1122/1.550747

Della Valle, G., Vergnes, B., & Lourdin, D. (2007). Viscous properties of thermoplastic starches from different botanical origin. *International Polymer Processing*, *22*(5), 471–479. https://doi.org/10.3139/217.2057

Dole, P., Joly, C., Espuche, E., Alric, I., & Gontard, N. (2004). Gas transport properties of starch based films. *Carbohydrate Polymers*, *58*(3), 335–343. https://doi.org/10.1016/j.carbpol.2004.08.002

Favis, B. D., & Chalifoux, J. P. (1987). The effect of viscosity ratio on the morphology of polypropylene/polycarbonate blends during processing. *Polymer Engineering and Science*, *27*(21), 1591–1600. https://doi.org/10.1002/pen.760272105

Favis, B. D., & Willis, J. M. (1990). Phase size/composition dependence in immiscible blends: Experimental and theoretical considerations. *Journal of Polymer Science Part B: Polymer Physics*, *28*(12), 2259–2269. https://doi.org/10.1002/polb.1990.090281208

Ferreira, W. H., Khalili, R. R., Figueira, M. J. M., & Andrade, C. T. (2014). Effect of organoclay on blends of individually plasticized thermoplastic starch and polypropylene. *Industrial Crops and Products*, *52*, 38–45. https://doi.org/10.1016/j.indcrop.2013.10.016

Fletcher, S. I., McMaster, T. J., Richmond, P., & Smith, A. C. (1985). Rheology and extrusion of maize grits. *Chemical Engineering Communications*, *32*(1–5), 239–262. https://doi.org/10.1080/00986448508911650

Fortelný, I. (2005). Theoretical Aspects of Phase Morphology Development. In *Micro- and Nanostructured Multiphase Polymer Blend Systems* (pp. 43–90). CRC Press. https://doi.org/10.1201/9781420026542-2

Geyer, R., Jambeck, J. R., & Law, K. L. (2017). Production, use, and fate of all plastics ever made. *Science Advances*, *3*(7), e1700782. https://doi.org/10.1126/sciadv.1700782

Giannelis, E. P., Krishnamoorti, R., & Manias, E. (1999). Polymer-Silicate Nanocomposites: Model Systems for Confined Polymers and Polymer Brushes. In *Polymers in Confined Environments* (pp. 107–147). Springer, Berlin, Heidelberg. https://doi.org/10.1007/3-540-69711-X_3

Grommers, H. E., & Van der Krogt, D. A. (2009). Potato Starch: Production, Modifications and Uses. In J. BeMiller & R. Whistler (Eds.), *Starch: Chemistry and Technology* (3rd ed., pp. 511–539). Elsevier. https://doi.org/10.1016/B978-0-12-746275-2.00011-2

Gupta, a. P., Sharma, M., & Kumar, V. (2008). Preparation and Characterization of Potato Starch Based Low Density Polyethylene/Low Density Polyethylene Grafted Maleic Anhydride Biodegradable Polymer Composite. *Polymer-Plastics Technology and Engineering*,

47(March 2015), 953–959. https://doi.org/10.1080/03602550802274597

Hong, J. S., Kim, Y. K., Ahn, K. H., Lee, S. J., & Kim, C. (2007). Interfacial tension reduction in PBT/PE/clay nanocomposite. *Rheologica Acta*, *46*(4), 469–478. https://doi.org/10.1007/s00397-006-0123-1

Huang, C.-H., Wu, J.-S., & Huang, C.-C. (2004). Predicting the Permeability and Tensile Properties of Multilayer Films from the Properties of the Individual Component Layers. *Polymer Journal*, *36*(5), 386–393. https://doi.org/10.1295/polymj.36.386

Huneault, M. A., & Li, H. (2007). Morphology and properties of compatibilized polylactide/thermoplastic starch blends. *Polymer*, *48*(1), 270–280. https://doi.org/10.1016/j.polymer.2006.11.023

Huneault, M. A., & Li, H. (2012). Preparation and properties of extruded thermoplastic starch/polymer blends. *Journal of Applied Polymer Science*, *126*(S1), E96–E108. https://doi.org/10.1002/app.36724

Jane, J. (2009). Structural Features of Starch Granules II. In J. N. BeMiller & R. Whistler (Eds.), *Starch: Chemistry and Technology* (3rd ed., pp. 193–236). Elsevier. https://doi.org/10.1016/B978-0-12-746275-2.00006-9

Jost, V., & Stramm, C. (2016). Influence of plasticizers on the mechanical and barrier properties of cast biopolymer films. *Journal of Applied Polymer Science*, *133*(2), n/a-n/a. https://doi.org/10.1002/app.42513

Karger-Kocsis, J., Kmetty, Á., Lendvai, L., Drakopoulos, S., & Bárány, T. (2014). Water-Assisted Production of Thermoplastic Nanocomposites: A Review. *Materials*, *8*(1), 72–95. https://doi.org/10.3390/ma8010072

Kaseem, M., Hamad, K., & Deri, F. (2013). Slit die rheology of thermoplastic starch during extrusion process. *International Journal of Plastics Technology*, *17*(1), 51–60. https://doi.org/10.1007/s12588-013-9044-x

Ketels, H. H. T. (1989). *Synthesis, characterization and applications of ethylene vinylalcohol copolymers*. T. U. Eindhoven.

Khanoonkon, N., Yoksan, R., & Ogale, A. A. (2016a). Effect of stearic acid-grafted starch compatibilizer on properties of linear low density polyethylene/thermoplastic starch blown film. *Carbohydrate Polymers*, *137*, 165–173. https://doi.org/10.1016/j.carbpol.2015.10.038

Khanoonkon, N., Yoksan, R., & Ogale, A. A. (2016b). Morphological characteristics of stearic acid-grafted starch-compatibilized linear low density polyethylene/thermoplastic starch blown film. *European Polymer Journal*, *76*, 266–277. https://doi.org/10.1016/j.eurpolymj.2016.02.001

Laohakunjit, N., & Noomhorm, A. (2004). Effect of Plasticizers on Mechanical and Barrier Properties of Rice Starch Film. *Starch - Stärke*, *56*(8), 348–356. https://doi.org/10.1002/star.200300249

Lee, D. S., Piergiovanni, L., & Yam, K. L. (2008). *Food packaging science and technology*. (D. S.

Lee & K. L. Yam, Eds.). Boca Raton, FL: CRC Press. https://doi.org/10.1201/9781439894071

Lee, S. Y., & Kim, S. C. (1997). Laminar morphology development and oxygen permeability of LDPE/EVOH blends. *Polymer Engineering and Science*, *37*(2), 463–475. https://doi.org/Doi 10.1002/Pen.11690

Li, G., & Favis, B. D. (2010). Morphology development and interfacial interactions in polycaprolactone/ thermoplastic-starch blends. *Macromolecular Chemistry and Physics*, *211*, 321–333. https://doi.org/10.1002/macp.200900348

Li, G., Sarazin, P., Orts, W. J., Imam, S. H., & Favis, B. D. (2011). Biodegradation of thermoplastic starch and its blends with poly(lactic acid) and polyethylene: Influence of morphology. *Macromolecular Chemistry and Physics*, *212*, 1147–1154. https://doi.org/10.1002/macp.201100090

Li, H., & Huneault, M. A. (2011). Comparison of sorbitol and glycerol as plasticizers for thermoplastic starch in TPS/PLA blends. *Journal of Applied Polymer Science*, *119*(4), 2439–2448. https://doi.org/10.1002/app.32956

Liu, H., Xie, F., Yu, L., Chen, L., & Li, L. (2009). Thermal processing of starch-based polymers. *Progress in Polymer Science (Oxford)*, *34*, 1348–1368. https://doi.org/10.1016/j.progpolymsci.2009.07.001

Ma, X. F., Yu, J. G., & Wan, J. J. (2006). Urea and ethanolamine as a mixed plasticizer for thermoplastic starch. *Carbohydrate Polymers*, *64*(2), 267–273. https://doi.org/10.1016/j.carbpol.2005.11.042

Ma, X., & Yu, J. (2004). The plasticizers containing amide groups for thermoplastic starch. *Carbohydrate Polymers*, *57*(2), 197–203. https://doi.org/10.1016/j.carbpol.2004.04.012

Martens, H. (2014). Hybrid polyolefin starch blown film. Geleen, The Netherlands.

Martin, O., Avérous, L., & Della Valle, G. (2003). In-line determination of plasticized wheat starch viscoelastic behavior: impact of processing. *Carbohydrate Polymers*, *53*(2), 169–182. https://doi.org/10.1016/S0144-8617(03)00040-7

Mazerolles, T., Heuzey, M. C., Soliman, M., Martens, H., Kleppinger, R., & Huneault, M. A. (2019). Development of co-continuous morphology in blends of thermoplastic starch and low-density polyethylene. *Carbohydrate Polymers*, *206*(November 2018), 757–766. https://doi.org/10.1016/j.carbpol.2018.11.038

McGlashan, S. A., & Halley, P. J. (2003). Preparation and characterisation of biodegradable starch-based nanocomposite materials. *Polymer International*, *52*(11), 1767–1773. https://doi.org/10.1002/pi.1287

Mokwena, K. K., & Tang, J. (2012). Ethylene Vinyl Alcohol: A Review of Barrier Properties for Packaging Shelf Stable Foods. *Critical Reviews in Food Science and Nutrition*, *52*(February 2015), 640–650. https://doi.org/10.1080/10408398.2010.504903

Mortazavi, S., Ghasemi, I., & Oromiehie, A. (2013). Effect of phase inversion on the physical and mechanical properties of low density polyethylene/thermoplastic starch. *Polymer Testing*,

32(3), 482–491. https://doi.org/10.1016/j.polymertesting.2013.01.004

Mortazavi, S., Ghasemi, I., & Oromiehie, A. (2014). Morphological and rheological properties of (low-density polyethylene)/thermoplastic starch blend: investigation of the role of high elastic network. *Journal of Vinyl and Additive Technology*, *20*(4), 250–259. https://doi.org/10.1002/vnl.21360

Muramatsu, M., Okura, M., Kuboyama, K., Ougizawa, T., Yamamoto, T., Nishihara, Y., … Kobayashi, Y. (2003). Oxygen permeability and free volume hole size in ethylene-vinyl alcohol copolymer film: Temperature and humidity dependence. *Radiation Physics and Chemistry*, *68*(3–4), 561–564. https://doi.org/10.1016/S0969-806X(03)00231-7

Otey, F. H., Westhoff, R. P., & Doane, W. M. (1980). Starch-Based Blown Films. *Industrial and Engineering Chemistry Product Research and Development*, *19*(4), 592–595. https://doi.org/10.1021/i360076a021

Paul, D. R., & Barlow, J. W. (1980). Polymer Blends. *Journal of Macromolecular Science, Part C*, *18*(1), 109–168. https://doi.org/10.1080/00222358008080917

Pérez, S., Baldwin, P. M., & Gallant, D. J. (2009). Structural Features of Starch Granules I. In J. N. BeMiller & R. Whistler (Eds.), *Starch: Chemistry and Technology* (3rd ed., pp. 149–192). Elsevier. https://doi.org/10.1016/B978-0-12-746275-2.00005-7

Pötschke, P., & Paul, D. R. (2003). Formation of Co-continuous Structures in Melt-Mixed Immiscible Polymer Blends. *Journal of Macromolecular Science, Part C: Polymer Reviews*, *43*(1), 87–141. https://doi.org/10.1081/MC-120018022

Qin, Y., Yang, J., Yuan, M., Xue, J., Chao, J., Wu, Y., & Yuan, M. (2014). Mechanical, barrier, and thermal properties of poly(lactic acid)/poly(trimethylene carbonate)/talc composite films. *Journal of Applied Polymer Science*, *131*(6), n/a-n/a. https://doi.org/10.1002/app.40016

Raquez, J.-M., Nabar, Y., Narayan, R., & Dubois, P. (2008). In situ compatibilization of maleated thermoplastic starch/polyester melt-blends by reactive extrusion. *Polymer Engineering & Science*, *48*(9), 1747–1754. https://doi.org/10.1002/pen.21136

Rindlav-Westling, A., Stading, M., Hermansson, A.-M., & Gatenholm, P. (1998). Structure, mechanical and barrier properties of amylose and amylopectin films. *Carbohydrate Polymers*, *36*(2–3), 217–224. https://doi.org/10.1016/S0144-8617(98)00025-3

Robertson, G. L. (2006). *Food Packaging: Principles and Practice*. (T. & F. Group, Ed.) (2nd ed.).

Robertson, G. L. (2013). *Food Packaging: Principles and Practice*. (CRC Press, Ed.) (3rd Editio).

Rodriguez-Gonzalez, F. J., Ramsay, B. A., & Favis, B. D. (2003). High performance LDPE/thermoplastic starch blends: A sustainable alternative to pure polyethylene. *Polymer*, *44*, 1517–1526. https://doi.org/10.1016/S0032-3861(02)00907-2

Rodriguez-Gonzalez, F. J., Ramsay, B. A., & Favis, B. D. (2004). Rheological and thermal properties of thermoplastic starch with high glycerol content. *Carbohydrate Polymers*, *58*, 139–147. https://doi.org/10.1016/j.carbpol.2004.06.002

Rodriguez-Gonzalez, F. J., Virgilio, N., Ramsay, B. A., & Favis, B. D. (2003). Influence of Melt Drawing on the Morphology of One-and Two-Step Processed LDPE/Thermoplastic Starch Blends. *Advances in Polymer Technology*, *22*(4), 297–305. https://doi.org/10.1002/adv.10057

Ronzani, A., & Baccaro, L. (2012). Barrier films, an opportunity for SABIC? Geleen, The Netherlands.

Sabetzadeh, M., Bagheri, R., & Masoomi, M. (2015). Study on ternary low density polyethylene/linear low density polyethylene/thermoplastic starch blend films. *Carbohydrate Polymers*, *119*, 126–133. https://doi.org/10.1016/j.carbpol.2014.11.038

Sabetzadeh, M., Bagheri, R., & Masoomi, M. (2016). Effect of nanoclay on the properties of low density polyethylene/linear low density polyethylene/thermoplastic starch blend films. *Carbohydrate Polymers*, *141*, 75–81. https://doi.org/10.1016/j.carbpol.2015.12.057

Sandoval, A. J., & Barreiro, J. A. (2007). Off-line capillary rheometry of corn starch: Effects of temperature, moisture content and shear rate. *LWT - Food Science and Technology*, *40*(1), 43–48. https://doi.org/10.1016/j.lwt.2005.09.001

Schwach, E., & Avérous, L. (2004). Starch-based biodegradable blends: Morphology and interface properties. *Polymer International*, *53*(April), 2115–2124. https://doi.org/10.1002/pi.1636

Shannon, J. C., Garwood, D. L., & Boyer, C. D. (2009). Genetics and Physiology of Starch Development. In *Starch: Chemistry and Technology* (pp. 23–82). Elsevier. https://doi.org/10.1016/B978-0-12-746275-2.00003-3

Shi, R., Zhang, Z., Liu, Q., Han, Y., Zhang, L., Chen, D., & Tian, W. (2007). Characterization of citric acid/glycerol co-plasticized thermoplastic starch prepared by melt blending. *Carbohydrate Polymers*, *69*(4), 748–755. https://doi.org/10.1016/j.carbpol.2007.02.010

Singh, N., Singh, J., Kaur, L., Sodhi, N. S., & Gill, B. S. (2003). Morphological, thermal and rheological properties of starches from different botanical sources. *Food Chemistry*, *81*(2), 219–231. https://doi.org/10.1016/S0308-8146(02)00416-8

Šoltýs, A., Hronský, V., Šmídová, N., Olčák, D., Ivanič, F., & Chodák, I. (2019). Solid-state 1 H and 13 C NMR of corn starch plasticized with glycerol and urea. *European Polymer Journal*, *117*(April), 19–27. https://doi.org/10.1016/j.eurpolymj.2019.04.042

St-Pierre, N., Favis, B. D., Ramsay, B. a., Ramsay, J. a., & Verhoogt, H. (1997). Processing and characterization of thermoplastic starch/polyethylene blends. *Polymer*, *38*(3), 647–655. https://doi.org/10.1016/S0032-3861(97)81176-7

Su, H., Xue, J., Cai, P., Li, J., & Guo, S. (2015). Structure and oxygen-barrier properties of (linear low-density polyethylene/ethylene-vinyl alcohol copolymer)/linear low-density polyethylene composite films prepared by microlayer coextrusion. *Journal of Applied Polymer Science*, *132*(27), n/a-n/a. https://doi.org/10.1002/app.42211

Tabatabaei, S. H., & Ajji, A. (2011). Structure-orientation-properties relationships for

polypropylene nanoclay composite films. *Journal of Plastic Film and Sheeting*, *27*(1–2), 87–115. https://doi.org/10.1177/8756087911405825

Taguet, A., Huneault, M. a., & Favis, B. D. (2009). Interface/morphology relationships in polymer blends with thermoplastic starch. *Polymer*, *50*, 5733–5743. https://doi.org/10.1016/j.polymer.2009.09.055

Tajuddin, S., Xie, F., Nicholson, T. M., Liu, P., & Halley, P. J. (2011). Rheological properties of thermoplastic starch studied by multipass rheometer. *Carbohydrate Polymers*, *83*(2), 914–919. https://doi.org/10.1016/j.carbpol.2010.08.073

Tester, R. F., Karkalas, J., & Qi, X. (2004). Starch - Composition, fine structure and architecture. *Journal of Cereal Science*, *39*, 151–165. https://doi.org/10.1016/j.jcs.2003.12.001

Thunwall, M., Kuthanová, V., Boldizar, A., & Rigdahl, M. (2008). Film blowing of thermoplastic starch. *Carbohydrate Polymers*, *71*(4), 583–590. https://doi.org/10.1016/j.carbpol.2007.07.001

Vaidya, U. R., & Bhattacharya, M. (1994). Properties of blends of starch and synthetic polymers containing anhydride groups. *Journal of Applied Polymer Science*, *52*(5), 617–628. https://doi.org/10.1002/app.1994.070520505

Van Soest, J. J. G., Benes, K., De Wit, D., & Vliegenthart, J. F. G. (1996). The influence of starch molecular mass on the properties of extruded thermoplastic starch. *Polymer*, *37*(16), 3543–3552. https://doi.org/10.1016/0032-3861(96)00165-6

Van Soest, J. J. G., Hulleman, S. H. D., De Wit, D., & Vliegenthart, J. F. G. (1996a). Changes in the mechanical properties of thermoplastic potato starch in relation with changes in B-type crystallinity. *Carbohydrate Polymers*, *29*, 225–232. https://doi.org/10.1016/0144-8617(96)00011-2

Van Soest, J. J. G., Hulleman, S. H. D., De Wit, D., & Vliegenthart, J. F. G. (1996b). Crystallinity in starch bioplastics. *Industrial Crops and Products*, *5*, 11–22. https://doi.org/10.1016/0926-6690(95)00048-8

Vergnes, B., & Villemaire, J. P. (1987). Rheological behaviour of low moisture molten maize starch. *Rheologica Acta*, *26*(6), 570–576. https://doi.org/10.1007/BF01333742

Wang, S. S., Chiang, W. C., Zhao, B., Zheng, X. G., & Kim, I. H. (1991). Experimental analysis and computer simulation of starch-water interactions during phase transition. *J. Food Sci.* Retrieved from http://www.scopus.com/inward/record.url?eid=2-s2.0-0000968570&partnerID=tZOtx3y1

Wang, S., Yu, J., & Yu, J. (2005). Compatible thermoplastic starch/polyethylene blends by one-step reactive extrusion. *Polymer International*, *54*(December 2004), 279–285. https://doi.org/10.1002/pi.1668

Wang, W., Song, P., Wang, R., Zhang, R., Guo, Q., Hou, H., & Dong, H. (2018). Effects of cationization of high amylose maize starch on the performance of starch/montmorillonite nano-biocomposites. *Industrial Crops and Products*, *117*(February), 333–339.

https://doi.org/10.1016/j.indcrop.2018.03.004

Willemse, R. C., Posthuma De Boer, a., Van Dam, J., & Gotsis, a. D. (1998). Co-continuous morphologies in polymer blends: The influence of the interfacial tension. *Polymer*, *40*(4), 827–834. https://doi.org/10.1016/S0032-3861(98)00307-3

Willett, J. L. (1994). Mechanical properties of LDPE/granular starch composites. *Journal of Applied Polymer Science*, *54*(11), 1685–1695. https://doi.org/10.1002/app.1994.070541112

Wu, S. (1982). *Polymer Interface and Adhesion*. *CRC Press* (1st ed.). New York, NY. Retrieved from https://www.taylorfrancis.com/books/9781351423533

Xie, F., Halley, P. J., & Avérous, L. (2012). Rheology to understand and optimize processibility, structures and properties of starch polymeric materials. *Progress in Polymer Science (Oxford)*, *37*(4), 595–623. https://doi.org/10.1016/j.progpolymsci.2011.07.002

Xie, F., Liu, H., Chen, P., Xue, T., Chen, L., Yu, L., & Corrigan, P. (2006). Starch gelatinization under shearless and shear conditions. *International Journal of Food Engineering*. Retrieved from http://www.scopus.com/inward/record.url?eid=2-s2.0-33846564029&partnerID=tZOtx3y1

Xie, F., Pollet, E., Halley, P. J., & Avérous, L. (2013). Starch-based nano-biocomposites. *Progress in Polymer Science*, *38*(10–11), 1590–1628. https://doi.org/10.1016/j.progpolymsci.2013.05.002

Yano, K., Usuki, A., & Okada, A. (1997). Synthesis and properties of polyimide-clay hybrid films. *Journal of Polymer Science, Part A: Polymer Chemistry*, *35*(11), 2289–2294. https://doi.org/10.1002/(SICI)1099-0518(199708)35:11<2289::AID-POLA20>3.0.CO;2-9

Zhang, G., Xu, H., MacInnis, K., & Baer, E. (2015). The structure-property relationships of LLDPE–EVOH blend films fabricated by multiplication extrusion. *Polymer*, *57*, 117–124. https://doi.org/10.1016/j.polymer.2014.12.025

Zhang, Z., Britt, I. J., & Tung, M. A. (2001). Permeation of oxygen and water vapor through EVOH films as influenced by relative humidity. *Journal of Applied Polymer Science*, *82*(8), 1866–1872. https://doi.org/10.1002/app.2030